Medical Laser-Induced Thermotherapy - Models and Applications

Sturesson, Christian

1998

Medical Laser-Induced Thermotherapy
-
Models and Applications

Christian Sturesson

Lund Reports on Atomic Physics
LRAP-235

Doctoral Thesis
Department of Physics
Lund Institute of Technology
October 1998

ISBN 91-628-3134-8

To Gunilla and Axel

Contents

ABSTRACT **6**

LIST OF PAPERS **7**

1. INTRODUCTION **9**
2. BIOLOGICAL BASIS OF HEAT TREATMENT **12**
2.1 HYPERTHERMIA 12
2.1.1 HYPERTHERMIA IN CONJUNCTION WITH PHOTODYNAMIC THERAPY 19
2.2 COAGULATION 21
2.3 VAPORISATION 24
3. INDUCTION METHODS FOR HEAT TREATMENT **25**
3.1 MICROWAVES 25
3.2 LASER LIGHT 27
3.2.1 LIGHT-TISSUE INTERACTION 27
3.2.2 MEASUREMENT OF OPTICAL PROPERTIES OF TISSUE 29
3.2.3 TEMPERATURE DEPENDENCE OF OPTICAL PROPERTIES 31
3.2.4 MONTE CARLO MODELLING 33
3.2.5 LASER APPLICATORS 34
4. HEAT TRANSFER IN TISSUE **39**
4.1 CONDUCTION 39
4.2 CONVECTION 42
4.3 EVAPORATION 44
4.4 RADIATION 46
4.5 HEAT TRANSFER BY BLOOD PERFUSION 47
4.6 METABOLIC HEAT GENERATION 51
5. MONITORING OF HEAT TREATMENT **53**
5.1 TEMPERATURE MEASUREMENTS 53
5.2 BLOOD FLOW MEASUREMENTS 57
6. CLINICAL APPLICATIONS OF LASER-INDUCED THERMOTHERAPY **62**
6.1 LIVER MALIGNANCIES 62
6.2 BENIGN PROSTATIC HYPERPLASIA 65
7. SUMMARY OF PAPERS **69**

ACKNOWLEDGEMENTS **70**

REFERENCES **71**

PAPERS **85**

Abstract

Heat has long been utilised as a therapeutic tool in medicine. Laser-induced thermotherapy aims at achieving the local destruction of lesions, relying on the conversion of the light absorbed by the tissue into heat. In interstitial laser-induced thermotherapy, light is focused into thin optical fibres, which are placed deep into the tumour mass. The objective of this work was to increase the understanding of the physical and biological phenomena governing the response to laser-induced thermotherapy, with special reference to treatment of liver tumours and benign prostatic hyperplasia. Mathematical models were used to calculate the distribution of light absorption and the subsequent temperature distribution in laser-irradiated tissues. The models were used to investigate the influence on the temperature distribution of a number of different factors, such as the design of the laser probe, the number of fibres, the optical properties of the tissue, the duration of irradiation, blood perfusion and boundary conditions. New results concerning transurethral microwave thermotherapy were obtained by incorporating the distribution of absorbed microwaves into the model. Prototypes of new laser applicators for anatomically correct treatment of benign prostatic hyperplasia were developed and tested *ex vivo*. Experimental work on liver tumours pointed to the importance of eliminating the blood flow in the liver during treatment to reduce convective heat loss. In addition, it was shown that hepatic inflow occlusion during treatment increased the thermal sensitivity of tumour tissue. The dynamic influence of interstitial laser thermotherapy on liver perfusion was investigated using interstitial laser Doppler flowmetry. Vessel damage after the combined treatment of laser-induced heat treatment and photodynamic therapy was studied.

List of papers

I. C. Sturesson and S. Andersson-Engels, "A mathematical model for predicting the temperature distribution in laser-induced hyperthermia. Experimental evaluation and applications," Phys. Med. Biol. **40**: 2037-2052, 1995.

II. C. Sturesson, "Interstitial laser-induced thermotherapy: influence of carbonization on lesion size," Lasers Surg. Med. **22**: 51-57, 1998.

III. K. Ivarsson, J. Olsrud, C. Sturesson, P.H. Möller, B.R.R. Persson and K.-G. Tranberg, "A feedback interstitial diode laser (805 nm) thermotherapy system: ex vivo evaluation and mathematical modelling with one and four fibers," Lasers Surg. Med. **22**: 86-96, 1998.

IV. A.M.K. Nilsson, C. Sturesson, D.L. Liu, and S. Andersson-Engels, "Spectral measurements of the optical properties of tissue in conjunction with laser-induced thermotherapy," Appl. Opt. **37**: 1256-1267, 1998.

V. C. Sturesson, D.L. Liu, U. Stenram and S. Andersson-Engels, "Hepatic inflow occlusion increases the efficacy of interstitial laser-induced thermotherapy in rat," J. Surg. Res. **71**: 67-72, 1997.

VI. C. Sturesson, K. Ivarsson, S. Andersson-Engels, and K.-G. Tranberg, "Changes in local hepatic blood perfusion during interstitial laser-induced thermotherapy of normal rat liver measured by interstitial laser Doppler flowmetry," submitted to Lasers Med. Sci.

VII. C. Sturesson, K. Ivarsson, S. Andersson-Engels, U. Stenram, and K.-G. Tranberg, "Interstitial laser-induced thermotherapy of a rat liver tumour: Effect of temperature and hepatic inflow occlusion," manuscript.

VIII. D.L. Liu, S. Andersson-Engels, C. Sturesson, K. Svanberg, C.H. Håkansson and S. Svanberg, "Tumour vessel damage resulting from laser-induced hyperthermia alone and in combination with photodynamic therapy," Cancer Lett. **111**: 157-165, 1997.

IX. C. Sturesson and S. Andersson-Engels, "Theoretical analysis of transurethral laser-induced thermo-therapy for treatment of benign prostatic hyperplasia. Evaluation of a water-cooled applicator," Phys. Med. Biol. **41**: 445-463, 1996.

X. C. Sturesson and S. Andersson-Engels, "Tissue temperature control using a water-cooled applicator. Implications for transurethral laser-induced thermo-therapy of benign prostatic hyperplasia," Med. Phys. **24**: 461-470, 1997.

XI. C. Sturesson, J. Olsrud, M. Bolmsjö, B.R.R. Persson, A. Mattiasson, and S. Andersson-Engels, "Side-firing laser catheter for treatment of benign prostatic hyperplasia: ex vivo evaluation," manuscript.

XII. M. Bolmsjö, C. Sturesson, L. Wagrell, S. Andersson-Engels, and A. Mattiasson, "Optimizing transurethral microwave thermotherapy: a model for studying power, blood flow, temperature variations and tissue destruction," Br. J. Urol. **81**: 811-817, 1998.

***

In addition to the above Papers, original material is presented in:

C. Sturesson and S. Andersson-Engels, "Mathematical modelling of dynamic cooling and pre-heating, used to increase the depth of selective damage to blood vessels in laser treatment of port wine stains," Phys. Med. Biol. **41**: 413-428, 1996.

C. Sturesson, S. Andersson-Engels and S. Svanberg, "A numerical model for the temperature increase in surface-applied laser-induced thermo therapy with applications to tumour blood flow estimations," in *Laser-induced interstitial thermotherapy*, G. Müller and A. Roggan, eds., (Bellingham, WA: SPIE Opt. Eng. Press, 1995), pp. 157-173.

K. Ivarsson, C. Sturesson A. Bruun, U. Stenram and K.-G. Tranberg, "Linomide augments the tumouricidal effect of interstitial laser thermotherapy in a rat liver tumour model," manuscript

1. Introduction

Ablation of lesions *in situ* is an attractive alternative to surgical resection for the treatment of patients with localised disease. Many different non- or minimally-invasive ablation techniques have been employed, aiming at producing predictable results as well as reducing the risk of complications. In tumour therapy, real-time monitoring of the outcome of the treatment is of paramount concern in order to ensure the complete destruction of the tumour. One of the most extensively investigated methods for local destruction of tumours is the use of heat.

Heat has been used as a therapeutic tool in medicine since ancient times. Treatment of breast tumours by cauterisation with glowing irons is described on an Egyptian papyrus roll, dating back to about 3000 BC. From the beginning of the 20th century, many reports exist describing the regression of malignant tumours after infection with pyrogenic bacteria.[1] Although it is difficult in fever-inducing treatments to distinguish the effect of the heat from unspecific immunological responses, these studies stimulated further investigations using heat for tumour therapy. In 1898, local heat treatment using hot water was found to have a good palliative effect on advanced cervical cancer. Other early reports described the therapeutic action of heat on penile and uterine carcinomas.[2]

Heat treatment has also been used to increase the efficacy of other cancer therapies. The application of heat as an adjuvant to radiotherapy was first described in 1910.[2] During recent decades, heat treatment has been used mainly to increase the sensitivity of tumours to ionising radiation. In combination with radiation therapy local heat treatment has been applied to recurrent breast cancer, cervical nodal metastases from head and neck cancers and superficial, metastatic or recurrent malignant melanoma.[3] These studies have shown an advantage of the combined therapy as compared with radiation therapy alone. In 1969, melanoma of the extremities was treated by perfusing the area with heated blood and a cytostatic agent, increasing survival. This technique is still used for treating inoperable melanomas.[4]

In tumour therapy, heat has generally been applied with the objective of increasing the temperature of the tissue by only a few degrees in order to exploit the heat-induced enhancement of the sensitivity of tumours to ionising radiation and certain drugs. The temperature range between approximately 41-47^{o}C is called *hyperthermia*. At hyperthermic temperatures an increased heat sensitivity of tumours over normal tissues has been observed experimentally. This potential benefit is difficult to fully explore clinically because of technical problems in delivering uniform heating to deep tumour sites, although the techniques for heat delivery have been refined since the use of glowing irons. Whole body and regional heat treatment by heated blood limits the temperatures that can be used because of patient tolerance.

When applied at higher temperatures, above approximately 50°C, the treatment is termed *thermotherapy*. Thermotherapy facilitates rapid tissue destruction. At these temperatures, no selectivity in heat sensitivity exists between neoplastic and normal tissues. Therefore, thermotherapy must be applied at precisely the right location because whatever tissue is heated, is necrosed.

Laser light offers an excellent means of inducing local temperature elevation in tissue, which can be explored for tumour therapy. Light energy is converted into heat upon absorption in the tissue. The light can be focused into thin optical fibres, which can be placed deep into the tumour mass or in natural body cavities in a minimally invasive way. Lasers have been used for both hyperthermia and thermotherapy. A clear-cut division between these two treatment modalities is difficult to make when using the laser as heat source. Because light penetrates only a few mm in tissue, large temperature gradients are created. The result is that some areas are treated at thermotherapeutic temperatures, and others at hyperthermic temperatures. The distinction between treatments is best made by considering the temperature at the border of the target area. However, most investigators prefer the use of the wording thermotherapy, alternatively photocoagulation, to hyperthermia when lasers are used for heat treatment because of the high central temperatures.

The advantage of using laser light for thermotherapy as compared with other methods lies in the ability it provides to deposit, in a minimally invasive way, a precise amount of energy in a well-defined region, inducing lesions of reproducible size. Patient cure after laser-induced thermotherapy is dependent on many different factors. An attempt to delineate the process from laser irradiation to patient cure, and associated determinants, is shown in Fig. 1.1. Rigorous knowledge about the underlying physical and biological processes is important for treatment optimisation.

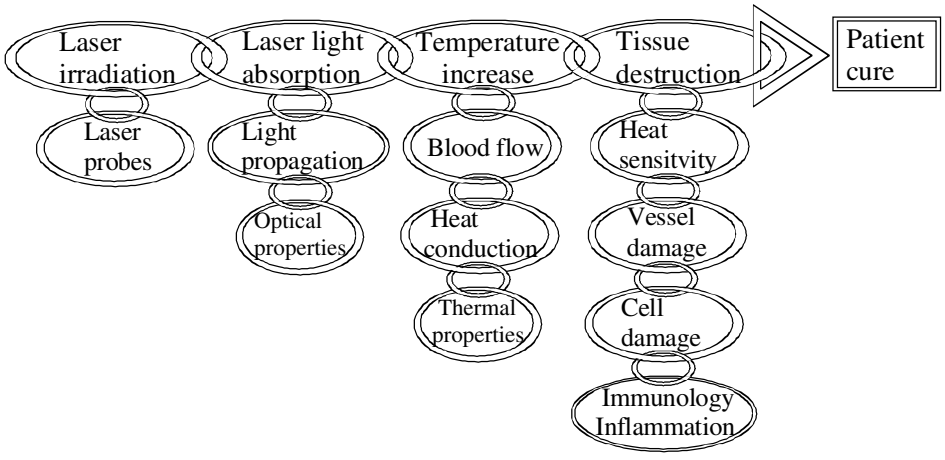

Fig. 1.1. *The chain of events and associated factors leading to patient cure by laser-induced thermotherapy.*

This thesis discusses the factors depicted in Fig. 1.1. The biological basis for heat treatment is described and the theoretical framework for light and heat propagation in tissue is presented. Mathematical models of the thermal response to laser thermotherapy were developed to predict the temperature distribution and the extent of damage. A complete model includes the calculation of the distribution of the light absorbed, the resulting time-dependent temperature distribution and the volume damaged. The results of the model can then be used to guide experimental and clinical work by aiding in the selection of the optimum set of irradiation parameters. The distribution of the absorbed laser light depends on the design of the laser applicator and the optical properties of the tissue. During coagulation the optical properties change, which was experimentally investigated. Blood perfusion plays a key role in determining the temperature distribution during laser-induced thermotherapy. The thermal influence of perfusion was investigated both theoretically and experimentally. The dynamic alterations in perfusion caused by heating are investigated and discussed. Different laser applicators are described, along with a new laser probe for transluminal application, making selective coagulation possible. Two clinical applications of laser-induced thermotherapy are presented. Finally, 12 papers covering the various topics discussed are reprinted.

2. Biological basis of heat treatment

Hyperthermia is defined as temperatures in the interval of about 41-47°C. In cancer therapy it is generally recognised that hyperthermic treatment should be combined with another therapeutic modality, such as ionising radiation, drugs or photodynamic therapy, in order to fully exploit the benefits of the treatment. At least three distinct effects of hyperthermia contribute to the result, namely the direct cell kill, the indirect cell kill due to the destruction of microvasculature, and the heat sensitisation to another treatment modality. Tumours show an apparent, albeit slight, increase in sensitivity to heat in the range 42-44°C as compared with normal tissue.[5] Clinical hyperthermia has therefore been applied in this temperature range for about one hour, attempting to cause tumour cell death while preserving normal tissue. Above 44°C the difference in heat sensitivity is lost. Thermotherapy employs temperatures which produce coagulation of the treated tissue. Rapid tissue destruction is accomplished by elevating the tissue temperature above approximately 50°C. No difference in heat sensitivity exists at this temperature; tumour and normal tissue are destroyed at the same high rate. Therefore, heat must be applied at precisely the right location so as not to induce gross damage to normal tissues. Increasing tissue temperature above 100°C results in boiling of tissue water, which leads to the formation of steam bubbles and may result in tissue carbonisation. This section discusses the biological basis of heat treatment and treats the cases of hyperthermia, coagulation and vaporisation separately.

2.1 Hyperthermia

Hyperthermia causes damage on the cellular level, mediated in a number of different ways. Heat induces structural changes in protein configuration by breaking hydrogen bonds and by disturbing ionic interactions within macromolecules.[6] The heat-induced conformational changes of proteins are extremely dependent on pH. Tumours are generally more acidic than normal tissue, due to rapid anaerobic glycolysis in the tumour and the production of lactic acid combined with an inadequate microcirculation.[5] Low pH in the tumour microenvironment is generally associated with an increased thermosensitivity.[7] In the different cell membranes, hyperthermia has been shown to remove proteins that go through the phospholipid layers. These proteins are needed to stabilise the membrane,[8] for transport functions[9] or as receptors.[10] A good correlation exists between deterioration of membrane protein function and cell killing. Hyperthermic treatment induces a sudden inhibition of the synthesis of cellular DNA, RNA and proteins.[11] The degree of inhibition has been shown to be related to the degree of heating.[12] Hyperthermia also leads to alterations in the organisation of various components in the cytoskeleton.[13] The above injuries are either reversible or lead to necrosis, depending on the thermal dose. Necrosis is an active degradation process which develops after the death of cells and tissues, mediated by the release of enzymes from dead and dying cells as well as from infiltrating inflammatory cells recruited from the blood supply. To

some extent, cell death is promoted through apoptosis (programmed cell death), which is the cell death mechanism responsible for the physiological elimination of cells.[14] Unlike necrosis, apoptosis does not induce an inflammatory reaction. Microscopically, the full extent of hyperthermic damage cannot be assessed with certainty until 24-72 h after treatment.[15,16]

Curves of *in vitro* cell survival show a strong dependence on the temperature of treatment (Fig. 2.1). The survival curves show, sometimes after an initial shoulder, an exponential decay and can then be described by an equation of the type:[17,18]

$$S = e^{-kt} \tag{2.1}$$

where S is the fraction of the cells surviving at any time t (s), and k (s^{-1}) is a constant representing the inactivation rate at a given temperature. In analogy to the curves showing dose effect obtained after irradiation with ionising radiation, a value for the inactivation time D_0 can be extracted from the curves of cell survival. This value represents, in the present context, the time of incubation at a certain temperature, after which the fraction of surviving cells is equal to 1/e. The rate constant k can then be represented as $1/D_0$.

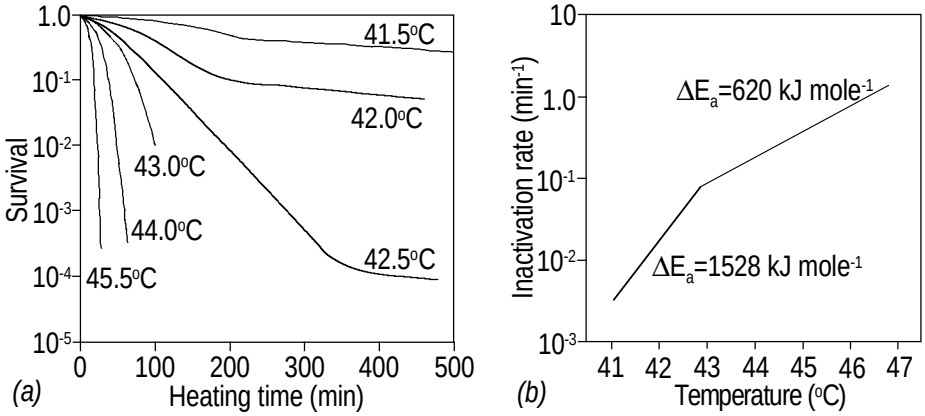

Fig. 2.1. *(a) Survival curves and (b) Arrhenius plot for the inactivation of Chinese hamster ovary cells at elevated temperatures (Redrawn from Ref. (19)).*

Thermal damage in cells and tissue has been described mathematically by thermal-chemical rate equations,[20] where the detailed temperature history determines the damage. The damage is then considered to be a unimolecular process, where native molecules transform into a denatured state through an intermediate, activated state, leading to cell death. The model states that through collision a native molecule M interacts with another molecule M, one of them becoming more energetically excited than the other and being transformed into a transition state, M*. In turn, the excited molecule might lose energy if it collides once again. There is also the possibility of the excited molecule being shaken into a new configuration, P, signifying denaturation:

$$M+M \rightleftharpoons M+M^* \qquad (2.2)$$

$$M^* \longrightarrow P$$

By assuming that the rate of formation of the excited molecules is the same as the rate of disappearance, and the rate of deactivation by M*+M collisions is much greater than the rate of unimolecular decay, the concentration of the excited molecules is then found to be:

$$-d[M]/dt = k\,[M] \qquad (2.3)$$

where the brackets indicate molar concentration and k is the resulting reaction rate.

A mathematical expression for the rate constant, k, can be obtained by assuming that in the reaction process leading to denaturation and cell death, thermally excited reactants jump over an energy barrier, ΔE_a, to form products (Fig. 2.2). The energy of the system can become distributed among an assembly of colliding molecules. The distribution of the total energy is the same as that of the kinetic energy, which is described by the Maxwell-Boltzmann distribution. The rate of product formation is proportional to the total concentration of molecules which can react, [M*], which is the product of the total concentration of molecules present [M] and the fraction that have an energy greater than ΔE_a:

$$-d[M]/dt = [M]\,A\,e^{-\Delta Ea/(RT)} \qquad (2.4)$$

where A (s^{-1}) is the frequency factor, ΔE_a (J $mole^{-1}$) is the activation energy, R (J $mole^{-1}$ K^{-1}) is the universal gas constant and T (K) is the temperature. Assuming a first-order reaction (Eq. 2.3) leads to the Arrhenius rate law:

$$k = A\,e^{-\Delta Ea/(RT)} \qquad (2.5)$$

The frequency factor as well as the activation energy can be shown to be linearly dependent on temperature. However, this dependence is extremely weak and its effect is negligible for all practical purposes.

In experimental measurements the value of the frequency factor depends on the numerical definition of the threshold of thermal damage, whereas the value of the activation energy is independent of this arbitrary definition. When a single value of the activation energy is used, it must be viewed as representing an average activation energy or the activation energy of the dominant component. The application of an Arrhenius analysis to identify the rate-limiting steps in the cell killing process violates the basic thermodynamic assumptions of reversibility.[21] In spite of this conceptual obstacle, the inflection point at about 43°C (Fig. 2.1) as given by the cell survival experiments, has been used to indicate different cell killing mechanisms above and below this point. In the range 43-47°C activation energies in the same range as those found for the denaturation of proteins have been observed.[19,22] Therefore, it has been assumed that the cell killing effect by heat between 43-47°C is mediated by protein denaturation.

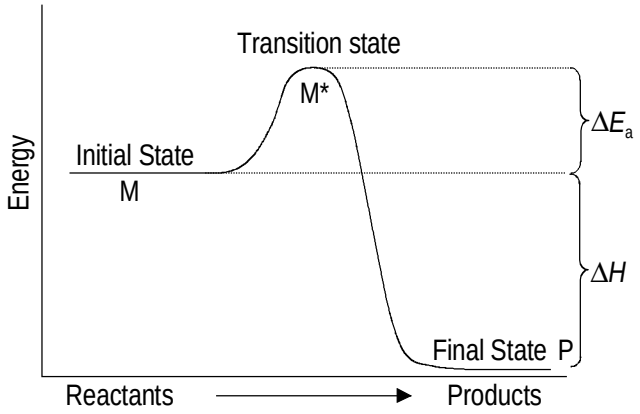

Fig. 2.2. *Energy-state diagram for a unimolecular process. Reactants in the initial state are native molecules of the cell. Products signify denatured molecules leading to cell death. It is assumed that the change in internal energy due to denaturation, ΔH, is much greater than the energy barrier, ΔE_a, so that products cannot revert to reactants without energy-consuming healing processes.*

The growth rates of tumours inoculated into the feet of mice after treatment at different temperatures and for different heating periods, have been investigated by Lindegaard and Overgaard.[23] An Arrhenius plot reveals the same inflection point at about 43°C as is found in cell survival experiments, indicating the universality of the method. Below 43°C and above about 47°C, the activation energies change, which might indicate that the cell killing mechanisms are completely different.[17]

Efforts have been made to define a thermal dose in terms of equivalent minutes at 43°C by using the Arrhenius relationship. The need for a concept of thermal dose is evident, considering that when the treatment temperature above 43°C is increased by one degree Celsius the treatment time can be halved to achieve the same therapeutic effect. The Arrhenius plot leads to the following equation, which can be used for the calculation of the thermal dose in equivalent minutes at 43°C:[19,24,25]

$$t_{43} = t_1 \times R^{(T_1-43)} \qquad (2.6)$$

where t_{43} is the thermal isoeffect dose given in equivalent minutes at 43°C, t_1 (min) is the treatment time at temperature T_1 (°C), and R is a factor which can be calculated from the activation energy and is about 2 for temperatures >43°C and about 4-6 for temperatures between about 39 and 43°C. Two different values of R are used due to the inflection point at about 43°C in the Arrhenius plot. It is then possible to calculate retrospectively an entity which can be compared between different clinical institutions by utilising the thermal dose concept. However, great differences in heat sensitivity exist between different cell types and tissues[25] so the optimal treatment has to be evaluated for each tissue type.

In vitro, it appears that the heat sensitivity of malignant cells is not greater than that of normal cells.[26] However, substantial evidence exists indicating that tumours *in*

vivo are more heat sensitive than normal tissue. It has been suggested that this is due to the difference in blood circulation between tumour and normal tissue. The microvasculature of most tissues has a biphasic response to hyperthermia. Initially, the flow increases (reactive phase), the increase being related to the temperature and duration of heating. Normal muscle and skin tissue can exhibit an enormous surge, up to 20 fold, in perfusion at heating temperatures of 41-45°C.[27] The level of perfusion greatly influences tissue temperature because blood perfusion dissipates heat by convection (see section 4.5). In this context both the perfusion level at rest and changes in perfusion induced by the treatment are important. At a constant deposition rate of thermal energy, a high perfusion level or an increase in tissue blood flow will lower the temperature. As a consequence the resulting thermal damage is unpredictable because of inter-individual variations.[28,29] This problem has recently been addressed regarding transurethral microwave thermotherapy (TUMT) of benign prostatic hyperplasia, where a constant microwave power is generally employed. Studies on human subjects[30] and canines[31] have revealed large variations in rest-flow as well as in treatment-induced changes in perfusion. The great variations in the volume of heat damage depending on blood perfusion has also been indicated on the basis of theoretical considerations (Paper XII).

After a certain time of heating, perfusion generally begins to decline. The trend is that the higher the temperature the greater the increase and the earlier the perfusion starts to decrease. The vasculature of some normal tissues is quite vulnerable to heat, which limits the capacity of blood flow increase upon heating. Exceptional thermosensitivity of the vasculature of the mouse jejunum has been described.[32] Also the circulation in the liver is considered to be thermosensitive.[33] The liver has a dual blood supply, where 25-30% of hepatic perfusion derives from the hepatic artery and the remaining part comes via the portal vein.[34] Intrinsic regulation of liver blood flow is proposed to be mediated only through the hepatic artery because of the presumed inability of the liver to regulate directly blood flow through the portal vein.[35] During hyperthermia of normal rat liver a transient increase in hepatic arterial flow at heating temperatures of 39 and 41°C has been observed, whereas no significant change in hepatic perfusion, which includes blood flow from both the hepatic artery and the portal vein, was found.[36] Other studies have consistently revealed decreases in hepatic blood flow during hyperthermia.[33,37] However, a transient increase in local hepatic perfusion by 30% was noted at a temperature of 41°C by employing more local techniques for liver heating and perfusion measurements. At 44°C liver perfusion showed a continuous decrease during and after heat treatment (Paper VI). Fig. 2.3 shows examples of blood perfusion measurements in normal rat liver obtained using interstitial laser Doppler flowmetry (see section 5.2).

The perfusion rates in tumours are generally less than those in normal tissues.[38] Tumour blood flow is heterogeneous with consequent foci of relative hypoxia and acidosis.[39,40] In addition, the tumour periphery has generally a higher blood flow than

the core.[41,42] The microcirculation in experimental tumours has been shown to be more sensitive to elevated temperatures than that of normal tissue.[43] Heating of normal tissue leads to an increase in blood flow,[44] whereas the blood flow in tumours decreases upon heating at the same temperature level.[45] Very likely the mechanisms of action of hyperthermia on experimental tumours include the indirect effect of ischemia due to the interruption of the blood flow. The number of studies on perfusion during hyperthermia of human tumours is small. A heterogeneous response to hyperthermia has been observed. Perfusion has been shown to increase,

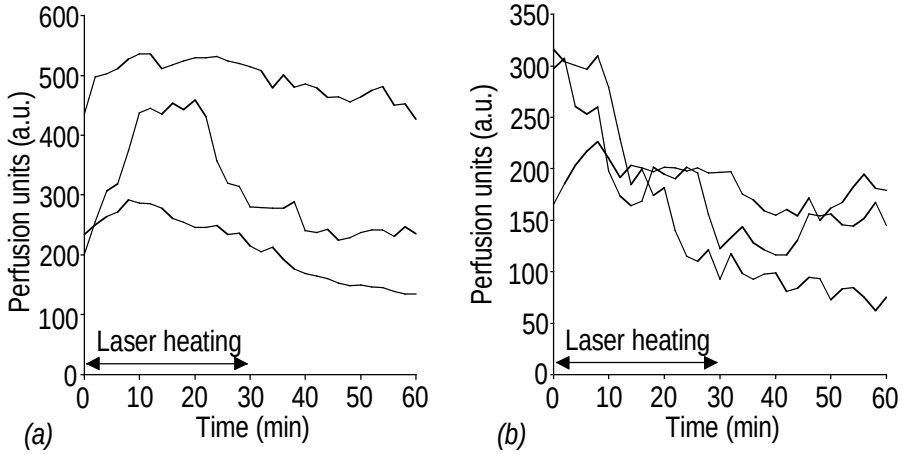

Fig. 2.3. *Local perfusion in rat liver in different subjects measured by interstitial laser Doppler flowmetry. Interstitial laser heating was performed for 30 min. The temperature at the measurement site was (a) 41°C and (b) 44°C.*

decrease or remain essentially unchanged during treatment.[42,46]

The decrease in blood perfusion observed during heat treatment is suggested to be due to a number of different factors. Tumour vessels are thin-walled and have a poor architectural array.[47] They are often tortuous, of variable diameter, contain many arterio-venous shunts and blind-end vessels. Due to the leaky nature of the vessels and the absence of adequate lymphatic drainage, the deeper vessels may collapse by the increased interstitial pressure, leading to nutritional deprivation and an acidic intra-tumour environment. Sluggish tumour blood flow may also lead to a preferential heating of the tumour. Tumour vessels lack appropriate innervation and therefore cannot dilate in response to heat.[48] The relatively fragile tumour capillaries, which are devoid of an elastic basement membrane, may not be able to cope with the stress imposed by an increased inflow of blood provided by the surrounding normal tissue. However, in some tumours a slight initial increase in blood flow is seen during hyperthermia.[49]

In addition, the endothelial cells of the walls of the tumour vessels have been shown to be thermosensitive.[50] After hyperthermic treatment, the endothelial cells show oedema and protrusion, which narrow the vessel lumen (Paper VIII). A common

phenomenon after thermal injury is an increased adherence of leukocytes to the vascular wall.[51] This would further impede blood flow. Another possible mechanism for the cessation of blood flow is the heat-induced extravasation of plasma proteins in the tumour, which may increase the extravascular pressure on the capillaries, eliciting vascular occlusion.[26] In total, the occlusion of tumour blood flow will result in poorer convective cooling and impede the entrance of nutrients and oxygen. The reduced oxygen level makes the tumour cells switch to anaerobic metabolism, which in addition to the increased metabolic rate, due to the increase in temperature, renders the tumour more acidotic.[52] The acidic environment then further increases the thermal damage. The drop in pH develops early during hyperthermic treatment and persists for many hours after the treatment.[53]

By mechanically restricting blood flow during treatment, the above-mentioned detrimental changes in tumour micromilieu are aggravated. Occlusion of the blood supply to experimental, subcutaneous tumours during hyperthermia has shown to potentiate the effect of heat.[54,55] The effect of occlusion of the hepatic inflow during laser heat treatment of liver tumours in rats was studied in Paper VII. It was shown that the combination of occlusion and laser treatment resulted in reduced growth tumour as compared to when heat was applied alone. The reduced growth of the tumour was associated with a pronounced, immediate decline in tumour blood perfusion. Fig. 2.4 shows measurements of local blood perfusion during treatment with inflow occlusion alone and in combination with laser heat treatment of rat liver tumours. For the treatment of liver tumours, the most important aspect of hepatic inflow occlusion during interstitial laser treatment is, however, the elimination of convective heat loss (Paper V).

The microscopic signs of hyperthermic treatment consist of tissue oedema and haemorrhage, which develop within minutes to hours after the treatment. Blood vessels are generally dilated and packed with erythrocytes (Paper IV).[45] Scattered intravascular thrombi and interstitial fibrin are seen in the area of treatment.[56] A few days after the treatment, an inflammatory response develops at the margin between the dead and healthy tissues (Paper V). Polymorphonuclear cells infiltrate the peripheral parts of the necrosis, which becomes enclosed by granulation tissue rich in fibroblasts and capillaries. This leads to the removal of cell debris and, in tumours, to the formation of permanent scar tissue.[57] In normal tissues, heat damaged tissue can be completely restored by regeneration.[58]

Although attractive theoretically because of its tumour selectivity, treatment with pure hyperthermia is difficult to achieve in practice because of the difficulties in generating a homogenous temperature distribution, which is influenced by factors such as the heating technique used and tissue perfusion. As discussed above, treatment may be locally inadequate if the local temperature is but one or a few degrees Celsius below the desired treatment temperature. Hyperthermia is most important as an adjuvant to radiation therapy in the treatment of locally advanced,

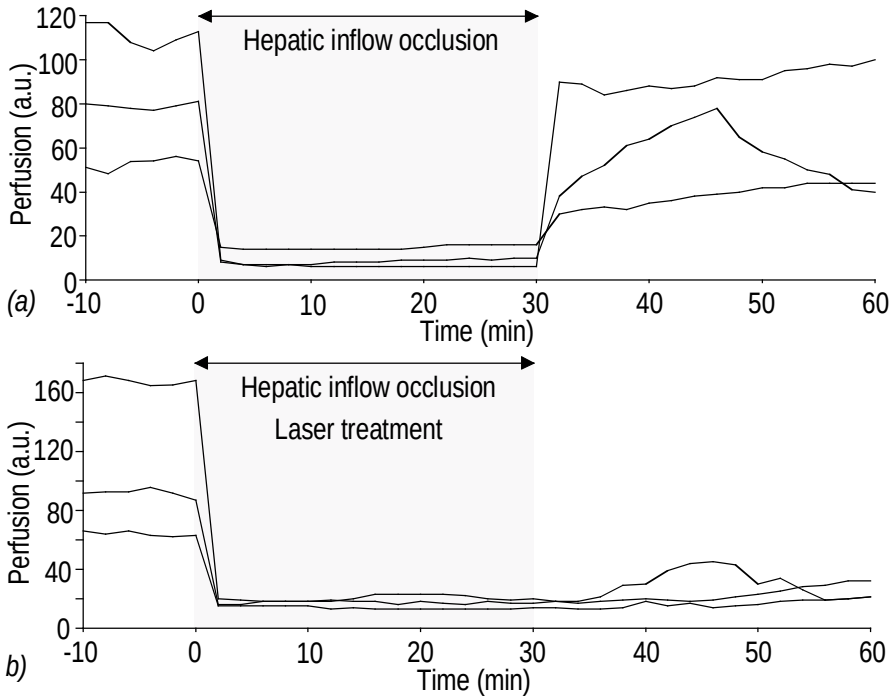

Fig. 2.4. *Effect on tumour blood perfusion of (a) hepatic inflow occlusion alone and (b) in combination with interstitial laser-induced thermotherapy. Local perfusion was measured at the tumour border, the temperature of which was maintained at 44°C for 30 min (Paper VII)*

solid tumours.[59,60] Hyperthermia significantly improved local tumour control when applied in association with radiation in the treatment of malignant melanoma.[61]

2.1.1 Hyperthermia in conjunction with photodynamic therapy

When utilised in the clinic, hyperthermia is most often combined with ionising radiation. Hyperthermia acts as a radiosensitising agent, which means that the radiation damage to cells is considerably increased by the additional application of heat.[62] Hyperthermia has also been shown to potentiate the effect of photodynamic therapy (PDT).[63] This section gives a brief introduction to PDT and describes the interaction of PDT with hyperthermia.

Photodynamic therapy is a tumour treatment modality utilising light to induce chemical reactions, the products of which are cytotoxic. The treatment requires the administration of a photosensitising agent, which is selectively retained in the tumour, and a subsequent exposure of the tumour to light at a wavelength which matches the absorption spectrum of the photosensitiser. When the molecules of the photosensitiser have been transferred to an excited state by the absorption of light two kinds of reactions are known to occur: type I reaction, which involves electron transfer to a target molecule, and type II reaction, which leads to energy transfer mainly to oxygen. The type I reaction produces different radicals, most often

involving oxygen, such as hydrogen peroxide, superoxide anion and hydroxyl radicals.[64] The most important type II reaction is the conversion of ground state oxygen to excited singlet state. Singlet oxygen reacts with amino acids, unsaturated fatty acids and nucleic acids, causing damage to these macromolecules, with resulting damage to cell function and structure.[65] Oxygen thus plays an important role in the generation of tissue damage, and without oxygen the photodynamic action does not occur.[66]

Different photosensitisers exist, such as haematoporphyrin derivative[67] (Hpd), a mixture of various porphyrins, and Photofrin,[68] which is a substance derived from Hpd and enriched in the photodynamically active fraction. Amino laevulinic acid (ALA) is a new photosensitising agent.[69] ALA is in itself photodynamically inactive, but is an endogenous precursor to haeme. An intermediate product in the haeme cycle is the effective photosensitiser protoporphyrin IX. Through the introduction of an excess of ALA the regulatory feedback system is bypassed, which results in a selective accumulation of protoporphyrin IX in the tumour cells. Effective photodynamic therapy is achieved by irradiating the sensitised tissue with a laser tuned to the absorption peak of porphyrins at about 630 nm. ALA can be administered either intravenously, for the treatment of deep-seated tumours,[70] or topically, for the treatment of superficial lesions.[71]

PDT damages the cell membrane,[72] mitochondria[73] and DNA.[74] *In vitro* photodynamic cell killing is characterised by cell lysis within one hour after a lethal PDT dose.[75] However, explanting of tumour tissue treated *in vivo* at doses sufficient for macroscopic eradication has shown an almost unaffected clonogenicity of the tumour cells, indicating the importance of vascular collapse for the treatment result.[76] Decrease and interruption of blood flow in both normal and tumour tissue have been observed after PDT when employing systemic administration of photosensitiser.[77,78] A correlation between tumour growth delay and reduction in tumour perfusion after PDT has been shown.[79] Damage to blood vessels after PDT is marked by two processes. Vessel constriction and platelet aggregation occur early during treatment. Fluid and macromolecular leakage from vessels occur shortly after the completion of the treatment, leading to tissue oedema.[80] These events contribute to blood flow stasis which induce regional tissue hypoxia. However, PDT using topical ALA results in an increase in blood perfusion immediately after treatment.[81]

The result of PDT depends on the amount of the administered drug and the dose of the irradiating light. Because the penetration depth of the light in tissue is limited to a few millimetres, PDT is suitable mainly for superficial lesions in the skin[82] and in body cavities such as the urinary bladder[83] and the bronchi.[84] Interstitial PDT is performed by implanting one or more optical fibres into the target tumour. In this way, tumours in the liver, prostate and pancreas can be treated.[85]

It has been established that the combination of hyperthermia and photodynamic therapy is more effective than the sum of the individual treatments.[86,87] By enhancing

the tumouricidal effect of PDT with hyperthermia it would be possible to reduce the dose of photosensitiser drug and thereby minimise the photosensitivity of the skin associated with the intake of systemic drugs. Also, with an increased treatment depth, thicker tumours can be treated.

The potentiation of PDT by heat has been shown to be greatest when hyperthermia is applied simultaneously or directly following the photodynamic treatment.[63,88] The mechanism of the synergism has not been clarified, but may at the cellular level include damage to a common protein target.[89] It has been is suggested that PDT increases heat sensitivity because of the decreased pH due to vascular damage.[88] A synergistic action of damage to the vasculature has been reported.[90] In a scanning electron microscopy study the combined treatment of PDT and hyperthermia has been shown to cause extreme damage to tumour vessels. Fig. 2.5 shows a scanning electron micrograph of an experimental tumour subjected to the combined treatment.

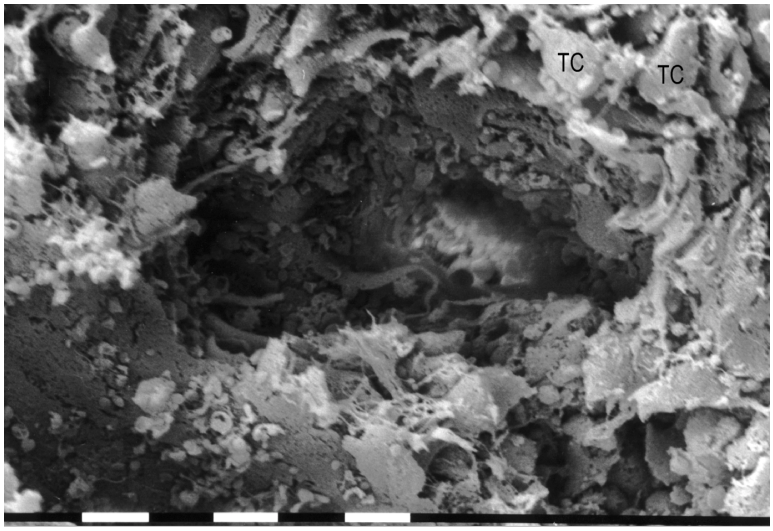

Fig. 2.5. *Micrograph of rat liver tumour after combined treatment of PDT and hyperthermia, showing destroyed tumour cells, TC. Platelets and fibrin networks appear in the vessel lumen (Bar length 10 μm).*

2.2 Coagulation

In thermotherapy, higher temperatures than those used in hyperthermic treatment are employed. It is clear that thermotherapy has no selectivity for tumours, which makes it essential to ensure that only the right areas are treated. The goal is to destroy the tumour tissue by means of thermal coagulation. The duration of treatment is typically 15-30 min. Thermal coagulation is indicated by the visible whitening of the tissue and is defined as the thermally-induced, irreversible alterations of cellular proteins and other biological molecules.[15] With this definition, structural changes after thermotherapy can be seen microscopically immediately after the treatment

while the observable histopathological treatment result after hyperthermia is delayed several days.

Henriques[91] used a general Arrhenius equation expressed as a damage integral to describe the accumulated thermal damage to pig basal epidermis:

$$\Omega = A \int e^{-\Delta Ea/(RT)} dt \qquad (2.7)$$

where Ω is the accumulated damage (dimensionless), for which an arbitrary threshold for thermal damage can be defined. As the endpoint to indicate complete necrosis Henriques chose $\Omega = 1$, which corresponds to denaturation of 63% of the native proteins. The values of the frequency factor and activation energy found in that study were $A = 3.1\times10^{98}$ s^{-1} and $\Delta E_a = 6.3\times10^{5}$ J mole^{-1}. The threshold temperature for coagulation necrosis versus irradiation time, using the above coefficients, is shown in Fig. 2.6. The damage integral is identical to Eq. 2.4 integrated over time, and can thus be applied to hyperthermic treatments. This analysis of thermal damage has also been applied to human tissues.[92] When measuring the coefficients in Eq. 2.7, it is important to indicate the particular end point chosen. This is because different end points in the same tissue will have different accumulation rates of damage. The Arrhenius description of thermal damage to tissue can be used in thermal dosimetry to assess the inflicted damage during treatment. This concept has been applied to laser (Paper II) and microwave heat treatment (Paper XII).

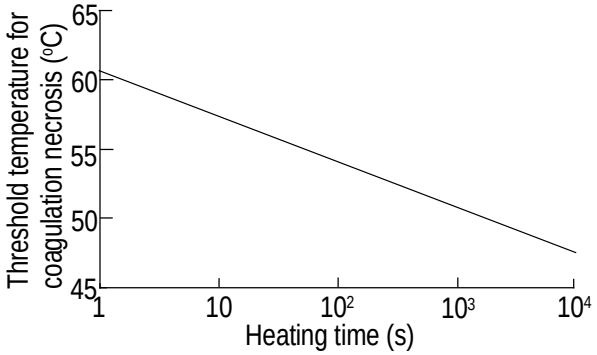

Fig. 2.6. *Temperature required for coagulation as function of heating time for basal epidermis of porcine skin.*

The healing response of coagulated tissues differs from the healing response after hyperthermia. In the central parts of thermally coagulated areas rapid cell removal and tissue healing do not occur. The necrotic core is devoid of functioning degradative enzymes due to complete denaturation. Also, by the destruction of blood vessels, the inner region is isolated from the inflammatory cells of the body.[57] Therefore, degradation and healing of the central portion of the coagulated lesion may take weeks, the healing depending on the invasion of peripheral blood vessels. Although the primary mode of action in laser-induced thermotherapy is coagulation,

hyperthermic conditions prevail in the periphery of the treatment region. Therefore, knowledge of the tissue response to both high (thermotherapy) and low (hyperthermia) temperatures is important in laser treatment.

2.3 Vaporisation

Increasing the tissue temperature to 100°C induces boiling of tissue water. Water vapour is trapped in the extracellular matrix as vacuoles or dissects along the lines of mechanical weakness.[93] Steam contained in vacuoles expands rapidly, disrupting cells and compressing surrounding tissue structures. Vapour bubbles then coalesce to form larger holes in the tissue. Tissue defects result from compression, desiccation and shrinkage. Surface irradiation using the Nd:YAG laser creates a subsurface temperature peak (Paper I),[94] because dehydration occurs at the surface (see section 4.3). Depending on the extent of subsurface pressure build up, surface tearing and tissue ejection may follow.

Continued heating of dehydrated tissue to about 400°C will initiate burning with the production of char tissue and smoke.[95] Because of limited penetration of light in tissue, vaporisation is easily produced in laser treatment. In interstitial laser-induced thermotherapy, carbonisation around an implanted optical fibre creates a central cavity delineated by a rim of charred tissue. Due to the high temperatures associated with carbonisation, charring may lead to the destruction of the laser probe.[96] Vapour bubbles resulting from vaporisation during interstitial laser-induced thermotherapy of porcine liver has subsequently been detected in the heart, which theoretically could lead to air embolus in certain patients.[97] Degradation of carbonised tissue takes time; charred tissue can still be found one year after treatment.[98] Fig. 2.7. displays the histological findings after interstitial laser-induced thermotherapy with carbonisation of a rat liver tumour.

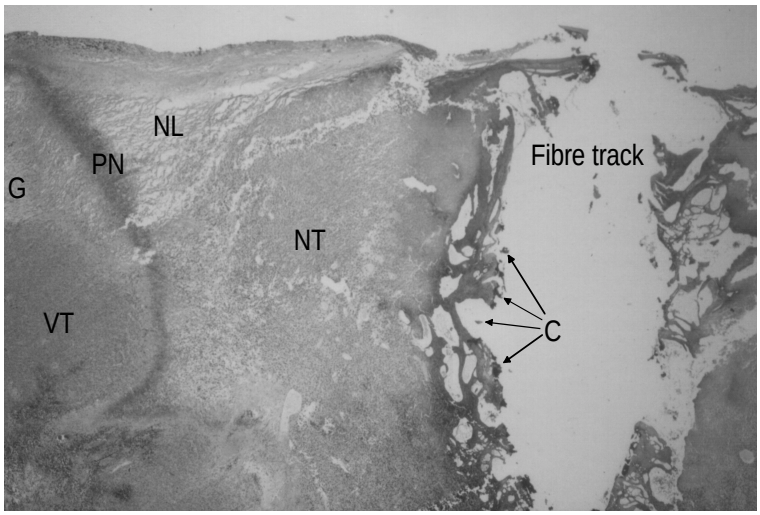

Fig. 2.7. *Microscopic findings 6 days after interstitial laser-induced thermotherapy of a rat liver tumour. The region around the fibre track contains black carbonised material, C, and empty spaces. The crater is surrounded by necrotic tumour, NT, and necrotic liver, NL. In the periphery, granulation tissue, G, a band of polymorphonuclear leucocytes, PN, and vital tumour, VT, are shown.*

3. Induction methods for heat treatment

Different methods for local deposition of heat are employed in tumour therapy. Microwaves are used both non-invasively to treat superficial tumours, and invasively for the treatment of deep-seated tumours.[99,100] Ultrasound can be applied from outside the body and be focused onto a small region to produce localised heating at depth.[101] Ferromagnetic seeds can be implanted into the tumour. The seeds are heated by applying an external magnetic field, elevating the temperature of the surrounding tissue by conduction.[102] Interstitially positioned catheters containing electrically resistive heating elements have been used to treat human brain tumours.[103] The method which is the most similar to laser-induced heat treatment is microwave heating. Therefore, it is appropriate to include a brief discussion of the similarities and differences between these two methods.

3.1 Microwaves

Microwaves are electromagnetic waves in the frequency range of about 300 MHz to 300 GHz, which correspond to wavelengths between 1 m and 1 mm (Fig. 3.1).[104] The electromagnetic field interacts with tissue by inducing oscillations of free electrons and ions, and rotation of polar molecules at the wave frequency. Through these processes, energy is removed from the electromagnetic field and converted into kinetic energy of the tissue molecules, resulting in a rise in temperature. The penetration depth in soft tissue is on the order of centimetres, with decreasing penetration depth as the frequency increases.[105] This can be compared with the penetration depth of laser light which is on the order of millimetres.[106]

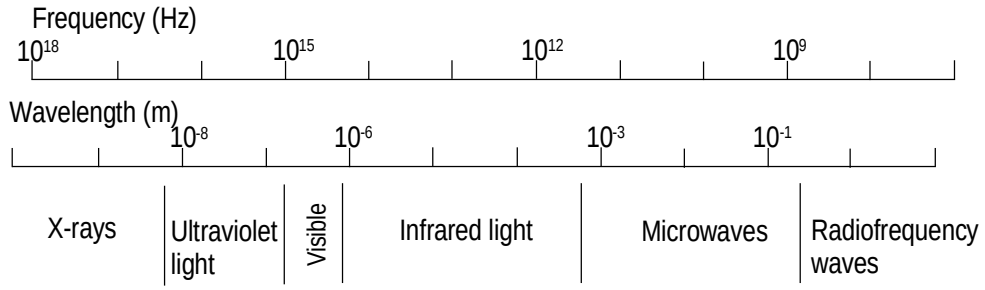

Fig. 3.1. *The electromagnetic spectrum.*

To characterise the heating pattern induced by a microwave applicator, the concept of specific absorption rate (SAR) is commonly used.[107] SAR is defined as deposited power per mass unit. The amount of microwave power absorbed by the tissue can be derived by Maxwell's equations in conjunction with a knowledge of the radiation pattern of microwave antenna, the dielectric constant and the electrical conductivity of the tissue. As an alternative, the SAR distribution can be estimated from measurements of the rise in tissue temperature resulting after a short burst of high power. A short duration of irradiation is necessary in order to minimise the effects of thermal conduction and blood perfusion (see section 4). The SAR is then given by

$$SAR = c\,\Delta T/\Delta t \qquad (3.1)$$

where c (J kg^{-1} ^{o}C^{-1}) is the specific heat of the tissue and T (^{o}C) is the tissue temperature after an irradiation time t (s).

Electrically, tissue can roughly be divided into two types based on water content. Tissues of high water content, such as muscle, liver and prostate, attenuate microwaves to a greater extent than tissues of low water content, such as fat and bone. Tissue-equivalent phantoms have been developed in order to allow the determination of SAR by temperature measurements. The phantom can be constructed as consisting of two separable parts. The cross-sectional plane is viewed by an infra-red camera (see section 5.1) after irradiation and separation of the phantom parts. Alternatively, multiple temperature sensors implanted in the phantom can be used.[108] The most widely utilised muscle-equivalent phantom consists of water, salt, polyethylene and a gelling material.[109] In dosimetry, the SAR measured on phantoms can be used as an approximation of the tissue SAR. However, these values should be regarded with caution because of the following complicating factors which come into play in the realistic situation. Tissue is not homogeneous, resulting in microwave absorption and reflection at biological interfaces. In addition, the radiation reflected at interfaces interferes with transmitted radiation and may create standing waves, inducing hot-spots in the tissues.

Microwave antennas have been constructed which can be inserted into interstitial catheters used for brachytherapy with radioactive sources.[110] Antennas with a diameter of 1 mm have been made, the typical size of the catheter being 2.2 mm.[111] For some antenna types, such as monopole types, the radiation pattern is sensitive to the depth to which the antenna is inserted in the tissue.[112] Because the insertion depth is determined by the location of the target tumour, this imposes problems in dosimetry and leads to the requirement of implanting multiple temperature sensors. In laser-induced interstitial thermotherapy, the longitudinal length of the irradiated volume is determined mainly by the length of the optical fibre tip. Multiple microwave antennas can be implanted and activated simultaneously in order to treat large lesions.[113]

Clinically, microwave heating is used extensively for transurethral treatment of benign prostatic hyperplasia. In the first investigations, which were performed in the early 1980s, the goal was to elevate the temperature of the tissue to hyperthermic temperatures. For this kind of treatment, microwaves are well suited. A large portion of the hyperplastic prostate can be treated at a quite homogenous temperature. However, hyperthermia has proved to be ineffective, although better than sham treatment.[114] The results obtained with hyperthermia suggested that the utilisation of higher temperatures would be more effective. The trend during recent years has therefore been towards higher powers for treatment at thermotherapeutic temperatures, with encouraging results (see section 6.2).

3.2 Laser light

Like microwaves, light is electromagnetic waves. The distinction between light and microwaves is based on wavelength or frequency (Fig. 3.1). Compared to light from other sources, laser light has the unique features of high intensity, coherence, monochromaticity and the possibility of producing short pulses. Following the invention of the laser in 1960, it has been used extensively for medical purposes. The therapeutic response depends in a complex manner on the choice of the wavelength of the light, the duration of irradiation and the power of the light. Different sets of these parameters are employed to transform light energy into mechanical, thermal or chemical energy (see section 2.1.1). Generally, mechanical effects are produced by employing short pulses (on the order of nanoseconds) and high energies. In this way mechanical stress waves can be induced sufficient in strength to disintegrate urinary stones.[115] Thermal effects are produced by lowering the laser power. Short laser pulses are used to ablate thin tissue layers in refractive surgery, utilising laser light which penetrates only a few micrometers in tissue.[116] The wavelength of the laser light can be chosen such that the light is absorbed selectively by the target. Selective coagulation of enlarged, disfiguring blood vessels in the skin can be performed by using laser light which is selectively absorbed by haemoglobin.[117] The pulse length is then chosen sufficiently short so as not to damage the surrounding, normal tissue, but sufficiently long to allow coagulation over the entire diameter of the vessel.

For non-selective heating near-infrared light, which penetrates comparatively deeply into the tissue, is commonly used. Laser heating has been used to treat bleeding peptic ulcers, where the thermal contraction of the tissue seals blood vessels.[118] Tumour vaporisation has been shown effective for palliative treatment of oesophageal cancer.[119] For the heating of large volumes, as desired in laser-induced hyperthermia and thermotherapy, the continuous wave mode is preferentially employed because thermal dissipation due to heat conduction is the principal determinant of tissue damage.

An understanding of the processes occurring in the interaction between light and tissue is important in order to choose the right laser parameters in a given situation. In this section, the basic concepts for the optical response of laser-irradiated tissues are introduced. In laser-induced heat treatment, light is conveyed through optical fibres to the area to be treated. Therefore, a brief discussion of optical fibres and modified fibre tips is included below.

3.2.1 Light-tissue interaction

In tissue, light is preferably envisioned as a stream of particles, photons, each carrying a discrete amount of energy. Light propagation in tissue is usually described using transport theory, mathematically expressed by the radiative transport equation.[120] This equation is derived by considering the energy balance of incoming, outgoing, absorbed and emitted photons in an infinitesimal volume

element in the medium. Transport theory does not include effects such as polarisation, diffraction and interference. Only properties such as power or intensity are considered, while wave properties such as amplitude and phase are ignored. In transport theory photons move in all directions and interact with tissue through absorption and scattering. Absorption terminates light propagation. Most of the absorbed light is converted into heat, which raises the temperature of the tissue. Scattering deflects the light from the original direction of flight, while preserving photon energy. For near-infrared light, the probability of scattering is much higher than that of absorption. The average distance between two scattering events is about 0.1 mm, to be compared with the average distance of about 20 mm travelled by the photon until it is absorbed. Tissue can be optically characterised by the absorption, μ_a (mm^{-1}) and scattering coefficient, μ_s (mm^{-1}) by considering the absorption and scattering centres as small and uniformly distributed throughout the tissue. These coefficients signify the inverse of the mean free path until absorption and between scattering events, respectively.

Tissue components which absorb light are called chromophores. Examples of important chromophores in the visible and near-infrared region of the spectrum are haemoglobin of blood and melanin of skin. Further out in the infrared, water is the dominant absorber. Fig. 3.2 shows the absorption spectra of oxygenated haemoglobin, DOPA-melanin and water. At about 1000 nm the light absorption in tissue falls to a minimum, resulting in a comparatively deep penetration of the light. The region between approximately 650 nm, where the absorption of blood decreases, and approximately 1300 nm, where water absorption starts, is called the therapeutic window. Although the penetration depth is comparatively great in this region, it is still limited to a few millimetres because of extensive scattering.

Scattering is due to microscopic variations in refractive index. Cell constituents such as mitochondria and membranes exhibit a refractive index slightly different from

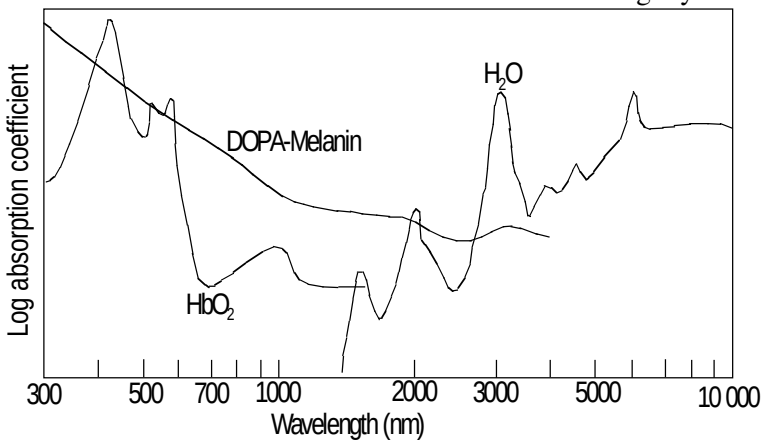

Fig. 3.2. *Absorption spectra for a selected number of important tissue chromophores. (Adapted from Ref. (121))*

that of extra- and intracellular fluid. The deflection angle of the scattering depends on the size of the scattering particle. If the particle is large in comparison to the wavelength of the light, the photon will be scattered in the forward direction. This type of scattering is called Mie scattering. To express the angular distribution of the scattered photons mathematically, a scattering phase function is usually employed. This function describes the probability that a photon will be scattered in a certain direction. A phase function which has been shown to describe scattering in tissue well is the Henyey-Greenstein phase function,[122] which was originally developed to describe light scattering in interstellar dust:[123]

$$p(\cos\theta) = \frac{1}{4\pi} \frac{1-g^2}{(1+g^2-2g\cos\theta)^{3/2}} \tag{3.2}$$

where p is the phase function (dimensionless), θ is the scattering angle and g (dimensionless) is called the anisotropy factor. The anisotropy factor equals the expectation value of $\langle\cos\theta\rangle$, and is thus the mean cosine of the scattering angle. The value of g can vary between -1 and 1. The g-values of -1, 0 and 1 describe complete backward, isotropic and complete forward scattering, respectively. For tissue in the visible and near-infrared region of the spectrum, the value of g is typically larger than 0.9, indicating the forward-scattering nature of tissue.

The wavelength of the laser light thus determines the penetration of light in tissue. Near-infrared light exhibits the greatest penetration depth obtainable with laser light. For a defined maximum rise in tissue temperature, a deeper penetration of the light makes possible a higher power deposition, and thus a greater volume of necrosis. Therefore, the Nd:YAG laser, emitting light at 1064 nm, has been the most widely used laser for thermotherapy. This laser is employed in many surgical disciplines for ablation and cutting, and is found at most large hospitals. The Nd:YAG laser is quite bulky and requires a high power supply. More recently, portable high-power diode lasers emitting in the near-infrared are being explored for thermotherapy (Paper III).[124,125] When carbonisation is induced around the fibre tip, light is strongly absorbed in the charred tissue and the penetration of light is drastically reduced.[126] The wavelength of the light is then of minor importance.

3.2.2 Measurement of optical properties of tissue

The efficacy of laser-induced thermotherapy depends on light and heat propagation. Light propagation in tissue can be described with a knowledge of the optical properties defined above. Mathematical models can then be used to gain a deeper understanding of the therapeutic procedure. Similarly, the propagation of heat is characterised by the thermophysical properties of tissue (see section 4.1). A number of different experimental techniques and theoretical models have been used to find the optical properties of tissue of which only a few will be reviewed in this section. A more detailed description is found in Ref. 127.

The total attenuation coefficient, $\mu_t=\mu_a+\mu_s$, is obtained according to Beer-Lambert's law by measuring the unscattered transmittance, that is, the fraction of light passing straight through a sample without interacting with the tissue:

$$T_c = e^{-\mu_t d} \tag{3.3}$$

where T_c is the unscattered transmittance and d is the thickness of the slice of tissue. In practice, measuring the unscattered transmittance is problematic due to the difficulty of separating the unscattered, transmitted light from the scattered light. To separate them, the light is detected far away from the sample and a small aperture is placed in front of the detector.[128,129]

In order to determine the complete set of optical properties (μ_s, μ_a and g), the measurement of the unscattered transmittance can be combined with measurements of total, diffuse reflectance, R_d, and transmittance, T_d, for collimated irradiation. Frequently, an integrating sphere is employed for these measurements. An integrating sphere is a hollow sphere coated on the inside with a both highly and diffusely reflective material, such as barium sulphate. Light entering the sphere will then be uniformly distributed over the entire inner surface of the sphere, where a detector measures light power (W), which is proportional to the total power entering the sphere. Diffuse transmittance is measured by placing a slice of tissue in front of a hole in the sphere and illuminating the slab with collimated light. Illuminating the side of the slice facing the sphere gives the diffuse reflectance. A schematic picture of the measurement set-up used in Paper IV is shown in Fig. 3.3. This method requires that slices of tissue are cut out from the tissue and is therefore an *in vitro* technique.

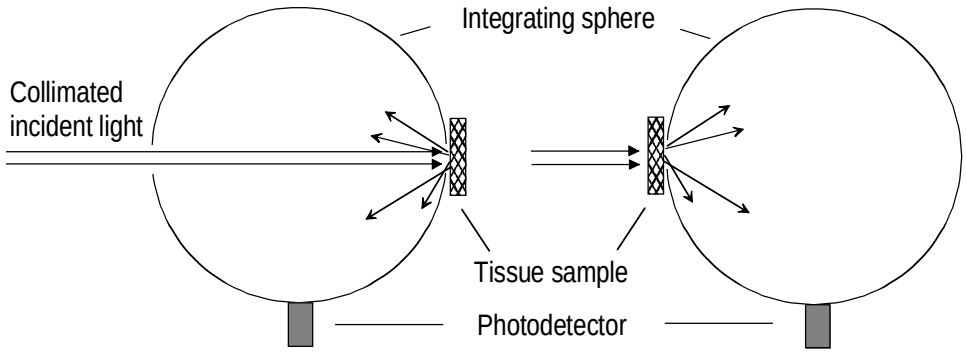

Fig. 3.3. *Experimental set-up for the measurement of diffuse reflectance (left) and transmittance (right) using the integrating sphere.*

With the three parameters, T_c, R_d and T_d, the optical properties can be derived using a mathematical model. One method is to perform Monte Carlo simulations (see below), calculating the reflectance and transmittance for a large set of optical properties. The simulations make up a reference table which is used to extract the optical properties through interpolation. Examples of optical properties derived from measurements using the integrating sphere method are shown in Table 3.1, including values of the effective depth of penetration based on diffusion theory. The effective penetration depth is defined as $\delta_{eff} = 1/\sqrt{(3\mu_a(\mu_a+\mu_s(1-g)))}$. Reported values of optical properties of tissue display significant inconsistencies, as exemplified for rat liver in Table 3.1. The investigations differ concerning tissue preparation (fresh, frozen, thawed), sample size, irradiation source, experimental set-up and theoretical analysis. In addition, instrument calibration has been a problem. Recent work includes calibration measurements on absorbing India ink and scattering latex spheres (Paper IV) or Intralipid.[136]

Table 3.1. *Optical properties of mammalian tissues measured at 1064 nm.*

Tissue	μ_s (mm^{-1})	μ_a (mm^{-1})	g	μ_s' (mm)	δ_{eff} (mm)	Ref.
Liver - rat	7.6	0.06	0.78		1.8	Paper IV
Liver - rat	6.09	0.59	0.92		0.72	130
Liver - rat	15.1	0.2	0.948		1.3	131
Liver - rat	20.8	0.88	0.93		0.40	132
Liver - bovine		0.053		0.176	5.2	133
Liver - bovine	10	0.04	0.90		2.8	134
Liver - porcine	8	0.05	0.97		4.8	134
Liver - human	15	0.03	0.93		3.2	134
Prostate - canine	11	0.04	0.96		4.2	134
Prostate - canine		0.037		0.82	3.2	135
Prostate - human	8	0.03	0.95		5.1	134

An alternative technique to determine the optical properties *in vivo* is to use time-resolved reflectance measurements,[137] which have been used to deduce the reduced scattering coefficient, $\mu_s' = \mu_s(1-g)$, and absorption coefficient by employing the diffusion approximation of the radiative transfer equation. The above properties have also been estimated by means of pulsed photothermal radiometry, which involves the measurement of the blackbody radiation emitted by a sample after the absorption of an optical pulse.[138]

3.2.3 Temperature dependence of optical properties

Heat induces changes in the optical properties of tissue, and these changes have an impact on the temperature distribution during laser irradiation. Perhaps the most striking example is the coagulation of egg white, where the medium changes from clear to completely turbid. In interstitial laser-induced thermotherapy high

temperatures are reached which make the tissue visibly opaque and white around the implanted fibres (Fig. 3.4). A knowledge of these changes and the rate at which they occur is valuable in thermal dosimetry.

Fig. 3.4. *Photograph of porcine muscle coagulated by a cylindrical diffuser.*

Thermally induced changes in the optical properties of tissue have generally been measured on slowly heated, *in vitro* samples using variations of the integrating sphere set-up described above. All studies on heated tissue have reported an increase in reduced scattering coefficient upon heating (Paper IV).[134,139,140,141] This increase is attributed both to an increase in the scattering coefficient and a decrease in the anisotropy factor. Changes of the absorption coefficient measured have been less consistent, where changes ranging from a slight decrease in absorption to an increase by a factor 2.5 have been observed upon heating. The changes in optical properties seem to start at approximately 45°C, to reach a plateau at about 65°C. These changes do not solely depend on the temperature but also on the heating time. Continuous measurement of the heat-induced changes in the optical properties of rat liver has been performed by Pickering *et al*.[142] Their results indicated that the changes in the optical properties constitute a continuous process. The dynamic behaviour of the parameter change can be described by introducing rate parameters in an Arrhenius model.[143,144] In this way dynamic mathematical models have been elaborated, showing the significance of laser-induced changes in the optical properties of tissue for the temperature distribution.[145,146]

Coagulation induces the creation of numerous small granules from the degeneration of fibrillar contractile proteins as well as from the disintegration of mitochondria and myofilaments. The general trend upon heating is thus a change in the number and size of scattering particles. From Mie theory it is known that the anisotropy factor decreases for a spherical scatterer as it decreases in diameter, which is consistent with the experimental findings. Coagulation will thus substantially decrease the penetration depth of light in tissue. Consequently the temperature at the surface of

an irradiated surface, alternatively near an implanted fibre tip, will increase as coagulation is induced.

3.2.4 Monte Carlo modelling

The Monte Carlo method is a common technique of modelling the propagation of light in tissue.[147,148] The technique is founded on the radiative transport equation, and describes the stochastic nature of radiation interactions. A single photon or photon package is launched into the tissue and the photon trajectory is simulated until the photon exits the tissue or is absorbed. The absorption distribution of light can be calculated with any desired accuracy by simulating a large number of photons. The degree of accuracy desired, and thus the required number of photons, depends on the application. A high accuracy can be achieved only by the expenditure of extensive computational effort. When modelling laser-induced thermotherapy, the accuracy needed is relatively low because subsequent heat conduction will smear out minor discontinuities. The time required for the computation of each Monte Carlo simulation then becomes quite reasonable.

The advantage of the model is that any irradiation geometry can be considered. In addition, no restriction on boundary conditions or optical homogeneity of tissue is imposed. However, Monte Carlo modelling of laser-induced thermotherapy is usually performed by considering the tissue as optically homogeneous, because the values generally obtained from measurements of optical properties are average values. Monte Carlo modelling has also been applied to laser Doppler flowmetry (see section 5.2), where a shift in wavelength is incorporated in a certain fraction of interaction events.[149]

In this work the Monte Carlo computer program written by Wang and Jacques[150] was utilised extensively. The original version calculates the photon absorption distribution in cylindrical coordinates resulting from a pencil beam hitting the tissue surface at right angles. Layers with different optical properties can be defined to simulate the light propagation in, for instance, skin.[151] A convolution facility allows the consideration of different beam profiles. The program was modified to calculate the light distribution from implanted plane-cut or cylindrically diffusing fibres. Initially a photon packet of weight W is launched into the tissue in a given direction. The step size before interaction is randomly sampled from the probability distribution for the free path of the photon according to Beer-Lambert's law. The step size is then given by: $s = -\ln(1-\xi)/\mu_t$, where s (m) is the step size, ξ is a random number between 0 and 1, and μ_t (m^{-1}) is the total interaction coefficient. After the photon has been moved the distance s, a fraction of the photon weight is deposited in the local grid element to account for absorption at the interaction site. The amount of deposited photon weight, ΔW, is calculated as $\Delta W = W \times \mu_a/\mu_t$. The weight of the photon packet is then decreased by a corresponding amount. At this stage, the photon packet is scattered. The deflection angle, θ, is sampled from the Henyey-

Greenstein phase function, and the azimuthal angle, ψ, is sampled from a uniform distribution between 0 and 2π, determining the scattering direction.

A further step is sampled and the photon packet is moved in the scattering direction. This procedure is iterated until the photon packet leaves the tissue or until the weight of the photon packet falls below a pre-set threshold value, W_{th}. A technique called roulette is used to terminate the photon when $W < W_{th}$. Based on a random number, the chance for the photon packet of surviving the roulette is $1/m$. If the photon packet survives, the weight of the photon packet is multiplied by a factor m, and the photon packet continues along its trajectory. If the photon packet does not survive the roulette, the photon weight is reduced to zero and the photon is annihilated. Fig. 3.5 shows the simulated trajectories of a few photons in liver tissue.

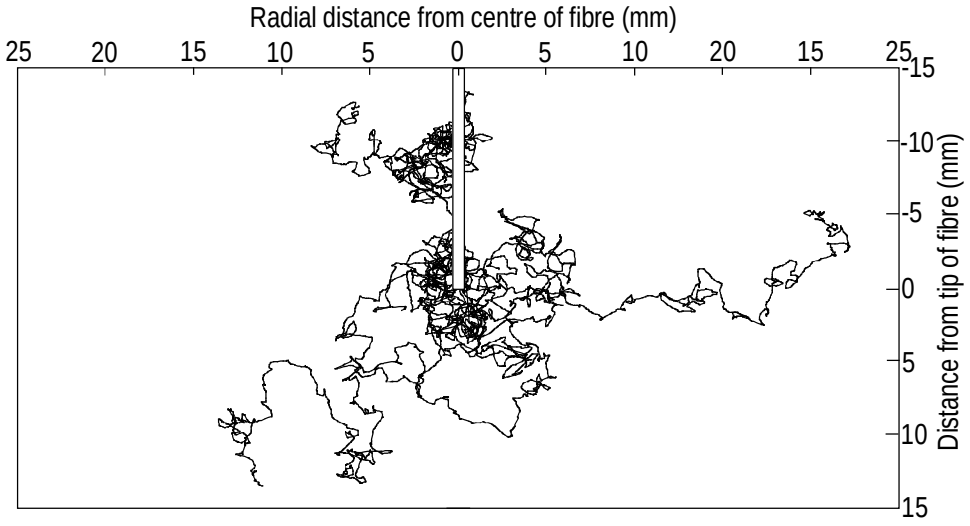

Fig. 3.5. *Trajectories of 7 simulated photons emitted from a plane-cut fibre. The optical properties used were measured at 1064 nm in rat liver (Paper IV).*

3.2.5 Laser applicators

In laser heat treatment, the laser light has to be transported from the laser to the treatment area. The most effective and practical way of transportation for most wavelengths is to use fibre optics. An optical fibre consists of a central core, surrounded by a cladding and a jacket to increase its mechanical strength. For the purpose of laser-induced thermotherapy, multimode optical fibres capable of high-power light throughput are used. They have an overall diameter of approximately 1 mm. Light is transmitted through total internal reflection, requiring the refractive index of the core to be greater than the refractive index of the cladding. Generally, the core is made of silica which has a refractive index close to 1.45. The cladding can be made of soft silicone, hard fluoropolymer or silica, which is doped with

fluorine to reduce its refractive index. The acceptance angle for a fibre is defined as the maximum angle of incidence at the fibre entrance for which the light will be transported by total internal reflection. The acceptance angle, a, depends on the refractive indices of the core, n_1, cladding, n_2, and the surrounding medium, n_0 according to

$$\sin(a) = \frac{1}{n_0}\sqrt{n_1^2 - n_2^2} \tag{3.3}$$

The above expression is called the numerical aperture, characterising the fibre. Eq. 3.3 also defines the divergence angle, which is the maximum angle at which light exits the fibre, where n_0 now is the refractive index of the surrounding medium at the exit.

Light in the fibre can be divided into a number of rays, with different rays having entered the fibre at different angles with respect to the optical axis of the fibre. A fibre permitting propagation of a number of rays is called a multimode fibre. During propagation in a fibre, different rays will be reflected at different positions at the core/cladding interface and will consequently exit a plane-cut fibre at different positions. The intensity distribution at the exit plane will follow the distribution of the refractive index of the core. With a core of uniform refractive index, the spatial distribution at the fibre exit will also be uniform. However, at distances much greater than the fibre diameter the intensity distribution will be Gaussian. The angular distribution of light at the surface of a plane-cut, multimode fibre can be expressed as

$$I(\alpha) = I_0 \exp(-2\alpha^2/a^2) \tag{3.4}$$

where I_0 is the irradiance at the fibre surface on the optical axis, α is the angle to the optical axis and a is the angle of divergence. To generate a uniform distribution for surface irradiation of tissue, a microscope objective (Papers I, IV, VIII), or a micro-lens attached to the fibre tip,[152] can be used. The lens images the fibre end on the tissue surface, yielding a flat field illumination. Reduction of the temperature gradients perpendicularly to the surface during surface irradiation will result in a more homogeneous heating pattern. This can be accomplished with surface cooling. Surface cooling with a forced flow of air[153] or nitrogen gas[154] has been tried, but has proved to be insufficient. Significant reduction of the temperature gradients has been shown to result simply by keeping the surface of the tissue moist (Paper I). The surface temperature decrease is due to evaporation of surface water (see section 4.3). Deep thermal coagulation has been achieved by combining laser irradiation with water cooling.[155] The simultaneous use of cryogen spray and laser heating has been shown to produce subsurface coagulation while avoiding thermal damage to the most superficial tissue, which could be useful in the treatment of haemangiomas.[156]

Interstitial laser-induced thermotherapy (ILT), as first described by Bown *et al.*,[157] utilises optical fibres inserted into the deep-seated target tumour. The first

approaches employed plane-cut fibres. In tissue, the absorption of light and hence the heat production with this fibre is concentrated around the tip. This results in high central temperatures. Using the Nd:YAG laser, vaporisation and carbonisation is produced at power levels exceeding 2-3 W. The charred material absorbs the laser light efficiently.[158] The charred fibre tip then acts as a point heat source, and tissue damage depends only on heat diffusion.[159,160] Using the same irradiation parameters, charring, as compared with no charring, at the fibre tip has been shown to increase the size of the lesion.[161] This effect is more pronounced in lightly pigmented tissues (for example, breast tissue) and for short irradiation times (Paper II). At higher power levels, there is the risk of the laser beam dissecting along the axis of the fibre, creating lesions of unpredictable size. The size of the spherical lesion produced using a single, plane-cut fibre with minimal vaporisation and carbonisation is limited to approximately 1.5 cm in diameter.[162] Because many tumours have a larger diameter they cannot be destroyed by a single treatment.

One way of increasing the size of the lesion is obviously to increase the laser power. The more energy deposited in the tissue, the greater the lesion. As mentioned above, this may result in lesions of unpredictable size, which is the main apparent reason why carbonisation and vaporisation should be kept to a minimum. In addition, the high temperatures associated with carbonisation may cause disintegration of the fibre. The local temperature rise in the tissue in the vicinity of an implanted optical fibre depends mainly on the intensity of the emitted light. By increasing the light-emitting area of the fibre, a higher power can be used, which increases the size of the lesion, while keeping the intensity at the surface of the applicator constant. Increasing the dimensions of the plane-cut fibre is unacceptable for interstitial use; the idea is to be minimally invasive. Therefore, efforts have been made construct fibre-endings which emit light over an extended length.

Diffusing fibres

Artificial sapphire tips emitting diffuse light have been designed in a variety of shapes and sizes.[163] The diffuse illumination pattern is obtained by frosting the tip. Sapphire conducts heat well and has a high melting temperature. The tip is attached to the optical fibre by a metal collar. Light loss at the fibre/tip interface leads to significant heating of the collar (Paper III).[164] Without cooling the sapphire probe acts much like a hot conducting probe due to the heating of the tip.[165] With air cooling, these tips have been associated with fatal air embolism in the treatment of hepatic tumours.[166]

A cone-shaped fibre tip emitting light along its length can be made using mechanical grinding[167] or chemical etching of the core of an optical fibre (Paper II). Because the fibre stripped of its jacket is very fragile, the tip must be protected by a coating. The radiation emitted by these probes is forward-directed. Placed in tissue, these tips act as diffusers because of strong scattering in tissue; the original direction of the light is of little importance. A diffuse illumination pattern and a better mechanical

stability are achieved by covering the tapered tip with a scattering coating (Paper X).[168] Scattering within the probe leads to a greater probability of light absorption, increasing the temperature of the probe. Therefore, the cylindrical diffuser has to be made of heat-resistant material. Examples of materials used for the outer aspect of cylindrical diffusers are glass and Teflon FEP. Teflon withstands temperatures of up to 250°C. With plastic diffusers, care must be taken not to induce carbonisation at the probe/tissue interface, which may result in the destruction of the probe. Glass is heat resistant but there is the risk of breaking the probe, making these probes less suitable for interstitial thermotherapy. A glass covered cylindrical diffuser for experimental use is shown in Fig. 3.6. Simultaneous application of multiple fibres makes possible the coagulation of large volumes.[169]

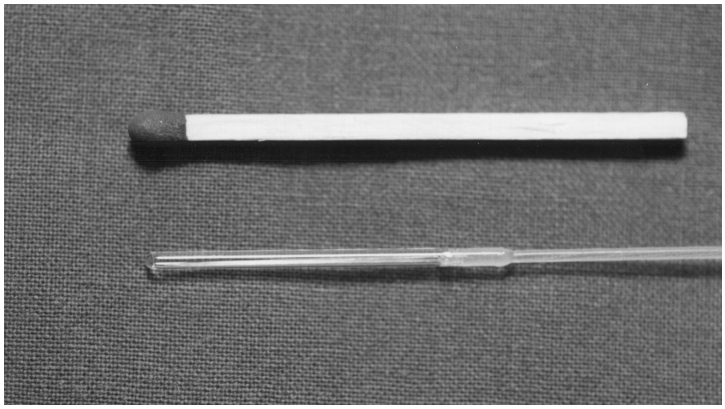

Fig. 3.6. *Photograph of the cylindrical diffuser used in Paper II.*

The volume of necrosis around each fibre can be increased while carbonisation is prevented by cooling the laser applicator during ILT (Papers IX, X). Constant liquid cooling of the fibre tip has been used by Dowlatshahi *et al.*[170] An internally water-cooled probe 2.5 mm in diameter has been constructed by Orth *et al.*[171], permitting insertion into parenchymatous organs such as the liver. Internally water-cooled applicators intended for transluminal use are also being developed (Papers X, XI).[172] In transluminal application the diameter of the probe should be as large as practically possible. A larger probe diameter allows the use of greater powers without increasing the fluence rate at the wall of the probe (Paper IX). The outer surface of a applicator can be increased by incorporating an inflatable balloon around the light-emitting part of the probe. The pressure exerted on the tissue by the balloon is claimed to reduce the blood flow of the tissue,[173] which in turn would reduce the temperature gradients even further. Water cooling results in innocuous temperatures close to the catheter wall, which is considered advantageous in certain applications. Asymmetrical coagulation can be produced by partially shielding the circumference of the applicator from laser irradiation.[174,175] A new fibre tip made of highly reflective material is presented in Paper XI. The probe emits light through an elongated but narrow slit, making possible selective coagulation (Fig. 3.7).

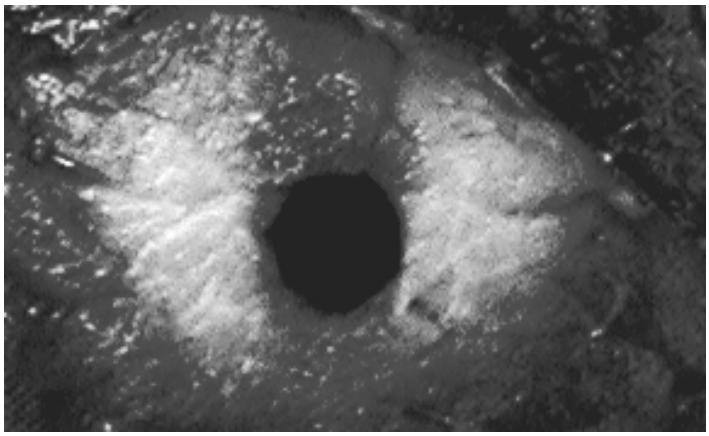

Fig. 3.7. *Contrast-enhanced image of the coagulated area resulting from irradiation in bovine muscle with the new, elongated side-firing probe (Paper XI). During irradiation, the probe was inserted into the hole in the centre of the picture and emitted light in the 3 and 9 o'clock directions.*

4. Heat transfer in tissue

In the context of heat treatment of tissue the four principal modes of heat transfer are conduction, convection, evaporation and radiation.[176] This section briefly describes these different modes.

4.1 Conduction

Thermal conduction is the transfer of energy from the more energetic particles in a substrate to the adjacent, less energetic ones as a result of interactions between the particles. This mode of heat transfer is described by Fourier's law, which states that the heat flow, $\vec{q}$ (W m^{-2}), at a given point in the tissue is proportional to the gradient of the temperature $T(x,y,z,t)$ (K):

$$\vec{q} = -\lambda \nabla T \tag{4.1}$$

where the proportionality constant λ (W m^{-1} K^{-1}) is the thermal conductivity of the tissue. The thermal conductivity depends on the type of tissue and temperature. Since most tissues can be considered as being composed of a combination of water, proteins and fat, the magnitude of the conductivity can be estimated with a knowledge of the proportions of these components. Different relations connecting the mass fractions of the different constituents to the thermophysical properties of tissue have been suggested (see below).

An energy balance for an infinitesimal volume element gives the following relation for transient conduction

$$\rho c \frac{\partial T}{\partial t} = \nabla\left(\lambda \nabla T\right) \tag{4.2}$$

where ρ (kg m^{-3}) is the density and c (J kg^{-1} K^{-1}) is the specific heat capacity. The ratio $\lambda/(\rho c)$ is called the thermal diffusivity, α (m^2 s^{-1}), which describes the dynamic behaviour of the thermal process. As for the thermal conductivity, the values of these properties can be related to the mass fractions of the different constituents making up the tissue:[177,178]

$$\begin{aligned} \lambda &= \rho\times(\lambda_w/\rho_w\times mf_w+\lambda_p/\rho_p\times mf_p+\lambda_f/\rho_f\times mf_f) && \text{(W m}^{-1}\text{ K}^{-1}\text{)} \\ \rho &= 1/(mf_w/\rho_w+mf_p/\rho_p+mf_f/\rho_f) && \text{(m}^3\text{ kg}^{-1}\text{)} \\ c &= c_w\times mf_w+c_w\times mf_p+c_w\times mf_f && \text{(kJ kg}^{-1}\text{ K}^{-1}\text{)} \end{aligned} \tag{4.3}$$

where mf is the mass fraction (dimensionless), and the subscripts w, p, and f signify water, protein and fat, respectively. Cooper and Trezek[177] recommended the following values for the different constants in Eq. 4.3: λ_w=0.628 W m^{-1} K^{-1}, λ_p=0.180 W m^{-1} K^{-1}, λ_f=0.188 W m^{-1} K^{-1}, ρ_w=1.00×10^3 kg m^{-3}, ρ_p=1.54×10^3 kg m^{-3}, ρ_f=0.815×10^3 kg m^{-3}, c_w=4.2 kJ kg^{-1} K^{-1}, c_p=1.09 kJ kg^{-1} K^{-1}and c_f=2.3 kJ kg^{-1} K^{-1}.

One suggested relationship between the thermophysical properties of tissue and the mass fraction of water, which is easily measured by determining the weight of tissue samples before and after drying, is given by[179,180]

$$\begin{aligned} \lambda &= (0.557 + 5.69\ mf_w) \times 10^{-1} && (W\ m^{-1}\ K^{-1}) \\ \rho &= (1.3 - 0.3\ mf_w) \times 10^{3} && (kg\ m^{-3}) \\ c &= 1.55 + 2.64\ mf_w && (kJ\ kg^{-1}\ K^{-1}) \end{aligned} \qquad (4.4)$$

The thermal properties of tissue change with temperature. Valvano[181] measured the temperature dependence of thermal properties in various tissues from 3-45°C. A linear relationship between thermal conductivity/diffusivity and temperature was found. The temperature dependence of the thermophysical properties of water, protein, fat and a number of other constituents has been measured by Choi and Oko,[178] where each solid component was in the form of aqueous suspensions of varying concentrations. For solid components the density was found to decrease linearly with increasing temperature. The behaviour of the thermal conductivity and specific heat was better described by a quadratic model of the type

$$\Theta = a_1 + a_2 T + a_3 T^2 \qquad (4.5)$$

where Θ indicates a thermal property, a_1, a_2 and a_3 are constants depending on the component and T is the temperature in °C. Values of the constants for density, conductivity and specific heat are shown in Table 4.1.

Table 4.1. *Temperature dependence of thermal properties (From Ref. (178))*

Thermal property	Component	a_1	$a_2 \times 10^3$	$a_3 \times 10^6$
	Water	0.57109	1.7625	-6.7036
Conductivity	Protein	0.17881	1.1958	-2.7178
($W\ m^{-1}\ K^{-1}$)	Fat	0.18071	-0.27604	-0.17749
	Water	997.18	3.1439	-3757.4
Density	Protein	1329.9	-518.4	
($kg\ m^{-3}$)	Fat	925.59	-417.57	
	Water	4.1762	-0.090864	5.4731
Specific heat	Protein	2.0082	1.2089	-1.3129
($kJ\ kg^{-1}\ K^{-1}$)	Fat	1.9842	1.4733	-4.8008

Using the above values the thermophysical properties of water, protein and fat can be calculated at different temperatures. The thermal property of a biological material is then given by Eq. 4.3. At 37°C the above relations give: λ_{water}=0.627 W m^{-1} K^{-1}, $\lambda_{protein}$=0.219 W m^{-1} K^{-1}, λ_{fat}=0.170 W m^{-1} K^{-1}, ρ_{water}=0.992×10^3 kg m^{-3}, $\rho_{protein}$=1.310×10^3 kg m^{-3}, ρ_{fat}=0.910×10^3 kg m^{-3}, c_{water}=4.18 kJ kg^{-1} K^{-1}, $c_{protein}$=2.05 kJ kg^{-1} K^{-1} and c_{fat}=2.03 kJ kg^{-1} K^{-1}. With the exception of the heat capacity of protein, the above values are similar to the values given by Cooper and Trezak.[177]

Fig. 4.1 shows the thermal conductivity and diffusivity as a function of temperature for water and a tissue with mass fractions of water, protein and fat equal to 0.70, 0.20 and 0.10, respectively, as modelled according to Eqs. 4.3 and 4.5. As depicted in the figure, the temperature dependence of the thermophysical properties of soft tissue with a high water content is close to the temperature dependence of the thermophysical properties of water.

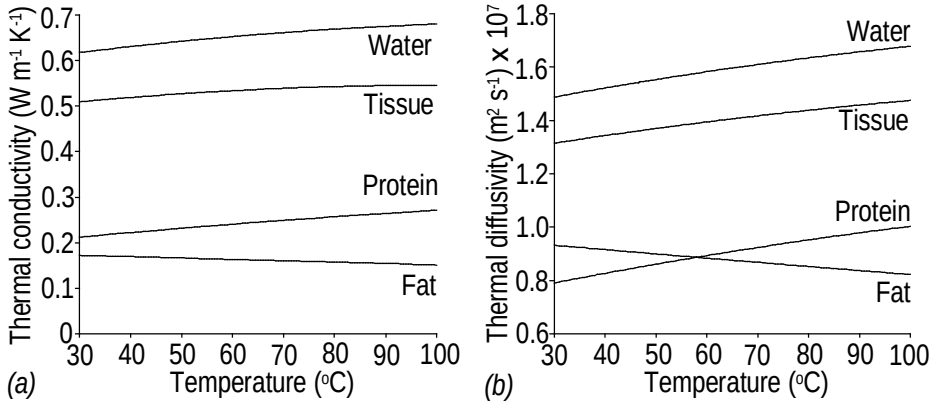

Fig. 4.1. *Temperature dependence of (a) thermal conductivity and (b) diffusivity for tissue constituents and typical soft tissue with a mass fraction of water of 70 %.*

Table 4.2 shows selected data on the thermophysical properties of tissue measured at room or body temperature. It can be observed that water has the highest values of thermal conductivity and diffusivity of the components constituting tissue. Therefore, tissues with a high water content are the best thermal conductors and respond fastest to a thermal disturbance. The dependence on temperature of the thermophysical properties of tissue has been incorporated into models of laser-induced heat treatment.[184] However, in treatment planning exact values of thermal properties at body temperature are difficult to conclude beforehand. Previously measured values of thermal properties, even on the same type of tissue, vary

Table 4.2. *Thermophysical properties of human tissue and water (Adapted from Refs. (182, 183))*

Material	Conductivity ($W\ m^{-1}\ K^{-1}$)	Density ($kg\ m^{-3}$)$\times 10^{-3}$	Specific heat ($kJ\ kg^{-1}\ K^{-1}$)	Diffusivity ($m^2\ s^{-1}$) $\times 10^{7}$
Muscle	0.38-0.54	1.01-1.05	3.6-3.8	0.90-1.5
Fat	0.19-0.20	0.85-0.94	2.2-2.4	0.96
Kidney	0.54	1.05	3.9	1.3
Heart	0.59	1.06	3.7	1.4
Liver	0.57	1.05	3.6	1.5
Brain	0.16-0.57	1.04-1.05	3.6-3.7	0.44-1.4
Water @ 37°C	0.63	0.99	4.2	1.5

significantly, so the error made by disregarding the temperature dependence may well be smaller than the error made by having inexact starting values.
The thermal diffusivity of tissue can be measured *in vivo* with the pulse-decay method.[185] This method utilises a small thermistor inserted into the tissue, which is first heated for a short period of time, inducing a temperature rise in the surrounding tissue. Subsequently, the thermistor is used to measure the temperature decay, which can be related to the thermal diffusivity. Thermal conductivity has been estimated by measuring the temperature of the thermistor when applying a constant power to it.[181] This value includes the intrinsic conductivity of tissue as well as the conduction-like contribution of perfusion (see section 4.5). The specific heat of tissue can be measured *in vitro* using a differential scanning calorimeter.[186] The tissue density is determined by weight and volume measurements of specimens of excised tissue.

4.2 Convection

Convection is the term applied to the heat transfer between a surface and a fluid, such as air or blood, moving over the surface. In the procedure of modelling heat treatment the most common convection problem encountered involves heat transfer between the surface of the body and the surrounding air, a problem which is treated in this section. Inside the tissue, convection occurs between blood and the vessel wall. The modelling of blood perfusion is covered in section 4.5. The heat transfer between a conducting solid, which in this context is tissue, and a convecting fluid is usually described using Newton's law of cooling, which states that the heat flow q (W m^{-2}) normal to the surface is proportional to the temperature difference between the surface T_s (K) of the tissue and the bulk temperature of the fluid T_∞:

$$q = h\,(T_s - T_\infty) \tag{4.6}$$

where the proportionality constant, h (W m^{-2} K^{-1}), is the coefficient of local heat convection. As shown in Fig. 4.2, there exists a thermal boundary layer if the temperature of the fluid free stream and the temperature of the tissue differ. The thickness of the boundary layer, δ, is usually defined as the distance from the surface for which the ratio $[(T_s - T)/(T_s - T_\infty)] = 0.99$.

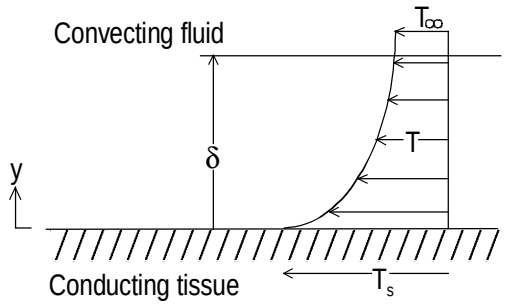

Fig. 4.2. *Schematic picture of the thermal boundary layer.*

At the tissue surface there is no fluid motion and energy transfer occurs only by conduction. Therefore, the heat flow at the surface is obtained by applying Fourier's law to the fluid at the surface (y = 0). That is,

$$q = -\lambda_f \left.\frac{\partial T}{\partial y}\right|_{y=0} \tag{4.7}$$

where λ_f is the thermal conductivity of the fluid. By combining Eq. 4.7 with Eq. 4.6 the expression of the heat convection coefficient becomes

$$h = \frac{-\lambda_f \left.\partial T/\partial y\right|_{y=0}}{T_s - T_\infty} \tag{4.8}$$

The temperature gradient at the surface is strongly dependent on the conditions in the boundary layer. Equations can be set up to account for the physical processes in this region. The solutions of these equations determine the heat convection coefficient. However, these solutions becomes very complex. Therefore, the convection coefficient is frequently calculated from empirical relations called correlations. These correlations, normally expressed in terms of dimensionless parameters or numbers, provide the most useful information in convective heat transfer as applied to thermotherapy.

Free convection

Consider a heated tissue surface in contact with air. If no external influences are applied to the fluid motion, such as using a fan, the resulting fluid motion is due to density gradients created by temperature differences in the fluid. The heat transfer by convection is then called free convection. In this case the free convection currents are due to buoyancy forces. To describe the heat transfer process due to free convection, the dimensionless Nusselt number, *Nu*, is used, which is defined by the following relation[176]

$$Nu = hL/\lambda_f \tag{4.9}$$

where h is the heat convection coefficient, L (m) is a characteristic length and λ_f is the conductivity of the fluid. The Nusselt number equals the dimensionless temperature gradient at the surface. Physically, the Nusselt number can be interpreted as the ratio of the conductive resistance of the fluid boundary layer to its convective resistance, or, as the ratio between the convective heat transfer in the boundary layer to its conductive heat transfer. Dimensional analysis of the basic momentum and energy balance equations shows that the Nusselt number is a function of two dimensionless parameters, namely the Grashof number (*Gr*) and the Prandtl number (*Pr*). The Grashof number expresses the ratio between the buoyant forces of the fluid to the viscous forces:[182]

$$Gr = g_{loc}\beta(T_s - T_\infty)L^3/\nu^2 \tag{4.10}$$

where g_{loc} (m s^{-2}) is the local acceleration due to gravity, β (K^{-1}) is the volume coefficient of expansion of the fluid, which for a perfect gas is equal to T^{-1}, and ν (m^2 s^{-1}) is the kinematic viscosity.

The Prandtl number gives the ratio between two transport coefficients: the kinematic viscosity for momentum transport and the thermal diffusivity for energy transport, that is, $Pr = \nu/\alpha$. Free convection from isothermal surfaces is usually described by correlations of the form

$$Nu = C\,(Gr\,Pr)^p \tag{4.11}$$

where the constants C and p are determined by fitting to experimental data. For laminar, free convection flow a p-value of 0.25 is recommended.[182] The free convection flow is considered laminar for Grashof numbers less than 1×10^9. The constant C is dependent on surface geometry. Values of C for different geometries for laminar flow are shown in Table 4.3.

Table 4.3. *Constants in free convection (Adapted from Ref. (182))*

Geometry	C	Characteristic length, L
Vertical planes	0.59	vertical length
Horizontal cylinders	0.53	diameter
Horizontal plates, heated surface up	0.54	average of plate sides
Spheres, short cylinders and blocks	0.60	$1/L=1/L_v+1/L_h$, where L_v and L_h are the vertical and horizontal dimensions, respectively.

4.3 Evaporation

The heat loss from moist tissue in contact with air will be dominated by the heat loss associated with the evaporation of water. The driving force for the loss of tissue moisture by diffusion is the difference in water concentration between the tissue and the surrounding air. For ideal gas mixtures, such as air and water vapour, the concentration of a component is proportional to its partial pressure. The water at the tissue surface is in thermodynamic equilibrium with the water vapour in air, that is, at the surface the pressure of the water vapour is equal to the pressure of saturated water vapour at the temperature of the surface. Therefore, water will migrate from the tissue surface to the air if the saturated vapour pressure at the surface is greater than the partial pressure of vapour in the surrounding air. The rate of water loss, m_w (kg m^{-2} s^{-1}) can then be described by the following expression:

$$m_w = h_m(p_{w,s}-p_{w,\infty})/R_wT_f \tag{4.12}$$

where h_m (m s^{-1}) is the convection coefficient of mass transfer, $p_{w,s}$ (N m^{-2}) is the saturated vapour pressure at the surface temperature, $p_{w,\infty}$ (N m^{-2}) is the partial

pressure of vapour in the surrounding air, R_w (J kg^{-1} K^{-1}) indicates the gas constant for water and T_f (K) is the temperature of the surface film, which is equal to $(T_s+T_\infty)/2$.

The convection heat and mass transfer are governed by dimensionless equations of the same form.[176] The two processes are therefore said to be analogous, which implies that between heat and mass transfer the relations for a particular geometry are interchangeable. By using the concept of a concentration boundary layer in analogy to the thermal boundary layer, the dimensionless concentration gradient at the surface is described by the Sherwood number (*Sh*):

$$Sh = h_m L/D_{AB} \tag{4.13}$$

where L (m) is a characteristic length and D_{AB} (m^2 s^{-1}) is the binary diffusion coefficient of, in this case, water vapour in air. The Sherwood parameter is to the concentration boundary layer what the Nusselt number is to the thermal boundary layer. The mass transfer analogous to the Prandtl number is the dimensionless Schmidt number (*Sc*) which is equal to ν/D_{AB}. Using the heat and mass transfer analogy leads to the following relation

$$Nu/Pr^p = Sh/Sc^p \tag{4.14}$$

where p is the exponent in Eq. 4.11. The equation above gives the relation between the heat and mass transfer convection coefficients as

$$h/h_m = \rho c Le^{1-p} \tag{4.15}$$

where ρ (kg m^{-3}) is the air density, c (J kg^{-1} K^{-1}) is the heat capacity of air and *Le* (dimensionless) is the Lewis number. The Lewis number is defined as $Le = Sc/Pr$, and is an approximate measure of the relative thickness of the thermal and concentration boundary layers. Eq. 4.15 connects the heat and mass transfer convection coefficients, the former being expressed using Eq. 4.11.

The energy associated with the phase change occurring during evaporation is the latent heat of vaporisation, h_{fg} (J kg^{-1}). The heat flow from the surface due to evaporation, q (W m^{-2}) is then equal to

$$q = m_{ev} h_{fg} \tag{4.16}$$

The above equations are valid when the surface is covered with a continuous layer of water and evaporation takes place mainly at the surface. Experimental verification of the mathematical expressions describing the thermal influence of surface evaporation has been made for laser-irradiated tissues (Paper I).[187] If the drying process by evaporation is intense enough the fraction of wet area will eventually decrease with decreasing surface moisture, leading to a decrease in the mass transfer coefficient. The process leading to the change in mass transfer is complex and depends on the transfer of internal moisture.[188,189] The modelling of this

drying process is of particular interest to the food industry and is beyond the scope of the present thesis.

4.4 Radiation

All objects emit electromagnetic radiation. The rate at which a surface at a certain temperature emits radiant energy per unit surface area and unit wavelength is termed monochromatic emissive power. Generally, the emissive power is a complex function depending on surface temperature, surface type, condition of the surface, and the wavelength of the radiation. For an ideal black body the electromagnetic radiation emitted, W (W m^{-3}), as a function of absolute temperature and wavelength is described by Planck's law:

$$W(\lambda,T)=\frac{2\pi hc^2}{\lambda^5}\frac{1}{e^{hc/\lambda kT}-1} \tag{4.17}$$

A black body is a theoretically-ideal "black" surface which emits and absorbs all incident radiation at all wavelengths. Fig. 4.3 shows the distribution of emitted thermal energy at two different temperatures. With increasing temperature, the curves shift towards shorter wavelengths. The higher the temperature the shorter the wavelength at which the maximum occurs.

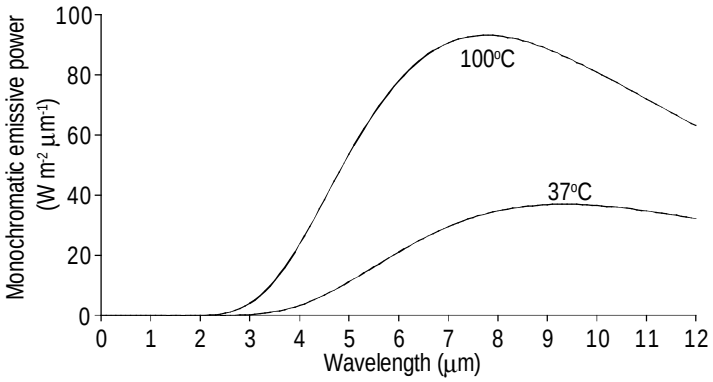

Fig. 4.3. *Emissive power of a black body as a function of wavelength for two different temperatures.*

For an ideal black body the electromagnetic radiation emitted is proportional to the fourth power of the absolute temperature, given by integrating Eq 4.17. The maximum heat flow, q (W m^{-2}) emitted from a black body is expressed by:

$$q=\sigma T^4 \tag{4.18}$$

where σ (W m^{-2} K^{-4}) is the Stefan-Boltzmann constant. A non-black body, such as tissue, emits radiation at a lower rate than a black body at the same temperature. Tissue is not a perfect black body. To describe the fraction of radiation emitted by a non-black body in relation to a black body, the dimensionless parameter called

emissivity, ε, is used. The rate of energy emission per unit surface area then becomes

$$q = \varepsilon\sigma T^4 \tag{4.19}$$

Because the emissivity depends on wavelength and the direction of the radiation relative to the radiant surface, the most frequently used value of the emissivity is the total hemispherical emissivity, which has been averaged over all wavelengths and directions. For human skin, the value of the emissivity is in the range 0.98-0.99.[190]

A tissue surface not only emits radiation but also absorbs infrared radiation from the environment. The fraction of incident radiation which is absorbed is denoted absorptivity. At thermal equilibrium, the absorptivity and emissivity are equal. Considering the absorptivity and emissivity to be equal, the radiant heat transfer between a small body in a large enclosure, such as the human body in a room, can be described by

$$q = \varepsilon\sigma(T_s^4 - T_\infty^4) \tag{4.20}$$

where T_s and T_∞ (K) are the temperature of the surface and of the environment, respectively. When comparing the heat transfer mediated by free convection, surface evaporation and radiation, it is found that evaporation is by far the most significant mechanism of heat transfer, even at moderate temperature elevations, as illustrated in Fig. 4.4.

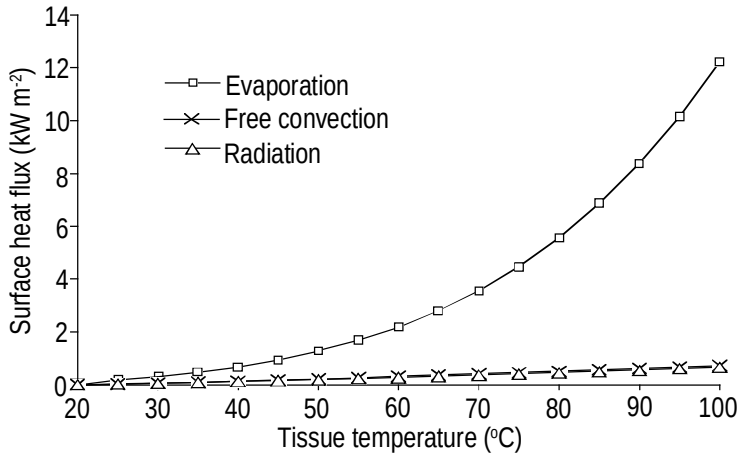

Fig. 4.4. *Surface heat flux as a function of temperature for a 4×4×4 cm tissue block heated at an ambient temperature of 20°C.*

4.5 Heat transfer by blood perfusion

The most difficult problem in calculating heat transfer in tissue is the modelling of the effect of blood perfusion. The thermal influence of perfusion depends on the vessel geometry, the blood flow rate through it and the thermophysical properties of

blood and the surrounding tissue. Also, adjacent blood vessels will influence each other thermally. Many attempts have been made to make a thermal model of blood perfusion. In this section, a number of models are presented. For a more extensive review, see Ref. (191).

Blood flow in a single vessel

As in the case of free convection, the convective heat transfer between a moving fluid in a circular duct and the duct wall is described by the Nusselt number (Eq. 4.9), where the characteristic length L is the duct, or vessel, diameter. The Nusselt number depends on whether the flow is laminar or turbulent. To characterise the degree of laminarity the dimensionless Reynolds number (Re) is used

$$Re = v_f D/\nu \tag{4.21}$$

where v_f (m s^{-1}) is the average fluid velocity, D (m) is the duct diameter and ν (m^2 s^{-1}) is the kinematic viscosity of the fluid. The Reynolds number expresses the ratio between the inertial and viscous forces in the fluid. Conventionally, the flow is considered laminar at a Reynolds number < 2300. The Nusselt number depends primarily on the dimensionless parameters Re, Pr and D/L, where Pr is the Prandtl number and L (m) is the duct length. For constant surface temperature and a fully developed velocity profile at the entrance, Victor and Shaw[192] proposed the following correlation for the average Nusselt number based on a non-Newtonian model for the convective heat transfer between flowing blood and the vessel wall:

$$Nu = 4 + 0.155\, Gz^{0.6862} \text{ for } Gz < 1000 \tag{4.22}$$

where Gz (dimensionless) is the Graetz number, which is equal to

$$Gz = (D/L)RePr \tag{4.23}$$

The equation describing the blood temperature T_b (K) in a vessel with constant wall temperature T_t (K) becomes

$$\rho_b c_b V_b \frac{dT_b}{dx} = -\pi\lambda_b Nu \left(T_b - T_t\right) \tag{4.24}$$

where ρ_b (kg m^{-3}) and c_b (J kg^{-1} K^{-1}) are the density and specific heat of blood, respectively, V_b (m^3 s^{-1}) is the blood flow rate and λ_b (W m^{-1} K^{-1}) is the thermal conductivity of blood. By inserting Eq. 4.22 in Eq. 4.24 and integrating over the length of the vessel, a parameter called heat transfer effectiveness, ε_b, can be determined.[190] This parameter is a measure of the heat exchange capacity of the vessel and is described by

$$\varepsilon_b = 1-(T_{be}-T_t)/(T_{bi}-T_t) \tag{4.25}$$

where T_{bi} (K) is the temperature of the incoming blood, T_{be} (K) is the temperature of the outgoing blood. Table 4.4 shows the value of the heat transfer effectiveness calculated for different blood vessels in a dog. The heat transfer effectiveness as

presented in Table 4.4 falls into three categories. For the largest vessels $\varepsilon_b \approx 0$, which implies that they have very little heat exchange with the surrounding tissue. The smallest blood vessels with a heat transfer effectiveness close to 1.0 behave like

Table 4.4. *Measured and estimated properties of blood vessels in a dog. (Adapted from Ref. (190))*

Blood vessel	Diameter (mm)	Length (mm)	Blood velocity (mm/s)	Reynolds number	Graetz number	Heat transfer effectiveness
Aorta	10	400	500	1667	1042	0.08
Large arteries	3	200	130	130	48.7	0.40
Main arterial branches	1	100	80	27	6.75	0.93
Terminal branches	0.6	10	60	12	18	0.68
Arterioles	2×10^{-2}	2	3	2×10^{-2}	5×10^{-3}	1.0
Capillaries	8×10^{-3}	1	0.7	1.9×10^{-3}	3.8×10^{-4}	1.0
Venules	3×10^{-2}	2	0.7	7×10^{-3}	2.6×10^{-3}	1.0
Terminal veins	1.5	10	13	6.5	24.4	0.59
Main venous branches	2.4	100	15	12	7.2	0.92
Large veins	6	200	36	72	54	0.38
Vena cava	12.5	400	330	1375	1074	0.08

ideal heat exchangers with the blood leaving at tissue temperature. Blood leaving the intermediate vessels ($0.38<\varepsilon_b<0.92$) can be at a significantly different temperature than the tissue itself. Therefore, it may be necessary to account for this when modelling heat treatment of tissue. Chen and Holmes[193] came to the conclusion that the primary heat transfer would occur in the small arteries.

The heat sink model

Pennes[194] introduced the conventional bioheat transfer equation with a term for a heat sink to describe the thermal influence of perfusion. The model assumes that the heat exchange between the blood vessels and the surrounding tissue occurs only at the level of the capillaries, where the blood velocity is very low. Based on the terminology above, this implies that the heat transfer effectiveness for the capillaries should be equal to unity, whereas the effectiveness for the other vessels should be equal to zero. Blood at an arterial temperature T_a (K) enters the capillary bed, where it equilibrates instantaneously with the surrounding tissue. Thus, the blood exits the capillary bed and enters the venous circulation at the local tissue temperature T (K). In a homogeneous medium the heat balance becomes

$$\rho c \frac{\partial T}{\partial t} = \nabla \cdot (\lambda \nabla T) - \omega_b \rho_b c_b \rho (T - T_a) + Q_s + Q_m \qquad (4.26)$$

where ρ (kg m^{-3}) and c (J kg^{-1} K^{-1}) are the density and the specific heat capacity of tissue, respectively, and λ (W m^{-1} K^{-1}) is the heat conductivity of tissue. The second term on the right represents the perfusion heat sink, where ω_b (m^3 kg^{-1} s^{-1}) is the volumetric perfusion rate and c_b (J kg^{-1} K^{-1}) is the specific heat of blood. Q_s (W m^{-3}) is the volumetric external source term, which in the present context represents laser light absorption. Q_m (W m^{-3}) is the volumetric heat production due to metabolism

(see section 4.6). The local arterial temperature, T_a, is usually assumed to be equal to the temperature of the body core.

The basic assumption in the heat sink model is that the arterial blood instantly reaches thermal equilibrium with the surrounding tissue in the capillaries and that all other vessels are thermally insignificant. However, general agreement now exists that the thermal equilibration process takes place in the precapillary vessels (see Table 4.4). The heat sink model would then describe the thermal equilibration process in these vessels instead of in the capillaries. Despite this weakness the model has proved to give useful approximations of the general temperature distribution during hyperthermia.[195] The model has been used extensively in the modelling of heat treatment due to its mathematical simplicity and because the perfusion rate parameter is readily measurable (see section 5.2).

The Chen and Holmes model

In this model the vessels are grouped into two categories: large vessels that are treated separately and small vessels that are considered as a continuum also including the tissue. The first category applies up to the point in the vascular tree where the heat transfer effectiveness approaches unity. Heat transfer between the smaller vessels and the tissue was considered to proceed by three different modes. The heat equation for the continuum, including three perfusion terms representing the different modes was proposed as[193]

$$\rho c \frac{\partial T}{\partial t} = \nabla \cdot (\lambda \nabla T) - \omega_b^* \rho_b c_b \rho \left(T - T_a^* \right) - \rho_b c_b \bar{u} \cdot \nabla T + \nabla \cdot (\lambda_p \nabla T) + Q_s + Q_m \quad (4.27)$$

The second term on the right in the above equation reflects the equilibration of blood, initially in a large vessel, to tissue temperature. This process is described by a heat sink term similar to the perfusion term in the heat sink model, where the quantities with an asterisk for the blood perfusion and arterial temperature refer to a specific vessel size. The third term on the right in Eq. 4.27 pertains to the contribution of convection due to thermally equilibrated small vessels, where $\bar{u}$ (m s^{-1}) represents the net velocity vector of blood. In tissue, arteries and veins frequently occur in counter-current vessel pairs, with blood flowing in opposite directions. This implies that the net velocity vector is small, which virtually cancels the effect of the third term. The fourth term on the right describes the thermal contribution of the small temperature fluctuations of nearly equilibrated blood along the temperature gradient of the tissue. This mode of heat transfer depends on the microvascular structure and is described by a perfusion conductivity, λ_p (W m^{-1} K^{-1}). The application of the model requires some knowledge of the local vascular geometry, which makes it more difficult to use than the heat sink model.

The Weinbaum and Jiji model

The model configuration consists of tissue surrounding a pair of thermally significant blood vessels directly connected by capillaries. Anatomical studies by

Weinbaum *et al.*[196] led to the conclusion that the main heat transfer contribution of local blood perfusion is associated with an incomplete counter-current heat exchange mechanism between pairs of arteries and veins. In this model it is assumed that the mean tissue temperature can be approximated by an average temperature of the adjacent counter-current pair of closely spaced and nearly equilibrated vessels. The resulting heat equation becomes[197]

$$\rho c \frac{\partial T}{\partial t} = \nabla \cdot (\lambda \nabla T) + \nabla \cdot (\lambda_{p'} \nabla T) + Q_s + Q_m \qquad (4.28)$$

where the heat transfer gives rise to a perfusion conductivity tensor $\lambda_{p'}$, which represents both the capillary bleed-off and the heat exchange between tissue and adjacent vessels. The perfusion conductivity in Eq. 4.27 and the perfusion conductivity in Eq. 4.28 look alike. However, the physical basis for them are quite different. The former refers to the thermal equilibration of a single vessel, whereas the latter describes the combined effect of small vessel bleed-off from counter-current pairs and convective heat transfer. If the assumption of isotropy is valid, the conductivity tensor will reduce to a simple scalar parameter. Added to the intrinsic tissue conductivity, this scalar constitutes the effective conductivity, which is a measurable quantity.[198] Because of mathematical simplicity, the heat sink model together with the Weinbaum and Jiji model assuming isotropy of flow have been the most frequently used models for blood perfusion in simulations of hyperthermic treatments.

4.6 Metabolic heat generation

The most widely used approach to estimate metabolic heat production, Q_m in the above equations, has been to set this term equal to the oxygen consumption multiplied by the caloric value of oxygen. The oxygen consumption of tumours has been shown to increase linearly with perfusion rate. The following relationship between the metabolic heat generation of tumour tissue and the local blood supply has been proposed[199]

$$Q_m = (2.83\ \omega - 0.22) \times 10^3 \quad (\mathrm{W\ m^{-3}}) \qquad (4.29)$$

where ω ($\mathrm{dm^3\ 100g^{-1}\ h^{-1}}$) is the tumour perfusion rate.

Metabolism, as any other chemical reaction, is accelerated with increasing temperature as long as the higher temperature does not lead to the inhibition of the metabolic process by, for example, the denaturation of enzymes. The temperature dependence can be written as[182]

$$Q_m = Q_{m0} \times 1.1^{\Delta T} \qquad (4.30)$$

where Q_{m0} ($\mathrm{W\ m^{-3}}$) is the basal metabolic heat production rate and ΔT is the temperature increase. The basal metabolic heat production rate is highly variable, ranging from approximately 5 $\mathrm{W\ m^{-3}}$ for subcutaneous fat to 50 $\mathrm{kW\ m^{-3}}$ for working

muscle.[182] Compared with the heating rate when using a laser for heat treatment, the metabolic heat production can be neglected.[200]

5. Monitoring of heat treatment

Laser-induced heat treatment is ideally performed during real-time, non-invasive monitoring of the developing thermal damage. This can help to confine the thermal lesion to the target tissue and prevent unwanted heating of the surrounding, healthy tissue by allowing intra-operative modification laser energy delivery. However, tissue response to heat treatment is delayed, which makes it difficult to identify immediate markers predictive of the final damage. At present, temperature seems to be the best indicator of the resulting tissue damage. The tissue temperature has most frequently been measured using invasive probes, but techniques for non-invasive temperature monitoring are being developed. Measurements of physiological parameters such as perfusion alterations and increased metabolic response to an elevated temperature is potentially achievable for monitoring of the treatment. This section reviews some techniques used for the measurement of temperature and blood perfusion.

5.1 Temperature measurements

Thermistors

The thermistor is an example of an invasive temperature probe. Invasive measurement is currently the most common method for temperature monitoring during heat treatment. Multiple probes are needed if the temperature distribution is to be mapped. Temperature control using the information from the probes has in most cases consisted of the use of a single feedback temperature sensor, which limits the maximum and minimum tissue temperature.[201,202,203] One problem with this control scheme is that the measurement point is somewhat arbitrary and generally its temperature cannot be assumed to be representative of temperatures in other parts of the treatment field.

With a thermistor the temperature-dependent parameter is the resistance of a semiconductor material. The resistance depends inversely on the number of charge carriers that are mobile under the influence of an applied electric potential. In a semiconductor the number of charge carriers is strongly dependent on temperature. The number is proportional to $e^{-Eg/(kTa)}$, where E_g is the energy band gap, k is the Boltzmann constant and T_a is the absolute temperature. A typical change in the resistance is 4% per degree Celsius.[204] Thermistor sensors are usually made of oxides of various metals such as nickel, iron and manganese. One disadvantage of the thermistor is the lack of intrinsic calibration. Three or more calibration points are needed to characterise the response curve of the thermistor. A mathematical expression of the relationship between thermistor resistance and temperature is given by the following expression[205]

$$T^{-1}=b_0+b_1\ln R+b_2\,(\ln R)^3 \qquad (5.1)$$

where T (K) is the temperature, b_o, b_1 and b_2 are constants and R (Ohm) is the thermistor resistance. Three calibration points are usually provided by the manufacturer, making it possible to determine the coefficients above. Once calibrated, thermistors show good long term calibration stability.

In order to measure the resistance of the thermistor, it must be part of a circuit. For this purpose, a four lead arrangement can be used (Fig. 5.1). This arrangement was used for thermistor resistance determination in Papers I, IV, V, IX. The current through the thermistor should be kept low to prevent Joule heating. The large lead resistances are important when measuring in microwave-heated areas. They keep the currents induced by the microwaves small, which minimises selective heating of the probe. The equipment for voltage measurement consisted in our case of an A/D converter connected to a computer. The A/D converter translated the voltage over the thermistor to an integer value between 0-4095. The computerised thermometry system developed also includes an optical shutter, which is controlled by one or more thermistors. The thermometry system can be programmed to intermittently switch off the laser whenever a pre-set maximum temperature is reached.

The response time of a thermistor is on the order 0.1 s, permitting detection of

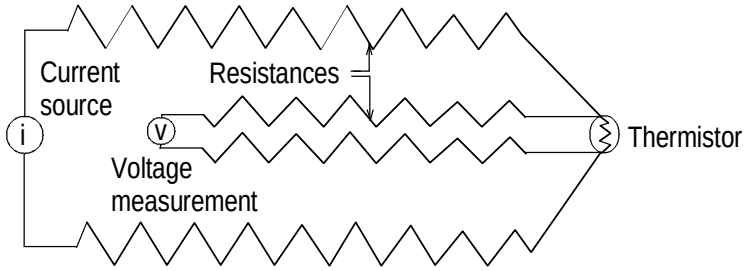

Fig. 5.1. *Schematic picture of the four lead arrangement for thermistor resistance determination.*

sudden temperature fluctuations. When measuring the temperature close to the source of laser radiation, care must be taken that the temperature recording is not influenced by direct absorption of laser light by the thermistor.[206] To avoid most of this problem, the laser can be switched off for a short period before the temperature is read. The temperature recording will then be more accurate due to the longer response time of tissue compared with the thermistor. In conclusion, the advantages of thermistor-based thermometry are high resolution and accuracy, good stability, small size and cost-effective technology.

A new method of estimating the tissue temperature during laser-induced thermotherapy is proposed in Paper IX. Information about the temperature of the tissue immediately surrounding the applicator can be obtained by measuring the temperature increase of the water flowing in a cooled applicator. Using a mathematical model, the maximum tissue temperature can also be estimated from the water temperature measurements. Cooling of the catheter forces the location of

the maximum tissue temperature a few millimetres into the tissue. *In vitro*, the method has been shown to be very accurate (Paper X). Orth *et al.*[171] have developed a similar method for temperature estimations. Experimentally, they found a linear relationship between the temperature rise of the water flowing in the laser probe and the tissue temperature. Measuring the temperature at the tissue-applicator interface is difficult using invasive probes, partly because of direct light absorption by the probe. To minimise light absorption by the implanted temperature probes, gold-coated thermocouples have been used.[175]

Water-cooled catheters are also employed in transurethral microwave thermotherapy of benign prostatic hyperplasia (see section 6.2). The temperature measured at the surface of the catheter wall has been used to control the treatment.[207] The urethral temperature has been shown to follow the intraprostatic temperature during treatment.[208] However, the treatment result is dependent on the intraprostatic temperature.[209] Deep inside the prostate, the temperature is mainly determined by blood perfusion.[210] Although changes in urethral and intraprostatic temperatures correlate, the absolute value of urethral temperature cannot be used to predict the absolute value of deep intraprostatic temperature due to inter-individual differences in prostatic blood perfusion.[28,208] The information on intraprostatic temperature provided by measurement of the urethral temperature is thus limited. The same conclusion was drawn based on theoretical considerations (Paper XII).

Infrared detectors

Surface temperature is readily measured non-invasively with an infrared radiometer utilising the infrared radiation emitted by all objects. Because infrared radiation is strongly attenuated in water the thermal radiation recorded by radiometric methods originates from a depth less than approximately 45 μm.[211] Thus, only the temperature of the most superficial tissue can be mapped. Infrared detectors can be divided into thermal and photon detectors. Thermal detectors measure the temperature rise produced in an absorbing receiver. Examples are the thermistor bolometer and the pyroelectric detector. Since the temperature rise is dependent on the energy absorbed and not the photon wavelength directly, these detectors have a flat spectral response. Due to the thermal processes involved most thermal detectors have a comparatively slow response.

For thermal imaging, photon detectors are commonly used. Photon detectors are made of semiconductor materials which release charge carriers after absorbing photons. The energy of the photons must exceed the energy of the band gap in the semiconductor material before the carriers can be released, which leads to the characteristic sharp cut-off in the long wavelength region. In general the energy band gap is decreased by cooling, resulting in a cut-off at longer wavelengths. Common detector materials include lead sulphide (PbS) and lead selenide (PbSe), which are sensitive to radiation between 1-3 μm and 2-5 μm, respectively. Mercury cadmium telluride (MCT) detectors are available for detection in the wavelength region 2-20

μm. The infrared camera used for the investigations reported in Papers II and X, was equipped with a MCT detector, which was cooled to -70°C using a Peltier element. The detection band was between 2-5 μm. In the above Papers, the thermocamera was used to measure the two-dimensional temperature profile resulting from interstitial irradiation. The laser probe was placed between two tissue slabs, which were separated before the thermal image was taken. The experimental set-up is shown in Fig. 5.2.

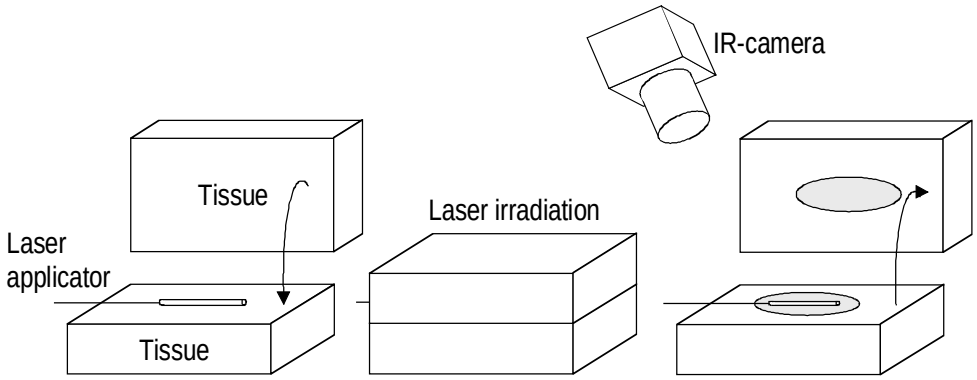

Fig. 5.2. *Experimental set-up for measuring the two-dimensional temperature distribution resulting from interstitial laser irradiation.*

Non-invasive monitoring of deep temperature

For the non-invasive monitoring of heat treatment the most important requirement is to identify a measurable quantity which is dependent only on temperature. Several methods of measuring temperature and damage deep inside the tissue non-invasively have been proposed. These include magnetic resonance imaging (MRI), X-ray computed tomography and ultrasonography.

MRI seems to have the greatest potential of the above-mentioned methods. The method is based on the interaction of applied magnetic fields and radiofrequency radiation with the natural magnetic moment of protons in free water found in the body. MRI has the advantage of being a non-ionising imaging modality, and of providing images of any desired plane. A number of different parameters can be measured by MRI, the two most important being the longitudinal relaxation time, T_1, and the transverse relaxation time, T_2. The relaxation mechanisms for nuclear magnetic moments are involved in thermal interactions with the surrounding medium. Both parameters are temperature sensitive. However, T_1 is probably best suited for temperature measurements as it is generally a simple exponential relaxation process.[204] Experimental work on liver tissue has shown that in the temperature range 37-50°C, T_1 varies approximately linearly with temperature at a rate of 1%/°C.[212] However, quantification of temperature changes using T_1 is difficult because the temperature coefficient of the individual tissue is usually

unknown.[213] In addition, T_1 temperature determination is sensitive to changes in perfusion and blood volume during monitoring.[213] Above 50°C, signal intensities cannot be related to tissue temperature due to coagulation, which induces irreversible changes in relaxation times. [214] These changes correspond roughly to the spatial extent of the thermally-induced tissue damage.[215,216]

Another parameter, the proton resonance frequency shift (PRF), also displays temperature dependence. The main advantage of measuring this parameter is its tissue independence, with the exception of adipose tissue.[217] The PRF method has proved to provide accurate temperature monitoring in tissue phantoms[218] and liver tissue.[217]

X-ray computed tomography (CT) has been proposed for non-invasive thermometry. The parameter depending on temperature is physical density, which is related to the measurable linear attenuation coefficient for X-rays. However, the density dependence of tissue with a high water content on temperature is small. When expressed in CT numbers, or Houndsfield numbers (HU), the variation is on the order -0.4 HU/°C.[219] The noise in a CT image is between 4-8 HU,[220] which implies that the temperature rise must be fairly large to be distinguishable from the noise. Data-processing techniques such as image subtracting, can to some extent eliminate this problem. With subtraction there exists the problem of motion artefacts, which can easily erase the temperature information. Dynamic CT imaging during bolus radiopaque tracer injection offers the ability to identify and discern between avascular and vascular areas. Complete avascularity of tumours evaluated using dynamic CT imaging performed a few days after heat treatment has been used as an indication of 100% tumour necrosis.[221] However, there are cases where this method has failed in predicting local tumour cure.[222]

Another radiodiagnostic technique that has been used for the direct visualisation of the coagulated lesion induced by thermotherapy is ultrasonography (US). The treatment results in an increased echodensity on the ultrasound image.[223] Real-time ultrasound has been claimed to predict reliably the extent of thermally-induced necrosis.[224] However, more recent results have led to the abandonment of the use of intra-operative US for depicting the final damage.[225,226,227,228]

5.2 Blood flow measurements

Tumour response to heat treatment does not depend solely on the temperature reached during treatment. Besides temperature another factor influencing tissue damage is blood flow. The local perfusion rate determines the microenvironment of the tumour cells (see section 2.1). Environmental factors such as pH and pO_2 can drastically alter the outcome of the treatment.[229,230] After hyperthermic treatment, correlation between tumour perfusion, as well as tumour oxygen tension, which is an indirect measure of blood perfusion, and tumour growth rate has been reported.[231,232] It is therefore of interest to monitor tumour blood perfusion during and after heat treatment.

Quantitative measurements of blood perfusion during heat treatment, in order to examine tumour vasculature response to heat, have with few exceptions been carried out on experimental animals. The use of radioactive microspheres is a common method for blood perfusion measurement, giving absolute values of regional perfusion.[233] When the microspheres (10-15 μm in diameter) are injected into the left ventricle of the heart, they are thoroughly mixed with circulating blood, transferred to organs and trapped in the capillary beds. The regional blood perfusion rate can then be calculated by counting the radioactivity in the tissue of interest and the reference blood withdrawn. Another method is to use radioactive tracers, such as ^{86}Rb, injected intravenously.[234] The fractional uptake of the tracer by tissues is equal to the fraction of the cardiac output flowing through them.[235] These methods require the animal to be sacrificed in order to measure the radioactivity.

Local blood perfusion of tumours can be measured by isotope clearance. With this method, the isotope, for example, ^{133}Xe, is injected locally into the tissue or delivered by inhalation. The washout rate of the isotope is then measured by external scintillation detectors. The rate of clearance is proportional to the capillary blood flow, which can be calculated from the clearance curves obtained and the partition coefficient between the tissue and the blood. With this method the animal does not have to be sacrificed to obtain values of blood flow. Another modality where the clearance of a distributed substance is measured is the hydrogen clearance method. Molecular hydrogen is administered with the inhalation gas until the tissue reaches saturation. The hydrogen supply is then turned off and the clearance rate of hydrogen is determined using platinum electrodes placed on, or into, the tissue of interest. The gradient of the clearance curve correlates directly with the magnitude of tissue blood perfusion within a radius of approximately 5 mm from the electrode.[236] As for the isotope clearance method, the hydrogen clearance method can provide absolute measurements of local blood flow in units of ml/min/100g tissue.

Different thermal methods have been used to estimate the blood perfusion of tissue.[237] Surface temperature recordings have been shown to correlate with perfusion in skin.[238,239] The thermal washout technique uses the transient response from a temperature perturbation introduced by extrinsic heating.[240,241] A common approach is to use self-heated thermistors, when both heating and temperature measurement can be done with the same probe.[242] The method provides values of the effective thermal conductivity, which can be used for modelling purposes (see section 4.5).

An estimation of the tissue perfusion in terms of ml/min/100g tissue can be obtained during heat treatment by matching the measured temperature decay after switching off the heating device to the temperature decay predicted by the heat sink model (see section 4.5). In the heat sink model, the blood perfusion parameter is the only free parameter. The mathematical solution can be made to match the measured temperatures by varying the value of the blood perfusion rate. During hyperthermic treatment, this technique is attractive because temperature measurement probes are

commonly already in place. The limitations of the method when thermal conduction is neglected have been pointed out.[243,244] Having a complete representation of the heating source term, steady-state values of the temperature can be used to estimate the blood perfusion. In this way, estimations of the blood perfusion rate in rat liver tumours have been obtained.[245]

Laser Doppler flowmetry

A technique suitable for measuring blood flow in human subjects is laser Doppler flowmetry (LDF).[246] The method has been used extensively for studying the response of skin microcirculation to various stimuli and treatments, such as laser treatment of port wine stains.[247] It has also been used in investigations of the vascular response to hyperthermia[248,249] and photodynamic therapy.[81] Generally the laser Doppler probe is placed on the surface of the tissue, providing a non-invasive and non-perturbing method for the registration of the microvascular flow. Information of deep perfusion can be obtained by inserting the probe into the tissue. The tissue trauma associated with the introduction of thin laser Doppler probes is considered minimal, causing little disturbance of the microvascular blood flow.[42,250] A schematic illustration of interstitial laser Doppler flowmetry is shown in Fig. 5.3.

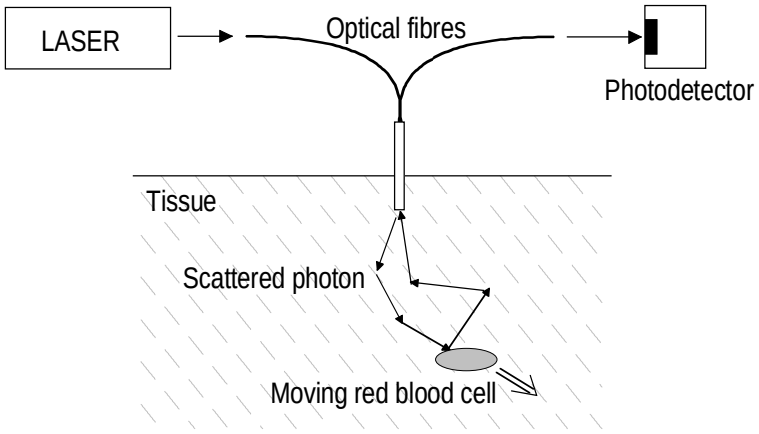

Fig. 5.3. *Principles of interstitial laser Doppler flowmetry.*

In LDF, laser light is sent into the tissue and the scattered light is detected. Light in the red or near-infrared part of the spectrum is chosen due to its low absorption in tissue. When a photon is scattered by a moving cell, such as a red blood cell in a vessel, the photon frequency is shifted by the quasielastic scattering process. The shift in frequency is the well-known Doppler shift. The Doppler shift in terms of frequency after scattering by a moving particle can be expressed as

$$\Delta f = \left(\vec{k}_s - \vec{k}_i\right)\frac{\vec{v}}{2\pi} \tag{5.2}$$

where $\vec{v}$ is the velocity vector, $\vec{k}_s$ and $\vec{k}_i$ are the scattering and the incident wave vectors, respectively. In blood perfusion studies the Doppler shift is small, approximately a factor 10^{-11} less than the frequency of the incident light.

Photons traversing tissue will generally be multiply scattered by stationary somatic cells before interacting with a moving red blood cell (RBC). The collisions between photons and stationary tissue result in the randomisation of the direction of light (that is, the incident wave vector in Eq. 5.2). Eventually the photons reach the moving erythrocytes. This randomisation precludes finding information on the direction of the blood flow. Scattered light is measured by a photodetector. At the photodetector surface photons scattered by moving RBC, which have experienced a Doppler shift in frequency, and photons scattered by the static tissue interfere, causing an intensity modulation in the detected signal. The frequency of the modulation equals the Doppler shift of the Doppler-shifted photons. Because the scattering process has a random nature, not every Doppler-shifted photon will have the same frequency. This is the case even if all RBC move in the same direction at the same speed, because the direction of the incident wave vector in Eq. 5.2. will vary due to the elastic scattering events. Therefore a spectrum of frequencies will be recorded, which in tissue has an approximately exponential decay in amplitude. It has been shown theoretically that the first weighted moment ‹ω› of the spectral power density S(ω) of the detector signal is proportional to the average velocity ‹v› of all moving particles in the optically sampled volume: [251]

$$\langle v \rangle \sim \langle \omega \rangle = M_1/M_0 \qquad \text{with } M_i = \int_{-\infty}^{+\infty} |\omega|^i S(\omega) d\omega \tag{5.3}$$

The numerator M_1 is the first moment of the spectral power density S(ω), which is considered to be proportional to the flow in the sampled volume (that is, the number of moving particles times the velocity). The denominator M_0 is proportional to the total amount of the Doppler-shifted light and thereby proportional to the number of moving particles in the optically sampled volume (RBC concentration), provided that multiple Doppler scattering effects are small. The probability of multiple Doppler scattering is low in perfusion measurement of skin, where the concentration of RBC is low, approximately 0.5 %.[252] In tissues with high perfusion, such as the liver, the likelihood that a photon is Doppler shifted more than once is high. The average RBC volume fraction of liver can be estimated to be 4-8%.[253,254] Multiple scattering leads to an underestimation of blood flow when employing the first moment of the spectral power density to represent perfusion. However, LDF output still varies linearly with mean blood cell velocity. The effect of multiple scattering can be compensated to some extent by electronic processing.[255]

In LDF laser light is generally delivered to the tissue via an optical fibre. The backscattered light is collected by the same or an adjacent fibre and registered by a photodetector. The parameter most often used to measure blood flow is the product

of velocity and concentration (first moment of the spectral power density), referred to as laser Doppler flow.[256] Conversion from laser Doppler flow to blood perfusion units in ml/min/100g is difficult. Even if laser Doppler flow has been found to correlate linearly to the values of blood flow obtained using conventional methods,[257,258] the relationship between laser Doppler flow and the absolute blood flow rate might vary between tissues.[256] The high resolution of the method (the optically sampled volume is about 1 mm^3)[259] makes it difficult to draw conclusions concerning tissue perfusion rate from point monitoring due to large local variations in perfusion. Variations in blood flow may be significant even at adjacent sites.[260]

Motion artefact is an important problem in LDF. When employing optical fibres for guiding laser light, a speckle pattern will form at the end of the fibre because of phase differences between the various rays of the beam. Signal artefacts can be produced by movement or vibration of the optical fibre itself, due to fluctuations of the speckle pattern at the detector surface. Also, relative movement between the laser Doppler probe and the tissue being studied creates artefacts. This can be a problem when measuring perfusion in rat liver, where there is considerable movement due to respiration. To minimise movement artefacts the probe should be allowed to move freely with the tissue. Even without a net tissue blood flow, laser Doppler flowmeters produce a signal well above electronic zero. In experiments on pig liver, total hepatic vascular exclusion resulted in a decrease to 11% of the initial LDF value.[261] In Paper VI, the same value was found in rat liver immediately after the animals were sacrificed. Some investigators subtract the zero-flow value from the laser Doppler flow value before further processing the results,[262] a technique which was employed in Paper VII. Possible causes for zero flow are tissue micromotions and Brownian motion of red blood cells.

6. Clinical applications of laser-induced thermotherapy

The goal of interstitial laser-induced thermotherapy (ILT) is to eradicate, by the application of heat, localised lesions in a safe and reproducible way. Through thin optical fibres placed in the target tissue, laser light is guided and emitted directly into the pathological tissue. The method has been used to treat localised tumours in the brain,[263] head and neck,[264] liver, pancreas,[265] breast[226,266] and prostate.[267] In addition, ILT is used for treatment of benign prostatic hyperplasia.[268]

Early approaches employed plane-cut fibres and high powers, creating considerable vaporisation and carbonisation. High power treatment is associated with the risk of damaging the probe, which lead some investigators to include probe cooling by a coaxial water or air flow. With high power ILT there is also the possibility that the beam from a plane-cut fibre dissects the tissue, creating a cylindrical lesion of unpredictable size. Therefore, ILT is generally performed with the intention of producing minimal vaporisation. Treatment time is typically 15-30 min.

Reproducible spherical lesions approximately 1.5 cm in diameter have been produced using the plane-cut fibre at a power of 1-2 W. The size of the lesion resulting from the simple use of a single plane-cut fibre at low powers is generally too small to be of clinical importance. To induce larger lesions, multiple treatments with the single fibre or simultaneous application of multiple fibres can be employed. To determine the optimal positions for the fibres in multifibre treatment, a mathematical model can be used (Paper III). Blood flow plays an important role in determining the size of the thermal lesion by dissipating heat. In the liver, many investigators have pointed to the importance of eliminating liver blood flow to reduce convective heat loss during ILT (Paper V).[228,269,270]

This section focuses on two clinical applications: laser treatment of liver tumours and benign prostatic hyperplasia.

6.1 Liver malignancies

Cancers of the liver are major medical problems. Primary liver cancer (hepatocellular carcinoma) is probably the most common malignant tumour of humans. The incidence of the tumour disease shows a striking geographic variability, being low in the industrialised Western world and high in Africa, Southeast Asia and Japan. Resection is the traditional method of surgical treatment for primary liver cancer.[271] Infrequently, liver transplantation is also performed for this condition when there is no evidence of extrahepatic disease.[272]

In the Western world, metastatic liver tumours are much more common than primary liver cancer. For liver metastases surgical resection is currently the only method to offer a real hope of cure. However, surgical resection is appropriate in only 10-20% of patients with liver tumours, either primary or secondary. Systemic metastatic disease and intra-abdominal disease outside the liver account for the bulk

of contraindications. The location of the lesions may be such that resection is not possible. In addition, patients may have medical conditions which make them unsuitable for major liver resection. For the majority of patients treatment is therefore palliative and survival is short.[273] There is thus a need for alternative treatment modalities.

Various methods have been developed for destroying the tumour *in situ* in a fashion to control the disease and minimise complications. These include cryotherapy,[274] brachytherapy,[275] injection of absolute alcohol[276] and ILT. Studies on ILT for treatment of liver tumours published to date have essentially been descriptions of the method and without comparison to conventional treatment modalities. Treatment has generally been focused on palliation and not on cure.

Clinical experience of ILT

Clinically, Hashimoto *et al.*,[277] in 1985, were the first to apply interstitial laser heating for the treatment of liver tumours. Ten patients were treated at laparotomy using a modified quartz fibre tip, positioned by ultrasound guidance. Levels of serum markers of malignancy showed a dramatic decrease within 3 months of treatment, suggesting a significant reduction in tumour bulk. The influence on patient survival of the treatment is not known. Hahl *et al.*[278] treated 7 patients using a sapphire probe inserted into the middle of the tumours. The temperature 1.5-2 cm from the probe was kept at 41-44°C for 10 min. Cytology of fine needle aspirates showed suspect cancer cells in 30% of the samples. Using air cooling of the fibre probe, one patient died of massive air embolism.

Percutaneous insertion of laser fibres with a conical tip was utilised by Nolsøe *et al.*[279] for the treatment of 11 patients. Treatment was interrupted when the temperature, measured with thermistors, at the tumour border had risen to 60°C or had been kept at 45°C for 15 min. Based on fine needle biopsies, ultrasound scanning and/or a second look operation, 12 of 16 treated colorectal liver metastases were considered completely destroyed. No serious complications were encountered. Three patients experienced minor pain, two patients had small temperature rises, and one patient developed a small pleural effusion. Amin *et al.*[221] introduced 4 plane-cut fibres percutaneously into the tumours of 21 patients. Nd:YAG laser light at a power of 2W per fibre was used for heating for 500 s. The fibres were then withdrawn 1.5 cm and the treatment was repeated. The number of repetitions depended on tumour size. Computed tomography showed that complete tumour necrosis was achieved in 38% of the tumours treated. The procedure was well tolerated by most patients. Mild abdominal discomfort was common during treatment and for 48h after treatment. During the treatment of lesions just below the liver capsule patients experienced shoulder pain and/or back pain. In 6 cases, small pleural effusions were noted on computed tomography scans. All patients were discharged within 24 hours after ILT.

Tranberg *et al.*[222] treated 7 patients with a total of 13 metastatic or primary liver tumours. They employed a diffusing sapphire probe inserted into the tumours after laparotomy. Multiple punctures, the number depending on tumour size, were made. The 5 min treatments were done during total occlusion of arterial and portal inflow. Computed tomography performed 1 week after treatment showed the eradication of 2 tumours. Germer *et al.*[280] used multiple cylindrical diffusers in the treatment of 10 patients with colorectal liver metastases. The average heating time was 840 s. Within a follow-up period of 3-24 months, no renewed growth of intrahepatic metastases was observed in 6 patients. In the postoperative period pleural effusion was observed in 4 patients. Bile leakage was observed in 1 patient, while transitory ascites developed in 2 patients. None of the patients died of the therapy.

The only study claiming a prolonged survival after ILT as compared to no treatment was done by Vogl *et al.*[281] They treated 99 patients, 54 of whom had developed metastases after liver resection. Thirty-six had metastases in both liver lobes, and 9 had other contraindications for surgery. Excluded were patients with more than 5 metastases; with metastases larger than 4 cm in diameter; or with extrahepatic tumours. Percutaneous ILT was performed under local anaesthesia. The median survival time was 36.4 months. Treatment was well tolerated by all patients. Six patients had mild nausea and a symptomless right subphrenic haemorrhage developed in one patient. There were no treatment-related deaths, infections, or liver or bile-duct injury.

Conclusions

Interstitial laser-induced thermotherapy of liver tumours is a local treatment modality in which the tumour is left *in situ* after thermal destruction. The aim of this technique is to eradicate the neoplasm while sparing the surrounding normal tissue. Clinical investigations have suggested the method to be safe and to prolong survival. To accomplish the complete destruction of the tumour, sophisticated imaging techniques are needed for exact fibre positioning and delineation of the thermal lesions. In most clinical investigations, ultrasound has been used to position the fibres. However, treatment-induced artefacts make it difficult to visualise the position of the fibre when repeated insertions are needed.[222] A CT scan can then be used to visualise the probe. Intra-operative MRI is a promising technique for imaging the thermal lesion in real time. The method is currently expensive and access for intra-operative monitoring of ILT is a problem. As of now, much of the future of ILT seems to depend on developments in the field of MRI.

6.2 Benign prostatic hyperplasia

With increasing age, a significant portion of the male population develops symptoms from the urinary tract. The symptoms include urgency, frequent urination, excessive urination at night, starting difficulties, poor stream, terminal dribbling, and incomplete voiding. Symptoms may be related to benign prostatic hyperplasia (BPH), which is a histopathological diagnosis. The prevalence of BPH with age is shown in Fig. 6.1.

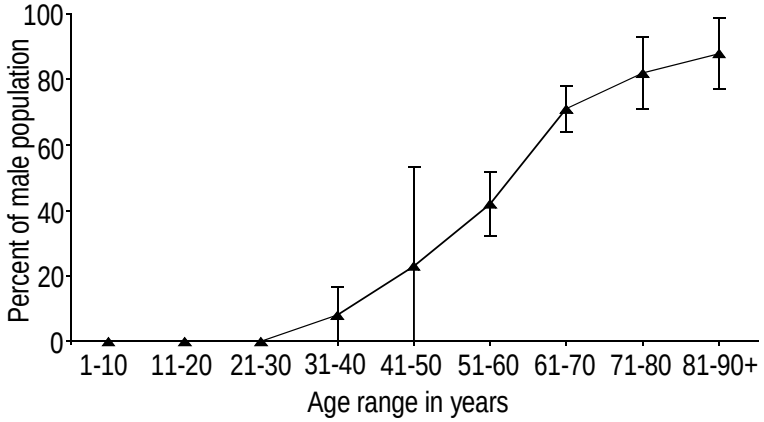

Fig. 6.1. *Prevalence of BPH with age (Redrawn from Ref. (282)).*

Benign prostatic hyperplasia is histologically characterised by the development of nodular tissues.[283] The hyperplasia begins in the submucosa of the proximal urethra. The nodules compress the urethral lumen and the surrounding normal prostate (Fig. 6.2). Outlet obstruction may ensue, which gives rise to lower urinary tract symptoms (LUTS). The symptoms caused by BPH are non-specific and differential diagnosis to consider are bladder neck sclerosis, urethral stricture, neurogenic bladder, detrusor insufficiency, urogenital infections, bladder stones, bladder cancer and prostatic cancer. In order to be able to make a reasonably safe diagnosis, the following investigations are recommended:[284] history and digital rectal examination of the prostate, flow measurements of micturition, a micturition diary, a symptom score and a quality of life questionnaire, urinalysis, serum creatinine, serum prostate specific antigen and measurement of residual urine. The outcome of treatment can be analysed by changes in urinary flow, postvoiding residual volume and symptom score. The international prostatic symptom score, I-PSS, is primarily recommended.

Outlet bladder obstruction caused by BPH is most frequently treated with transurethral resection of the prostate (TURP).[285] TURP is performed by inserting a resectoscope into the urethra. An electric current is passed through a metallic loop which facilitates the cutting of the prostatic tissue. Patients subjected to TURP are usually given a spinal or epidural anaesthesia. Following TURP, patients are provided with an indwelling catheter which can usually be removed on the following

day. Average hospital stay is 5 days. Generally, a marked increase in urinary flow is observed after TURP, as well as a decrease in symptom score. [286] Despite a high efficacy, the intra- and postoperative morbidity associated with TURP, including failure to void, bleeding requiring blood transfusions and genito-urinary infections[287,288] have led to investigations of alternative treatment modalities with fewer side-effects.

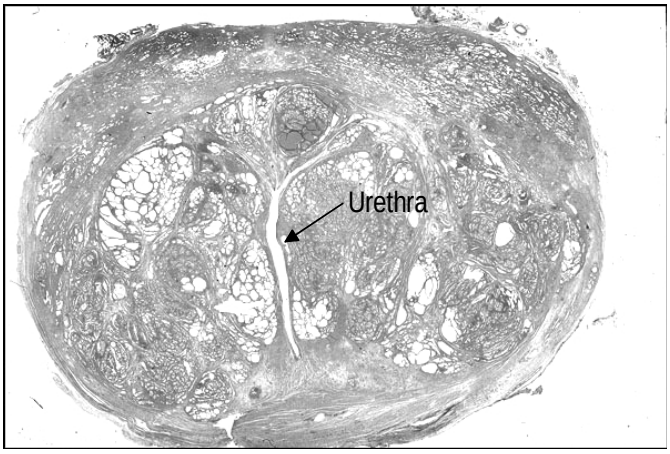

Fig. 6.2. *Cross-section of the prostate showing numerous irregular nodules (published with kind permission by Dr. James L. Fishback, University of Kansas School of Medicine).*

A number of medical treatment modalities for improving the symptoms from an obstructed bladder due to BPH are clinically investigated.[286] The non-medical interventions under investigation include balloon dilatation,[289] urethral stenting,[290] cryotherapy[291] as well as heat treatment. Prostatic thermal coagulation and hyperthermia have been induced using microwaves,[292,293] focused ultrasound,[294,295] radiofrequency heating[296] and laser irradiation. Hyperthermia seems to be ineffective in the treatment of BPH,[297] which has led to the utilisation of higher temperatures.

Many strategies of using the laser for the treatment of BPH have been proposed and employed. One of the most common laser methods is visual laser ablation of the prostate (VLAP) using the Nd:YAG laser. The method was first applied to humans in 1992.[298] The current procedure is performed in a non-contact mode by applying laser energy at four standard positions using high powers (40-60 W) for about 1 min. Side-firing fibres are employed in conjunction with standard operative endoscopes. The procedure begins just outside the bladder neck and is repeated every 1.5-2 cm until the verumontanum is reached. Laser treatment of BPH has proven to be safe, effective and cost-efficient.[299] A significant reduction in symptom score, increase in flow, and decrease in residual volume has been noted after treatment.[300,301] Studies comparing TURP and VLAP have shown the results obtained using the two methods to be similar in efficiency, while VLAP displayed

lower morbidity, shorter procedure and hospitalisation times.[302,303,304] Patients are discharged from hospital either on the same or the following day after the procedure. A significant difference between VLAP and TURP is the lack of acute tissue removal. This, in turn, leads to the lack of immediate relief of symptoms. The effect of VLAP results after delayed sloughing of the coagulated tissue. Due to post-procedure tissue swelling, an indwelling catheter is generally required for 3-5 days.

Benign prostatic hyperplasia frequently develops on the bilateral sides of the urethra. Selective coagulation of the hyperplastic tissue is accomplished with the treatment scheme described above, which, however, requires multiple repositionings of the laser fibre. A simpler procedure, in which the heat distribution is shaped according to the hyperplastic region, is proposed in Paper XI. Further development will include not only selective heating but also selective cooling in order to accentuate the butterfly-shaped heat distribution resulting from the irradiation. The advantage of the method compared with VLAP is thought to be ease of application, requiring only the insertion of the laser catheter into the urethra and fixation.

Another approach based on interstitial laser-induced thermotherapy was elaborated by Muschter *et al*.[305] They inserted fibres transuretrally emitting a conical emission pattern into the enlarged prostatic lobes. Since then cylindrical diffusing fibres have been used, inserted either from the urethra or perineum.[306] The concept is based on the idea that by creating intraprostatic lesions, the urethra would not be affected. As a consequence, no sloughing of tissue would occur, which would reduce post-procedure irritative symptoms, such as frequency and urgency. The necrotic tissue is expected to be resorbed, resulting in a shrunken gland. Indeed, a low incidence of postoperative irritative symptoms has been noted.[306] Treatment results are promising, although no randomised studies comparing this method with TURP have been made.

Simultaneous treatment of the entire circumference of the urethra can be performed using a cylindrical diffuser placed in the prostatic urethra.[307,308,309] Furuya *et al*.[310] treated 26 patients with symptomatic BPH, employing a diffusing fibre inserted into a balloon, which was inflated in the prostatic urethra. The prostatic urethra was left intact by flushing water through the balloon during laser irradiation. Without measuring the temperature of the tissue, they claimed to have generated a treatment temperature of more than 45°C. Significant improvement of the symptoms was achieved. Maintaining a low temperature of the urethral wall permits the use of local anaesthesia only.[311] The method described above of delivering energy to the hyperplastic prostate closely resembles the approach used in transurethral microwave thermotherapy (TUMT).[312,313] For TUMT the laser probe is replaced by a microwave antenna. Continuous development has led to the use of high temperatures, enabling coagulation. The method has proven to show comparable results to TURP.[314,315] However, the clinical results reported are very variable.[316] A correlation between treatment outcome after TUMT and intraprostatic temperature has been proposed, making monitoring of the tissue temperature important.[317]

TUMT is generally applied at a constant power and does not include any intraprostatic temperature measurements. Treatment temperature is dependent on the blood perfusion level, which displays large inter-individual variations.[318] Also, hyperplastic prostatic tissue is heterogeneous[319] causing local variations in blood perfusion which may result in spatial differences in tissue temperature. The striking importance of blood perfusion on temperature was shown mathematically in Paper XII. Measuring prostatic temperature during TUMT to regulate the microwave power during treatment has therefore been tried clinically with good results.[209]

Conclusions

An enormous number of minimally invasive techniques are under development for the treatment of BPH, most methods exploiting heat to induce thermal necrosis or vaporisation. The laser is but one among many alternatives for heat induction. No single method has so far proven superior to TURP in effectiveness, although encouraging results have been obtained. Quite a number of methods results in a decrease in morbidity, hospital stay, and late complications as compared to TURP, factors which may be increasingly important, not least when considering the financial situation of public health care in Sweden or elsewhere. The search for the ultimate treatment continues….

7. Summary of papers

Papers I-III report on mathematical modelling of laser-induced thermotherapy. The model utilises Monte-Carlo simulations for calculating the light absorption distribution, which is used as the source term in the heat conduction equation. The heat conduction equation is then solved using a finite difference technique. Experimental studies confirmed the results of the model, quantifying the importance of surface water evaporation on the temperature distribution (*Paper I*). Moistening the tissue surface provides an effective means to lower the surface temperature while facilitating deep tissue heating. In *Paper II*, the influence of carbonisation during interstitial laser-induced thermotherapy was investigated. Lesions were produced in porcine muscle *ex vivo* using a cylindrical diffuser covered with either a transparent glass cap or an optically opaque steel needle. Tissue coagulation was modelled using an Arrhenius relationship, and good agreement between theory and experiment was found. It was shown that the "hot tip", mimicking carbonisation during treatment, produced larger lesions as compared to the cylindrical diffuser. The difference in lesion size diminished as treatment time was prolonged and was more pronounced the greater the optical penetration depth. Modelling of four diffusing fibres activated simultaneously was performed in *Paper III*. Good agreement between theory and experiments was found, indicating the usefulness of the model for dosimetry.

Papers IV-VIII consider the biological response to thermotherapy *in vivo* of normal rat liver and rat liver tumours. A continuous wave or quasi-continuous wave Nd:YAG laser was used for all experiments. Changes in optical properties of normal liver after laser-induced thermotherapy were investigated (*Paper IV*). Coagulation resulted in an increase of 200% in the absorption coefficient, attributed to the accumulation of erythrocytes in the tissue due to heat-induced microvascular damage. Heat treatment also resulted in a two-fold increase in the reduced scattering coefficient, suggested to be due to a treatment-induced decrease in the average size of the scattering centres. The importance of occluding the hepatic blood flow during heat treatment was investigated in *Paper V*. At constant laser power, the elimination of convective heat dissipation resulted in higher temperatures, which led to complete tumour destruction. Changes in blood perfusion during interstitial laser-induced thermotherapy were measured with interstitial laser Doppler flowmetry in normal liver (*Paper VI*) and liver tumours (*Paper VII*). In *Paper VI*, temperature and blood flow were measured 4 mm from the laser fibre. The temperature was maintained at either 41 or 44°C for 30 min by regulating the laser power. At 41°C the blood flow initially increased by 30%. At 44°C blood flow decreased continuously during treatment. The results indicate a great sensitivity to heat of the liver vasculature. In *Paper VII*, the influence of hepatic inflow occlusion on the heat sensitivity of liver tumours was investigated. Treatment was performed by maintaining the temperature at the tumour border at 44°C for 30 min. Hepatic inflow occlusion during interstitial laser-induced thermotherapy resulted in an increase in the thermal sensitivity of the

tumour as evidenced by a reduction in the rate of tumour growth. Blood perfusion measured at the tumour border was greatly influenced by the combined treatment of hepatic inflow occlusion and thermotherapy. Only marginal recovery of perfusion was found after reversing the occlusion. The effect of the combined treatment of laser thermotherapy and photodynamic therapy on liver tumours was investigated in *Paper VIII*. Scanning electron microscopy pictures showed extreme damage to tumour vessels, which may indicate that vessel damage is responsible for secondary tumour cell death.

Papers IX-XII deal with different aspects of transurethral thermotherapy of benign prostatic hyperplasia. The relative importance of a number of different factors were investigated by modelling the temperature distribution during laser treatment (*Paper IX*). Simultaneous cooling of the urethral wall was theoretically found to greatly increase the therapeutic volume, otherwise limited by the small penetration depth of laser light into the prostate. Also, the importance of the dimension of the inserted catheter was quantified, and was found to be an important parameter for maximising the lesion size. A prototype of an internally water cooled applicator was developed (*Paper X*). Using the theoretical relationship between the maximum tissue temperature and the increase in temperature of the cooling water in the applicator, a new thermometry system was developed. *In vitro* experimental studies showed that the method can be used for minimally invasive and accurate temperature estimations of the maximum treatment temperature. A new laser applicator, which emits light from a narrow, elongated slit, was developed (*Paper XI*). Inserted into a water-cooled catheter selective coagulation was produced in bovine muscle *ex vivo*. Because benign prostatic hyperplasia frequently develops bilaterally around the urethra, this probe could be used for anatomically correct coagulation of the prostate. A mathematical model was used to investigate the influence of a number of different parameters on the temperature distribution and the damaged volume during transurethral microwave thermotherapy (TUMT). The great influence of blood perfusion was stressed. In order to minimise the apparent inter-individual differences in treatment response, it was proposed that TUMT should be performed in conjunction with intraprostatic temperature measurements for the regulation of microwave power.

The author is responsible for most of the work in Papers I, II, V-VII, IX-XI, including project design, programming, computer simulations, experimental work and the writing of manuscripts.

For Paper III the author was responsible for programming and computer simulations and for the writing of the parts of manuscript pertaining to the above-mentioned areas.

For Papers IV and VIII, the author contributed to the experimental work, the writing of manuscript, but not to the evaluation of the results.

For Paper XII, the author contributed to computer simulations and the scrutinising of the manuscript.

Acknowledgements

During the time of my Ph D studies I have received excellent help and support from numerous people, including my colleagues in the Medical Group and the staff at the Division. Especially I would like to express my sincere gratitude to:

My supervisor, Dr. *Stefan Andersson-Engels*, who initiated the project and who has guided me throughout my work. He always had time for discussions and gave invaluable advise. By providing a friendly and informal atmosphere, he made hard work seem easy.

Professor *Sune Svanberg* for being a constant source of inspiration.

Dr. *Karl-Göran Tranberg,* Department of Surgery, for his encouragement and enthusiasm. It was always a real pleasure working with him. His input regarding the biological and clinical aspects of laser treatment of liver tumours, including excellent scrutinising of manuscripts, has been invaluable.

Dr. *Kjell Ivarsson*, Department of Surgery, for friendship, fruitful collaboration and help with the experimental work.

Monica Radnell and *Karin Jansner* for kindness and great help with experiments.

Dr. *Magnus Bolmsjö*, Lund Instruments AB, and Professor *Anders Mattiasson*, Department of Urology, for productive collaboration and stimulating discussions concerning all kinds of heat treatment of benign prostatic hyperplasia.

Professor *Bertil Persson* and *Johan Olsrud*, Department of Radiation Physics, for friendship, fruitful collaboration and interesting discussions regarding the physics in laser heat treatment.

Professor *Unne Stenram*, Department of Pathology, for his interest in laser treatment and his great help in examining the histological specimens.

My wife, *Gunilla*, for her inspiring love and support. Without her contribution this work would never had been accomplished. Our wonderful son, *Axel*, has given a new dimension to our lives. It is amazing what a smile can do to you!

References

1. M. Molls, "Hyperthermia - the actual role in radiation oncology and future prospects, part I," Strahlenther. Oncol. **168**: 183-190, 1992.
2. K.H. Luk, T.L. Philips and R.M. Holse, "Hyperthermia in cancer therapy," West. J. Med. **132**:179-185, 1980.
3. R.A. Steeves, "Hyperthermia in cancer therapy: where are we today and where are we going?," Bull. N.Y. Acad. Med. **68**: 341-350, 1992.
4. H.R. Alexander Jr, D.L. Fraker and D.L. Bartlett, "Isolated limb perfusion for malignant melanoma," Semin. Surg. Oncol. **12**: 416-28, 1996.
5. J.A. Dickson and S.K. Calderwood, "Thermosensitivity of neoplastic tissues in vivo," in *Hyperthermia in cancer therapy*, F.K. Storm, ed., (Boston: Hall Medical Publishers, 1983), pp. 63-140.
6. D.B. Leper, "Molecular and cellular mechanisms of hyperthermia alone or combined with other modalities," in *Hyperthermic oncology*, J. Overgaard, ed., (London: Taylor and Francis, 1984), pp. 9-40.
7. L.E. Gerweck, "Hyperthermia in cancer therapy: The biological basis and unresolved questions," Cancer Res. **45**: 3408-3414, 1985.
8. C. Streffer, "Mechanism of heat injury," in *Hyperthermic oncology*, J. Overgaard, ed., (London: Taylor and Francis, 1984), pp. 213-222.
9. R.H. Burdon, S.M Kerr, C.M.M. Cutmore, J. Munro and V. Gill, "Hyperthermia, Na+K+ATPase and lactic acid production in some human tumour cells," Br. J. Cancer **49**: 437-445, 1984.
10. S.K. Calderwood and G.M. Hahn, "Thermal sensitivity and resistance of insulin-receptor binding," Biochem. Biophys. Acta **756**: 1-8, 1983.
11. G.M. Hahn, "Hyperthermia and cancer," (New York: Plenum, 1982)
12. J.E. Fuhr, "Effect of hyperthermia on protein biosynthesis in L5178Y murine leukemic lymphoblasts," J. Cell. Physiol. **84**: 365-372.
13. J.L. Roti Roti and A. Laszlo, "The effects of hyperthermia on cellular macromolecules", in *Hyperthermia and oncology* vol. 1, M. Urano and E. Douple, eds., (Utrecht: VSP, 1988), pp. 13-56.
14. B.V. Harmon, Y.S. Takano, C.M. Winterford and G.C. Gobé, "The role of apoptosis in the response of cells and tumours to mild hyperthermia," Int. J. Radiat. Biol. **59**:489-501, 1991.
15. H.M. Sweetland, A. Wyman and K. Rogers, "Evaluation of the effect on normal liver of interstitial laser hyperthermia using artificial sapphire probes," Lasers Med. Sci. **8**: 99-105, 1993.
16. S. Thomsen, "Pathologic analysis of photothermal and photomechanical effects of laser-tissue interaction," Photochem. Photobiol. **53**: 825-835, 1991.
17. C. Streffer and D. van Beunigen, "The biological basis for tumour therapy by hyperthermia and radiation," in *Hyperthermia and the therapy of malignant tumours*, C. Streffer, ed., Recent results in cancer research, vol 101, (Berlin: Springer, 1987), pp. 24-70.
18. O.S. Nielsen, "Evidence for an upper temperature limit for thermotolerance development in L1A2 tumour cells *in vitro*," Int. J. Hyperthermia **2**: 299-309, 1986.
19. W.C. Dewey, L.E. Hopwood, S.A. Sapareto and L.E. Gerweck, "Cellular responses to combinations of hyperthermia and radiation," Radiology **123**: 463-474, 1977.
20. P.W. Atkins, 2nd ed., "Physical chemistry," (Oxford: Oxford university press, 1982)
21. K.J. Henle, "Arrhenius analysis of thermal response," in *Hyperthermia in cancer therapy*, F.K. Storm, ed., (Boston: Hall Medical Publishers, 1983), pp. 47-53.
22. P.L Privalov, "Stability of proteins," in *Advances in protein chemistry*, C.B. Anfinsen, J.T. Edsall and E.M. Richards, eds., vol 33 (New York: Academic, 1979), pp. 167-241.
23. J.C. Lindegaard and J. Overgaard, "Factors of importance for the development of step-down heating effect in a C3H mammary carcinoma in vivo," Int. J. Hyperthermia **3**: 79-91, 1987.
24. C.A. Perez and S.A. Sapareto, "Thermal dose expression in clinical hyperthermia and correlation with tumor response/control," Cancer Res. (suppl.) **44**: 4818s-4825s, 1984.
25. W.C. Dewey, "Arrhenius relationships from the molecule to the clinic," Int. J. Hyperthermia **10**: 457-483, 1994.
26. C.W. Song, "Blood flow in tumours and normal tissues in hyperthermia," in *Hyperthermia in cancer therapy*, F.K. Storm, ed., (Boston: Hall Medical Publishers, 1983), pp. 187-206.
27. J.A. Dickson and S.K. Calderwood, "Temperature range and selective sensitivity of tumours to hyperthermia: a critical review," Ann. NY Acad. Sci. **335**: 180-205, 1980.
28. S.N. Venn, S.W. Hughes, B.S.I. Montgomery and A. Timoty, "Heating characteristics of a 434 MHz transurethral system for the treatment of BPH and interstitial thermometry," Int. J. Hyperthermia **12**: 271-278, 1996.
29. T.R. Larson, J.M. Collins and A. Corica, "Detailed interstitial temperature mapping during treatment with a novel transurethral microwave thermoablation system in patients with benign prostatic hyperplasia," J. Urology **159**: 258-264, 1998.
30. T.R. Larson and J.M. Collins, "Increased prostatic blood flow in response to microwave thermal treatment: preliminary findings in two patients with benign prostatic hyperplasia," Urology **46**: 584-590, 1995.

31. L.X. Xu, L. Zhu and K.R. Holmws, "Thermoregulation in the canine prostate during transurethral microwave hyperthermia, part II: blood flow response," Int. J. Hyperthermia **14**: 65-73, 1998.
32. P. Falk, "The effect of elevated temperature on the vasculature of mouse jejunum," Br. J. Radiol. **56**: 41-49, 1983.
33. S.D. Prionas, M.A. Taylor and L.F. Fajardo, "Thermal sensitivity to single and double heat treatments in normal canine liver," Cancer Res. **45**: 4791-4797, 1985.
34. P.D.I. Richardson and P.G. Withrington, "Liver blood flow. I. Intrinsic and nervous control of liver blood flow," Gastroenterology **81**: 159-173, 1981.
35. W.W. Lautt, "Intrinsic regulation of hepatic blood flow," Can. J. Physiol. Pharmacol. **74**: 223-233, 1996.
36. M. Uda, J.L. Osborn, C.K.K. Lee, R. Nakhleh and C.W. Song, "Pathophysiological changes after local heating of rat liver," Int J Radiat Oncol Biol Phys **18**: 587-594, 1990.
37. H. Matsuda, K. Sugimachi, H. Kuwano and M. Mori, "Hyperthermia, tissue microcirculation, and temporarily increased thermosensitivity in VX2 carcinoma in rabbit liver," Cancer Res **49**: 2777-2782,1989.
38. R.K. Jain and K. Ward-Hartley, "Tumor blood flow - charaterization, modifications, and role in hyperthermia," IEEE Trans. Sonics Ultrasonics **31**: 504-526, 1984.
39. H.A. Eddy and G.W. Casarett, "Development of the vascular system in the hamster malignant neurilemmoma," Microvasc. Res. **6**: 63-83, 1973.
40. W Rogers, R.F. Edlich and J.B. Aust, "Tumor blood flow II. Distribution of blood flow in experimental tumors," Angiology **20**: 374-387, 1969.
41. T.V. Samulski, P. Fessenden, R. Valdagni and D.S. Kapp, "Correlations of thermal washout rate, steady state temperatures, and tissue type in deep seated recurrent or metastatic tumors," Int. J. Radiat. Oncol. Biol. Phys. **13**: 907-916, 1987.
42. J.C. Acker, M.W. Dewhirst, G.M. Honoré, T.V. Samulski, J.A. Tucker and J.R. Oleson, "Blood perfusion measurements in human tumours: evaluation of laser Doppler methods," Int. J. Hyperthermia **6**: 287-304, 1990.
43. H.S. Reinhold and B. Endrich, "Tumour microcirculation as a target for hyperthermia," Int. J. Hyperthermia **2**: 111-137, 1986.
44. C.W. Song, M.S. Kang, J.G. Rhee and S.H. Levitt, "Effect of hyperthermia on vascular function, pH and cell survival," Radiology **137**: 795-803, 1980.
45. B. Emami, G.H. Nussbaum, N. Hahn, A.J. Piro, A. Dritschilo and F. Quimby, "Histopathological study on the effects of hyperthermia on microvasculature," Int. J. Radiat. Oncol. Biol. Phys. **7**: 343-348, 1981.
46. F.M. Waterman, R.E. Nerlinger, D.J. Moylan and D.B. Leeper, "Response of human tumor blood flow to local hyperthermia," Int. J. Radiat. Oncol. Biol. Phys. **13**: 75-82, 1987.
47. J. Denekamp, "Endothelial cell proliferation as a novel approach to targeting tumour therapy," Br. J. Cancer **45**: 136-139, 1982.
48. L.F. Fajardo and S.D. Prionas, "Endothelial cells and hyperthermia," Int. J. Hyperthermia **10**: 347-353, 1994.
49. C.W. Song, "Effect of local hyperthermia on blood flow and microenvironment: a review," Cancer Res. (suppl.) **44**: 4721s-4730s, 1984.
50. L.F. Fajardo, S.D. Prionas, J. Kowalski and H.H. Kwan, "Hyperthermia inhibits angiogenesis," Radiat. Res. **114**: 297-306, 1988.
51. T.E. Dudar and R.K. Jain, "Differential response of normal and tumor microenvironment to hyperthermia," Cancer Res. **44**: 605-612, 1984.
52. H.I. Bicher, F.W. Hetzel, T.S. Sandhu, P. Frinak, P. Vaupel, M.D. O'Hara and T. O'Brien, "Effects of hyperthermia on normal and tumor microenvironment," Radiology **137**: 523-530, 1980.
53. F.W. Hetzel, "Biologic rationale for hyperthermia," in *The radiologic clinics of north America*, vol. 27, R.A. Steeves, ed., (Philadelphia: Saunders), pp. 499-508.
54. J.R. Stewart, F.A. Gibbs, C.M. Lehman, J.W. Peck and M.J. Egger, "Change in the in vivo hyperthermic response resulting from the metabolic effects of temporary vascular occlusion," Int. J. Radiat. Oncol. Biol. Phys. **9**: 197-201, 1983.
55. C.A. Wallen, T.V. Colby and J.S. Stewart, "Cell kill and tumor control after heat treatment with and without vascular occlusion in RIF-1 tumors," Radiat. Res. **106**: 215-223, 1986.
56. S.F. Badylak, C.F. Babbs, T.M. Skojac, W.D. Voorhees and R.C. Richardson, "Hyperthermia-induced vascular injury in normal and neoplastic tissue," Cancer **56**: 991-1000, 1985.
57. S. Thomsen, "Identification of lethal thermal injury at the time of photothermal treatment," in *Laser-induced interstitial thermotherapy*, G. Müller and A. Roggan, eds., (Bellingham, WA: SPIE Opt. Eng. Press, 1995), pp. 459-467.
58. J. Overgaard, "Histopathologic effects of hyperthermia," in *Hyperthermia in cancer therapy*, F.K. Storm, ed., (Boston, MA:Hall Medical Publishing, 1983), pp. 163-185.
59. P. Gabriele, M. Amichetti, R. Orecchia and R. Valdagni, "Hyperthermia and radiation therapy for inoperable or recurrent parotid carcinoma. A phase I/II study," Cancer **75**: 908-913, 1995.

60. H.J. Feldmann, M.H. Seegenschmiedt and M. Molls, "Hyperthermia--its actual role in radiation oncology. Part III: Clinical rationale and results in deep seated tumors," Strahlenther. Onkol. **171**: 251-264, 1995.
61. J. Overgaard, D. Gonzalez Gonzalez, M.C. Hulshof, G. Arcangeli, O. Dahl, O. Mella, and S.M. Bentzen, "Randomised trial of hyperthermia as adjuvant to radiotherapy for recurrent or metastatic malignant melanoma. European Society for Hyperthermic Oncology," Lancet **345**: 540-543 1995.
62. J. Overgaard, "The current and potential role of hyperthermia in radiotherapy," Int. J. Radiat. Oncol. Biol. Phys. **16**: 535-549, 1989.
63. T.S. Mang, "Combination studies of hyperthermia induced by the Neodymium:Yttrium-Aluminum-garnet (Nd:YAG) laser as an adjuvant to photodynamic therapy," Lasers Surg. Med. **10**:173-178, 1990.
64. J. van Stevenick, K. Tijssen, J.P.J. Boegheim, J. van der Zee and T.M.A.R. Dubbelman, "Photodynamic generation of hydroxyl radicals by hematoporphyrin derivative and light," Photochem. Photobiol. **44**: 711-716, 1986.
65. K.R. Weishaupt, C.J. Gomer and T.J. Dougherty, "Identification of singlet oxygen as the cytotoxic agent in photo-inactivation of a murine tumor," Cancer Res. **36**: 2326-2329, 1976.
66. J. Moan and S. Sommer, "Oxygen dependence of the photosensitizing effect of hematoporphyrin derivative in NHIK 3025 cells," Cancer Res. **45**: 1608-1610, 1985
67. D. Kessel, P. Thompson, B. Musselman and C.K. Chang, "Probing the structure and stability of the tumour localizing derivative of hematoporphyrin by reduction with LiA1H4," Cancer Res. **47**: 4642-4645, 1987.
68. D.A. Bellnier, Y.K. Ho, R.K. Pandey, J.R. Missert and T.J. Dougherty, "Distribution and elimination of Photofrin II in mice," Photochem. Photobiol. **50**: 221-228, 1989.
69. J.C. Kennedy, R.H. Pottier and D.C. Pross, "Photodynamic therapy with endogenous protoporphyrin IX: basic principles and present clinical experience," J. Photochem. Photobiol. B: Biol. **6**: 143-148, 1990.
70. J. Regula, A.J. MacRobert, A. Gorchein, G.A. Buonaccorsi, S.M. Thorpe, G.M. Spencer, A.R. Hatfield and S.G. Bown, "Photosensitisation and photodynamic therapy of oesophageal, duodenal, and colorectal tumours using 5 aminolaevulinic acid induced protoporphyrin IX - a pilot study," Gut **36**: 67-75, 1995.
71. R.M. Szeimies, P. Calzavara-Pinton, S. Karrer, B. Ortel and M. Landthaler, "Topical photodynamic therapy in dermatology," J. Photochem. Photobiol. B **36**: 213-219, 1996.
72. J. Moan, J.V. Johannessen and T. Christensen, "Porphyrin-sensitized photoinactivation of human cells in vitro," Am. J. Pathol. **109**: 184-192, 1982.
73. R. Hilf, "Cellular targets of photodynamic therapy as a guide to mechanisms," in *Photodynamic therapy: basic principles and clinical applications*, B.W. Henderson and T.J. Dougherty, eds., (New York: Marcel Dekker, 1992), pp. 387-424.
74. J. Moan, J.B. McGhie and P.B. Jacobsen, "Photodynamic effects on cells in vitro exposed to hematoporphyrin derivative and light," Photochem. Photobiol. **37**: 599-604, 1983.
75. D.A. Bellnier and T.J. Dougherty, "Membrane lysis in Chinese hamster ovary cells treated with hematoporphyrin derivative plus light," Photochem. Photobiol. **36**: 43-47, 1982.
76. B.W. Henderson, S.M. Waldow, T.S. Mang, W.R. Potter and P.B. Malone, "Tumor destruction and kinetics of tumor cell death in two experimental mouse tumors following photodynamic therapy," Cancer Res. **45**: 572-576, 1985.
77. S.H. Selman, M. Kreimer-Birnbaum, J.E. Klaunig, P.J. Goldblatt, R.W. Keck and S.L. Britton, "Blood flow in transplantable bladder tumours treated with hematoporphyrin derivative and light," Cancer Res. **44**:1924-1927, 1984.
78. T.J. Wieman, T.S. Mang, V.H. Fingar, T.G. Hill, M.W.R. Reed, T.S. Corey, V.Q. Nguyen and E.R. Render, "Effect of photodynamic therapy on blood flow in normal and tumor vessels," Surgery **104**: 512-517, 1988.
79. I.P.J. van Geel, H. Oppelaar, Y.G. Oussoren and F.A. Stewart, "Changes in perfusion of mouse tumours after photodynamic therapy," Int. J. Cancer **56**: 224-228, 1994.
80. V.H. Fingar, T.J. Wieman, S.A. Wiehle and P.B. Cerrito, "The role of microvascular damage in photodynamic therapy: The effect of treatment on vessel constriction, permeability and leukocyte adhesion," Cancer Res. **52**: 4914-4921, 1992.
81. I. Wang, S. Andersson-Engels, G.E. Nilsson, K. Wårdell and K. Svanberg, "Superficial bloodflow following photodynamic therapy of malignant skin tumours measured by laser Doppler imaging," Br.J.Dermatol. **136**: 184-189, 1997.
82. K. Svanberg, T. Andersson, D. Killander, I. Wang, U. Stenram, S. Andersson-Engels, R. Berg, J. Johansson and S. Svanberg, "Photodynamic therapy of non-melanoma malignant tumours of the skin utilizing topical d-amino levulinic acid sensitization and laser irradiation," Br. J. Dermatol. **130**: 743-751, 1994.
83. B.P. Shumaker and F.W. Hetzel, "Clinical laser photodynamic therapy in the treatment of bladder cancer," Photochem. Photobiol. **46**: 899-901, 1987.
84. J.S. McCaughan, T.E. Williams and B.H. Bethel, "Photodynamic therapy of endobronchial tumors," Lasers Surg. Med. **6**: 336-345, 1986.
85. K.T. Moesta, P. Schlag, H.O. Douglass Jr. and T.S. Mang, "Evaluating the role of photodynamic therapy in the management of pancreatic cancer," Lasers Surg. Med. **16**: 84-92, 1995.

86. T. Christensen, A. Wahl and L. Smedshammer, "Effects of haematoporphyrin derivative and light in combination with hyperthermia on cells in culture," Br. J. Cancer **50**: 85-89, 1984.
87. S.M. Waldow, B.W. Henderson and T.J. Dougherty, "Hyperthermic potentiation of photodynamic therapy employing Photofrin I and II. Comparison of results using three animal tumor models," Lasers Surg. Med. **7**: 12-22, 1987.
88. S.M. Waldow, B.W. Henderson and T.J. Dougherty, "Potentiation of photodynamic therapy by heat: Effects of sequence and time interval between treatments in vivo," Lasers Surg. Med. **5**: 83-94, 1985.
89. C. Prinsze, T.M.A.R. Dubbelman and J. VanStevenick, "Potentiation of thermal inactivation of glyceraldehyde-3-phosphate dehydrogenase by photodynamic treatment. A possible model for the synergistic interaction between photodynamic therapy and hyperthermia," Biochem. J. **276**: 357-362, 1991.
90. S. Kimel, L.O. Svaasand, M. Hammer-Wilson, V. Gottfried, S. Cheng, E. Svaasand and M.W. Berns, "Demonstration of synergistic effects of hyperthermia and photodynamic therapy using the chich chorioallantoic membrane model," Lasers Surg. Med. **12**: 432-440, 1992.
91. F.C. Henriques, "Studies of thermal injury," Arch. Pathol. **43**: 489-502, 1947.
92. R. Agah, J.A. Pearce, A.J. Welch and M. Motamedi, "Rate process model for arterial tissue thermal damage: Implications on vessel photocoagulation," Lasers Surg. Med. **15**: 176-184, 1994.
93. J. Pearce and S. Thomsen, "Rate process analysis of thermal damage," in *Optical-thermal response of laser-irradiated tissue*, A.J. Welsh and M.J.C. van Gemert, eds., (New York: Plenum Press, 1995), pp. 561-603.
94. A.L. McKenzie, "Physics of thermal processes in laser-tissue interaction," Phys. Med. Biol. **35**: 1175-1209, 1990.
95. G.L. LeCarpentier, M. Motamedi, L.P. McMath, S. Rastegar and A.J. Welch, "Continuous wave laser ablation of tissue: analysis of thermal and mechanical events," IEEE Trans. Biomed. Eng. **40**: 188-200, 1993.
96. J. Heisterkamp, R. van Hillegersberg, E. Sinofsky and J.N.M. Ijzermans, "Heat-resistant cylindrical diffuser for interstitial laser coagulation: comparison with the bare-tip fiber in a porcine model," Lasers Surg. Med. **20**: 304-309, 1997.
97. D.E. Malone, L. Lesiuk, A.P. Brady, D.R. Wyman and B.C. Wilson, "Hepatic interstitial laser photocoagulation: demonstration and possible clinical importance of intravascular gas," Radiology **193**: 233-237, 1994.
98. A.C. Steger, W.R. Lees, P. Shorvon, K. Walmsley and S.G. Bown, "Multiple fibre low-power interstitial laser hyperthermia - studies in the normal liver," Br. J. Surg. **79**: 139-145, 1992.
99. C.E. Lindholm, E. Kjellén, P. Nilsson, L. Weber and S. Hill, "Prognostic factors for tumour response and skin damage to combined radiotherapy and hyperthermia in superficial recurrent breast carcinomas," Int. J. Hyperthermia **11**: 337-355, 1995.
100. H.I. Bicher, R.S. Wolfstein, A.G. Fingerhut, H.S. Frey, B.S. Lewinsky, "An effective fractionation regime for interstitial thermoradiotherapy - preliminary clinical results," in *Hyperthermic oncology*, vol. 1, J. Overgaard, ed., (London:Taylor and Francis, 1984), pp. 575-578.
101. P.P. Lele, "Physical aspects and clinical studies with ultrasonic hyperthermia," in *Hyperthermia in cancer therapy*, F.K. Storm, ed., (Boston, MA:Hall Medical Publishing, 1983), pp. 333-367.
102. R.F. Meredith, I.A. Brezovich, B. Wippelmann, "Ferromagnetic thermoseeds: Suitable for an afterloading interstitial implant," Int. J. Radiat. Oncol. Biol. Phys. **17**: 1341-1346, 1989.
103. J.A. DeFord, C.F. Babbs, U.H. Patel, N.E. Fearnot, J.A. Marchosky and C.J. Moran, "Accuracy and precision of computer-simulated tissue temperatures in individual human intracranial tumours treated with interstitial hyperthermia," Int. J. Hyperthermia **6**: 755-770, 1990.
104. C. Marchal, P. Bey, S. Hoffstetter and J. Robert, "Ultrasound and microwave hyperthermia in the treatment of superficial human cancerous tumors," in *Hyperthermia in cancer treatment*, L.J. Anghileri and J. Robert, eds., (Boca Raton, FL:CRC Press, 1986), pp. 211-265.
105. R.B. Roemer, "Thermal dosimetry," in *Thermal dosimetry and treatment planning*, M. Gautherie, ed., (Berlin:Springer, 1990), pp. 119-212.
106. L.O. Svaasand, T. Boerslid and M. Oeveraasen, "Thermal and optical properties of living tissue: Application to laser-induced hyperthermia," Lasers Surg. Med. **5**: 589-602, 1985.
107. P. Nilsson, *Physics and technique of microwave-induced hyperthermia in the treatment of malignant tumours.* PhD thesis, Lund University, Sweden, 1984.
108. M. Bolmsjö, L. Wagrell, A. Hallin, T. Eliasson, B.-E. Erlandsson and A. Mattiasson, "The heat is on - but how? A comparison of TUMT devices," Br. J. Urol. **78**: 564-572, 1996.
109. A.W. Guy, "Analysis of electromagnetic fields induced in biological tissues by thermodynamic studies on equivalent phantom models," IEEE Trans. Microwave Theory Tech. **19**: 205-214, 1971.
110. B. R. Paliwal and P. N. Shrivastava, "Microwave hyperthermia. Principles and quality assurance," in *The radiologic clinics of north America*, vol. 27, R.A. Steeves, ed., (Philadelphia: Saunders), pp. 489-497.
111. J.W. Strohbehn and E.B. Douple, "Hyperthermia and cancer therapy: A review of biomedical engineering contributions and challenges," IEEE Trans. Biomed. Eng. **31**: 779-787, 1984.

112. J.A. Mechling and J.W. Strohbehn, "Three-dimensional theoretical SAR and temperature distributions created in brain tissue by 915 and 2450 MHz diploe antenna arrays with varying insertion depth," Int. J. Hyperthermia **8**: 529-542, 1992.
113. T.P Ryan, B.S. Trembly, D.W. Roberts, J.W. Strohbehn, C.T. Coughlin and P.J. Hoopes, "Brain hyperthermia. I. Interstitial microwave antenna array techniques-the Dartmouth experience," Int. J. Radiat. Oncol. Biol. Phys. **29**: 1065-1078, 1994.
114. A.S. Bdesha, C.J. Bunce, J.P. Kelleher, M.E. Snell, J. Vukusic and R.O. Witherow, "Transurethral microwave treatment for benign prostatic hypertrophy - a randomized controlled clinical-trial," BMJ **306**: 1293-1296, 1993.
115. M.J. Copcoat, K.T. Ison, G. Watson and J.E.A. Wickham, "Lasertripsy for urethral stones in 120 cases: lessons learned," Br. J. Urol. **61**: 487-489, 1988.
116. D.S. Gartry, "Treating myopia with the excimer laser: the present position," BMJ **310**: 979-85, 1995.
117. O.T. Tan, P. Morrison and A.K. Kurban, "850 nm for the treatment of port-wine", Plast. Reconstr. Surg. **86**: 1112-1117, 1990.
118. P. Rutgeerts, G. Vantrappen, L. Broeckaert, G. Coremans, J. Janssens and K. Geboes, "A new and effective technique of YAG laser photocoagulation for severre upper gastrointestinal bleeding," Endoscopy **16**: 115-117, 1984.
119. J. Pietraffita and R. Dwyer, "Endoscopic laser therapy of malignant esophageal obstruction," Arch. Surg. **121**: 395-400, 1986.
120. A. Ishimaru, *Wave propagation and scattering in random media*, (Academic Press, New York, 1978).
121. J.-L. Boulnois, "Photophysical processes in laser-tissue interactions," in *Laser applications in cardiovascular diseases*, R. Ginsberg, ed., (New York: Futura, 1987).
122. S.L. Jacques, C.A. Alter, S.A. Prahl, "Angular dependence of HeNe laser light scattering by human dermis," Lasers Life Sci. **1**: 309-333, 1987.
123. L.G. Henyey and J.L. Greenstein, "Diffuse radiation in the galaxy," Astrophys. J. **93**: 70-83, 1941.
124. V. Prapavat, A. Roggan, J. Walter, J. Beuthan, U. Klingbeil and G. Müller, "In vitro studies and computer simulations to assass the use of a diode laser (850 nm) for laser-induced thermotherapy (LITT)," Lasers Surg. Med. **18**: 22-33, 1996.
125. U.G. Mueller-Lisse, A.F. Heuck, M. Thoma, R. Muschter, P. Schneede, E. Weninger, S. Faber, A. Hofstetter and M.F. Reiser, "Predictability of the size of laser-induced lesions in T1-Weighted MR images obtained during interstitial laser-induced thermotherapy of benign prostatic hyperplasia," J. Magn. Reson. Imaging **8**: 31-39, 1998.
126. D. Wyman, B. Wilson and K. Adams, "Dependence of laser photocoagulation on interstitial delivery parameters," Lasers Surg. Med. **14**: 59-64, 1994.
127. A.M.K. Enejder, *Light scattering and absorption in tissue - models and measurements*, Ph D thesis, Lund Reports on Atomic Physics, LRAP-219, 1997.
128. J.W. Pickering, S.A. Prahl, N. van Wieringen, J.F. Beek, H.J.C.M. Sterenborg and M.J.C. van Gemert, "Double-integrating-sphere system for measuring the optical properties of tissue," Appl. Opt. **32**: 399-410, 1993.
129. A.M.K. Nilsson, R. Berg and S. Andersson-Engels, "Measurements of the optical properties of tissue in conjunction with photodynamic therapy," Appl. Opt. **34**: 4609-4619, 1995.
130. P. Parsa, S.L. Jacques and N.S. Nishioka, "Optical properties of rat liver between 350 and 2200 nm," Appl. Opt. **28**: 2325-2330, 1989.
131. R. van Hillegersberg, J.W. Pickering, M. Aalders and J.F. Beek, "Optical properties of rat liver and tumor at 633 nm and 1064 nm: Photofrin enhances scattering," Lasers Surg. Med. **13**: 31-39, 1993.
132. J.W. Pickering, P. Posthumus and M.J.C. van Gemert, "Continuous measurement of the heat-induced changes in the optical properties (at 1064 nm) of rat liver," Lasers Surg. Med. **15**: 200-205, 1994.
133. J.L. Karagiannes, Z. Zhang, B. Grossweiner and L.I. Grossweiner, "Applications of the 1-D diffusion approximation to the optics of tissues and tissue phantoms," Appl. Opt. **28**: 2311-2317, 1989.
134. A. Roggan, K. Dörschel, O. Minet, D. Wolff and G. Müller, "Optical properties of biological tissues in the near-infrared wavelength range: review and measurements," in *Laser-induced interstitial thermotherapy*, G. Müller and A. Roggan, eds., (Bellingham, WA: SPIE Opt. Eng. Press, 1995), pp. 10-44.
135. S. Rastegar, S.L. Jaques, M. Motamedi and B.M. Kim, "Theoretical analysis of equivalency of high-power diode laser (810 nm) and Nd:YAG laser (1064 nm) for coagulation of tissue: predictions for prostate coagulation," Proc SPIE **1646**: 150, 1992.
136. R. Cubeddu, A. Pifferi, P. Taroni, A. Torricelli and G. Valentini, "A solid tissue phantom for photon migration studies, " Phys. Med. Biol. **42**: 1971-1979, 1997.
137. M.S. Patterson, B. Chance and B.C. Wilson, "Time resolved reflectance and transmittance for the non-invasive measurement of optical properties," Appl. Opt. **28**: 2331-2336, 1989.

138. S.A. Prahl, I.A. Vitkin, U. Bruggemann, B.C. Wilson and R.R. Anderson, "Determination of optical properties of turbid media using pulsed photothermal radiometry," Phys. Med. Biol. **37**: 1203-1217, 1992.
139. J.W. Pickering, S. Bosman, P. Posthumus, P. Blokland, J.F. Beek and M.J.C. van Gemert, "Changes in the optical properties (at 632.8 nm) of slowly heated myocardium," Appl. Opt. **32**: 367-371, 1993.
140. R. Splinter, R.H. Svenson, L. Littman, J.R. Tuntelder, C.H. Chuang, G.P. Tatsis and M. Thompson, "Optical properties of normal, diseased, and laser photocoagulated myocardium at the Nd:YAG wavelength," Lasers Surg. Med. **11**: 117-124, 1991.
141. G.J. Derbyshire, D.K. Bogen and M. Unger, "Thermally induced optical property changes in myocardium at 1.06 µm," Lasers Surg. Med. **10**: 28-34, 1990.
142. J.W. Pickering, P. Posthumus and M.J.C. van Gemert, "Continuous measurement of the heat-induced changes in the optical properties (at 1064 nm) of rat liver," Lasers Surg. Med. **15**: 200-205, 1994.
143. R. Meijerink, M. Essenpreis, J.W. Pickering, C.H. Massen, T.N. Mills and M.J.C. van Gemert, "Rate process parameters of egg white measured by light scattering," in *Laser-induced interstitial thermotherapy*, G. Müller and A. Roggan, eds., (Bellingham, WA: SPIE Opt. Eng. Press, 1995), pp. 66-80.
144. R. Agah, A.H. Gandjbakhche, M. Motamedi, R. Nossal and R.F. Bonner,"Dynamics of temperature dependent optical properties of tissue: dependence on thermally induced alteration," IEEE Trans. Biomed. Eng. **43**: 839-846, 1996.
145. T.N. Glenn, S. Rastegar and S.L. Jacques, "Finite element analysis of temperature controlled coagulation in laser irradiated tissue," IEEE Trans. Biomed. Eng. **43**: 79-87, 1996.
146. B.M. Kim, S. Rastegar and S.L. Jacques, "Finite element analysis of the role of dynamic perfusion and optical properties in laser coagulation of biological tissue," ASME Adv. Bioeng. **33**: 237-238, 1996.
147. B.C. Wilson and G. Adam, "A Monte Carlo model for the absorption and flux distributions of light in tissue," Med. Phys. **10**: 824-830, 1983.
148. M. Keijzer, S.L. Jacques, S.A. Prahl and A.J. Welch, "Light distributions in artery tissue: Monte Carlo simulations for finite-diameter laser beams," Lasers Surg. Med. **9**: 148-154, 1989.
149. F.F.M. de Mul, M.H. Koelink, M.L. Kok, P.J. Harmsma, J. Greve, R. Graaff and J.G. Aarnoudse, "Laser Doppler velocimetry and Monte Carlo simulations on models for blood perfusion in tissue," Appl. Opt. **34**: 6595-6611, 1995.
150. L. Wang and S.L. Jacques, "Monte Carlo modeling of light transport in multi-layered tissues in standard C," (Laser Biology Research Laboratory, M.D. Andersen Cancer Center, University of Texas, Houston, TX, USA, 1992).
151. C. Sturesson and S. Andersson-Engels, "Mathematical modelling of dynamic cooling and pre-heating, used to increase the depth of selective damage to blood vessels in laser treatment of port wine stains," Phys. Med. Biol. **41**: 413-428, 1996.
152. S.M. Waldow and G.E. Russel, "Response of the RIF-1 tumour to superficial or interstitial heating (46-50°C) using a Nd:YAG laser," Lasers Med. Sci. **8**: 171-178, 1993.
153. M. Panjehpour, A.V. Wilke, D.L. Frazier and B.F. Overholt, "Nd:YAG laser hyperthermia treatment of rat mammary adenocarcinoma in conjunction with surface cooling," Lasers Surg. Med. **11**: 356-362, 1991.
154. S. Andersson-Engels, J. Johansson, D. Killander, E. Kjellén, L.O. Svaasand, K. Svanberg and S. Svanberg, "Photodynamic therapy alone and in conjunction with near-infrared light-induced hyperthermia in human malignant tumours: a methodological case study," Proc. SPIE **908**: 116-125, 1988.
155. R. van Hillegersberg, W.J. Kort, F.J.W. Ten Kate and O.T. Terpstra, "Water-jet-cooled Nd:YAG laser coagulation. Selective destruction of rat liver metastases," Lasers Surg. Med. **11**: 445-454, 1991.
156. B. Anvari, B.S. Tanenbaum, W. Hoffman, S. Said, T.E. Milner, L.L. Liaw and J.S. Nelson, "Nd:YAG laser irradiation in conjunction with cryogen spray cooling induces deep and spatially selective photocoagulation in animal models," Phys. Med Biol. **42**: 265-282, 1997.
157. S.G. Bown, "Phototherapy of tumours," World. J. Surg. **7**: 700-709, 1983.
158. S.L. Jacques, "Role of tissue optics and pulse duration on tissue efects during high-power laser irradiation," Appl. Opt. **32**: 2447-2454, 1993.
159. D.R. Wyman, W.M. Whelan and B.C. Wilson, "Interstial laser photocoagulation: Nd:YAG 1064 nm optical fiber source compared to point heat source," Lasers Surg. Med. **12**: 659-664, 1992.
160. D.R. Wyman and W.M. Whelan, "Basic optothermal diffusion theory for interstitial laser photocoagulation," Med. Phys. **21**: 1651-1656, 1994.
161. Z. Amin, G. Buonaccorsi, T. Mills, S. Harries, W.R. Lees and S.G. Bown, "Interstitial laser photocoagulation: Evaluation of a 1320 Nd:YAG and a 805 nm diode laser: the significance of charring and the value of precharring the fibre tip," Lasers Med. Sci. **8**: 113-120, 1993.
162. M. Hiele, F. Penninckx, A.M. Gevers, P. van Eyken, K. Geboes, Y. Ni, G, Marchal, G. Vantrappen, J. Fevery, F. Frank, S. Hessel and P. Rutgeerts, "Interstitial thermotherapy for liver tumours: Studies of different fibres and radiation characteristics," Lasers Med. Sci. **8**: 121-125, 1993.
163. N. Daikuzono and S. Joffe, "Artificial sapphire probe for contact photocoagulation and tissue vaporisation with the Nd:YAG laser," Med. Instrum. **19**: 173-178, 1985.

164. S. Ashley, S.G. Brooks, A.A. Gehani, R.C. Kester and M.R. Rees, "Thermal characteristics of sapphire contact probe delivery systems for laser angioplasty," Lasers Surg. Med. **10**: 234-244, 1990.
165. P.J. van Eeden, A.C. Steger and S.G. Bown, "Fiber tip considerations for low power laser interstitial hyperthermia," Lasers Med. Sci. (abstr.) **3**:336, 1988.
166. T.M. Schroder, P.A. Puolakkainen, J. Hahl and O.J. Ramo, "Fatal air embolism as a complication of laser-induced hyperthermia," Lasers Surg. Med. **9**: 183-185, 1989.
167. C. Nolsøe, S. Torp-Pedersen, E. Olldag and H.H. Holm, "Bare fibre low power Nd:YAG laser interstitial hyperthermia. Comparison between diffuser tip and non-modified tip. An in vitro study," Lasers Med. Sci. **7**: 1-7, 1992.
168. R. van Hillegersberg, H.J. van Staveren, W.J. Kort, P.E. Zondervan and O.T. Terpstra, "Interstitial Nd:YAG laser coagulation with cylindrical diffusing fiber tip in experimental liver metastases," Lasers Surg. Med. **14**: 124-138, 1994.
169. A.C. Steger, P. Shorvon, K. Walmsley, R. Chisholm, S.G. Bown and W.R. Lees, "Ultrasound features of low power interstitial laser hyperthermia," Clin. Radiol. **46**: 88-93, 1992.
170. K. Dowlatshahi, D. Babish, J.D. Bangert and R. Kluiber, "Histologic evaluation of rat mammary tumor necrosis by interstitial Nd:YAG laser hyperthermia," Lasers Surg. Med. **12**: 159-164, 1992.
171. K. Orth, D. Russ, J. Duerr, R. Hibst, R. Steiner and H.G. Beger, "Thermo-controlled device for inducing deep coagulation in the liver with the Nd:YAG laser," Lasers Surg. Med. **20**: 149-156, 1997.
172. A. Roggan, D. Albrecht, H.-P. Berlien, J. Beuthan, B. Fuchs, C. Germer, I. Mesecke-von Rheinbaden, R. Rygiel, S. Schünder and G. Müller, "Application equipment for intraoperative and percutaneous laser-induced interstitial thermotherapy (LITT)," in *Laser-induced interstitial thermotherapy*, G. Müller and A. Roggan, eds., (Bellingham, WA: SPIE Opt. Eng. Press, 1995), pp. 224-248.
173. M, Hara, H. Sawa, H. Yokota and I. Saito, "Experimental studies of stereotactic laser balloon hyperthermic treatment," Lasers Surg. Med. **20**: 195-201 1997.
174. T. Suzuki, K. Kurokawa, K. Suzuki,K. Nakano, N. Diakuzono and H. Yamanaka, "Transurethral balloon laser thermotherapy: effects of a directionally shielded balloon in canine prostates," Int. J. Urol. **3**: 35-38, 1996.
175. H.-J. Schwarzmaier, R. Kaufmann, T. Kahn and F. Ulrich, Applicators for the laser-induced thermo-therapy-basic considerations and new developments," in *Laser-induced interstitial thermotherapy*, G. Müller and A. Roggan, eds., (Bellingham, WA: SPIE Opt. Eng. Press, 1995), pp.249-262.
176. F.P. Incropera and D.P. De Witt, *Fundamentals of heat and mass transfer*, 3rd edn., (New York: Wiley, 1990).
177. T.E. Cooper and G.J. Trezek, "Correlations of thermal properties of some human tissues with water content," Aerospace Med. **42**: 24-27, 1971.
178. Y. Choi and M.R. Okos, "Effects of temperature and composition on the thermal properties of food," in *Food engineering and process applications*, vol. 1, M. Le Maguer and P. Jelen, eds., (London: Elsevier, 1986).
179. A.J. Welch, "The thermal response of laser irradiated tissues," IEEE J. Quant. Electr. **20**: 1471-1481, 1984.
180. S.L. Jacques and S.A. Prahl, "Modeling optical and thermal distributions in tissue during laser irradiation," Lasers Surg. Med. **6**:494-503, 1987.
181. J.W. Valvano, "Tissue thermal properties and perfusion," in *Optical-thermal response of laser-irradiated tissue*, A.J. Welsh and M.J.C. van Gemert, eds., (London: Plenum Press), pp. 445-488.
182. A.F. Emery and K.M. Sekins, "Thermal science for physical medicine," in *Therapeutic heat and cold*, J.F. Lehmann, ed., (Baltimore, MD: Williams and Wilkins, 1982), pp. 70-132.
183. K. Giering, O. Minet, I. Lamprecht and G. Müller, "Review of thermal properties of biological tissues," in *Laser-induced interstitial thermotherapy*, G. Müller and A. Roggan, eds., (Bellingham, WA: SPIE Opt. Eng. Press, 1995), pp. 45-65.
184. A. Roggan and G. Mïller, "Dosimetry and computer based irradiation planning for laser-induced interstitial thermotherapy," in *Laser-induced interstitial thermotherapy*, G. Müller and A. Roggan, eds., (Bellingham, WA: SPIE Opt. Eng. Press, 1995), pp. 114-156.
185. M.M. Chen, K.R. Holmes and V. Rupinskas, "Pulse-decay method for measuring the thermal conductivity of living tissues," Trans. ASME J. Biomech. Eng. **103**: 253-260, 1981.
186. K. Giering, I. Lamprecht, O. Minet and A. Handke, "Determination of the specific heat capacity of healthy and tumourous human tissue," Thermochimica Acta **251**: 199-205, 1995.
187. J.H. Torres, M. Motamedi, J.A. Pearce and A.J. Welch, "Experimental evaluation of mathematical models for predicting the thermal response of tissue to laser irradiation," Appl. Opt. **32**: 597-606, 1993.
188. A.V. Luikov, *Heat & mass transfer in capillary-porous bodies*, (Oxford: Pergamon Press, 1966).
189. P. Chen and D.C. Pei, "A mathematical model of drying processes," Int. J. Heat Mass Transfer **32**: 297-310, 1989.
190. J.C. Chato, "Fundamentals of bioheat transfer," in *Thermal dosimetry and treatment planning*, M. Gauthrie, ed., (Berlin:Springer, 1990), pp. 1-56.
191. H. Arkin, L.X. Xu and K.R. Holmes, "Recent developments in modeling heat transfer in blood perfused tissues," IEEE Trans. Biomed. Eng. **41**: 97-107, 1994.

192. S.A Victor and V.L. Shaw, "Steady state heat transfer to blood flowing in the entrance region of a tube," Int. J. Heat Mass Transfer **19**: 777-783, 1976.
193. M.M. Chen and K.R. Holmes, "Microvascular contributions in tissue heat transfer," Ann. N.Y. Acad. Sci. **335**: 137-150, 1980.
194. H.H. Pennes, "Analysis of tissue and arterial blood temperatures in the resting human forearm," J. Appl. Physiol. **1**: 93-122, 1947.
195. E.G. Moros, A.W. Dutton, R.B. Roemer, M. Burton and K. Hynynen, "Experimental evaluation of two simple thermal models using hyperthermia in muscle in vivo," Int. J. Hyperthermia **9**:581-598, 1993.
196. S. Weinbaum, L.M. Jiji and D.E. Lemons, "Theory and experiment for the effect of vascular temperature on surface tissue heat transfer - part I: anatomical foundation and model conceptualization," ASME J. Biomech. Eng. **106**: 321-330, 1984.
197. S. Weinbaum and L.M. Jiji, "A new simplified equation for the effect of blood flow on local average tissue temperature," ASME J. Biomech. Eng. **107**: 131-139, 1985.
198. J. Crezee and J.J.W. Lagendijk, "Experimental verification of bioheat transfer theories: measurement of temperature profiles around large artificial vessels in perfused tissue," Phys. Med. Biol. **35**: 905-923, 1990.
199. H.P. Sien and R.K. Jain, "Temperature distributions in normal and neoplastic tissues during hyperthermia: lumped parameter analysis," J. Therm. Biol. **4**: 157-164, 1979
200. R.K. Jain, "Bioheat transfer: mathematical models of thermal systems," in *Hyperthermia in cancer therapy*, F.K. Storm, ed., (Boston, MA: Hall medical publishers, 1983), pp. 9-46.
201. K.-G. Tranberg, K. Ivarsson and P.H. Möller, "Interstitial laser thermotherapy using feedback control and monitoring with electrical impedance tomography: review of studies in vitro an in vivo," in *Laser-induced interstitial thermotherapy*, G. Müller and A. Roggan, eds., (Bellingham, WA: SPIE Opt. Eng. Press, 1995), pp. 354-365.
202. S.N. Joffe, H. Tajiri, Y. Oguro, N. Diakuzono and S. Suzuki, "Laserthermia A new method of interstitial local hyperthermia using the contact Nd:YAG laser," in *The radiologic clinics of North America*, vol 27, R.A. Steeves, ed., (Philadelphia:Saunders, 1989), pp. 611-620.
203. S.W. Waldow, G.E. Russel and P.E. Wallner, "Microprocessor-controlled Nd:YAG laser for hyperthermia induction in the RIF-1 tumor," Lasers Surg. Med. **12**: 417-424, 1992.
204. T.V. Samulski and P. Fessenden, "Thermometry in therapeutic hyperthermia," in *Methods of hyperthermia control*, M. Gauthrie, ed., (Berlin:Springer, 1990), pp. 1-34.
205. J.S. Steinhart and S.R. Hart, "Calibration curves for thermistors," Deep-sea Res.**15**: 497-503, 1968.
206. F. Manns, P.J. Milne, X. Gonzalez-Cirre, D.B. Denham, J.-M. Parel and D.S. Robinson, "In situ temperature measurements with thermocouple probes during laser interstitial thermotherapy (LITT): quantification and correction of a measurement artefact," Lasers Surg. Med. **23**: 94-103, 1998.
207. M.J.A.M. de Wildt and J.J.M.C.H. de la Rosette, "Transurethral microwave thermotherapy: an evolving technology in the treatment of benign prostatic hyperplasia," Br. J. Urol. **76**: 531-538, 1995.
208. T.R. Larson, J.M. Collins and A. Corica, "Detailed interstitial temperature mapping during treatment with a novel transurethral microwave thermoablation system in patients with benign prostatic hyperplasia," J. Urol. **159**: 258-264, 1998.
209. L. Wagrell, S. Schelin, M.Bolmsjö and L. Brudin, "High-energy transurethral microwave thermotherapy (TUMT) with intraprostatic temperature monitoring," J. Urol. **159**: 1583-1587, 1998.
210. M. Devonec, N. Berger, J.P. Fendler, P. Joubert, M. Nasser and P. Perrin, "Thermoregulation during transurethral microwave thermotherapy: experimental and clinical fundamentals," Eur. Urol. **23**: 63-67, 1993.
211. T.J. Love, "Analysis and application of thermography in medical diagnosis," in *Heat transfer in medicine and biology*. Vol 2, A. Shitzer and R.C. Eberhart, eds., (New York: Plenum Press, 1985), pp. 333-352.
212. R. Matsumoto, K. Oshio and F.A. Jolesz, "T1-weighted MR monitoring for interstitial laser- and freezing-induced ablation in the liver," J. Magn. Reson. Imaging **2**: 555-562, 1992.
213. I. Young, J.W. Hand, A. Oatridge, M.V. Prior and G.R. Forse, "Further observations on the measurement of tissue T1 to monitor temperature in vivo by MRI," Magn. Reson. Med. **31**: 342-345, 1994.
214. F.A. Jolesz, A.R. Bleier, P. Jakab, P.W. Ruenzel, K. Huttl and G.J. Jako, "MR imaging of laser-tissue interactions," Radiology **168**: 249-253, 1988.
215. A.R. Bleier, F.A. Jolesz, M.S. Cohen, R.M. Weisskoff, J.J. Dalcanton, N. Higuchi, D.A. Feinberg, B.R. Rosen, R.C. McKinstry and S.G. Hushek, "Realtime magnetic resonance imaging of laser heat deposited in tissue," Magn. Reson. Med. **21**: 132-137, 1991.
216. F.A. Jolesz and G.P. Zientara, "MRI-guided laser-induced interstitial thermotherapy: basic principles," in *Laser-induced interstitial thermotherapy*, G. Müller and A. Roggan, eds., (Bellingham, WA: SPIE Opt. Eng. Press, 1995), pp. 294-324.
217. T. Harth, T. Kahn, M. Rassek, B. Schwabe, H.J. Schwarzmaier, J.S. Lewin and U. Mödder "Determination of laser-induced temperature distributions using echo-shifted TurboFLASH," Magn. Reson. Med. **38**: 238-245, 1997.

218. J. Olsrud, R. Wirestam, S. Brockstedt, A.M.K. Nilsson, K.-G. Tranberg, F. Ståhlberg and B.R.R. Persson, "MRI thermometry on phantoms by use of the proton frequency shift method: application to interstitial laser thermometry," Phys. Med. Biol. (in press).
219. B.G. Fallone, P.R. Moran and E.B. Podgorsak, "Noninvasive thermometry with a clinical X-ray CT scanner," Med. Phys. **9**: 715-721, 1982.
220. S.M. Bentzen, J. Overgaard and J. Jorgensen, "Isotherm mapping in hyperthermia using subtraction X-ray computed tomography," Radiother. Oncol. **2**: 255-260, 1984.
221. Z. Amin, J.J. Donals, A. Masters, R. Kant, A.C. Steger, S.G. Bown and W.R. Lees, "Hepatic metastases: interstitial laser photocoagulation with rea-time US monitoring and dynamic CT evaluation of treatment," Radiology **187**: 339-347, 1993.
222. K.-G. Tranberg, P.H. Möller, P. Hannesson and U. Stenram, "Interstitial laser treatment of malignant tumours: initial experience," Eur. J. Surg. Oncol. **22**: 47-54, 1996.
223. A.H. Dachman, J.A. McGehee, T.E. Beam, J.A. Burris and D.A. Powell, "US-guided percutaneous laser ablation of liver tissue in a chronic pig model," Radiology **176**: 129-133, 1990.
224. A. Masters, A.C. Steger, W.R. Lees, K.M. Walmsley and S.G. Bown, "Interstitial laser hyperthermia: A new approach for treating liver metastases," Br. J. Cancer **66**: 518-522, 1992.
225. H.R.S. Roberts, J. Brookes, W.R. Lees and S.G. Bown, "Guidance and control of interstitial laser photocoagulation in liver tumours," in *Laser-induced interstitial thermotherapy*, G. Müller and A. Roggan, eds., (Bellingham, WA: SPIE Opt. Eng. Press, 1995), pp. 344-353.
226. S.A. Harries, Z. Amin, M.E.F. Smith, W.R. Lees, J. Cooke, M.G. Cook, J.H. Scurr, M.W. Kissin and S.G. Bown, "Interstitial laser photocoagulation as a treatment of breast cancer," Br. J. Surg. **81**: 1617-1619, 1994.
227. D.E. Malone, D.R. Wyman, D.J. Moote, F.G. DeNardi, H. Mori, C. Swift, R. Lewis, G.W. Stevenson and B.C. Wilson, "Sonographic changes during hepatic interstitial laser photocoagulation," Invest. Radiol. **27**: 804-813, 1992.
228. P.H. Möller, P.H. Hannesson, K. Ivarsson, J. Olsrud, U. Stenram and K.-G. Tranberg, "Interstitial laser thermotherapy in pig liver: effect of inflow occlusion on extent of necrosis and ultrasound image," Hepato-Gastroenterol. **44**: 1302-1311, 1997.
229. L.E. Gerweck, "Modification of cell lethality at elevated temperatures: The pH effect," Radiat. Res. **70**: 224-235, 1977.
230. G.M. Hahn, "Metabolic aspects of the role of hyperthermia in mammalian cell inactivation and their possible relevance to cancer treatment," Cancer Res. **34**: 3117-3123, 1974.
231. Y. Nishimura, Y. Shibamoto, S. Jo, K. Akuta, M. Hiraoka, M. Takahashi and M. Abe, "Relationship between heat-induced vascular damage and thermosensitivity in four mouse tumours," Cancer Res. **48**: 7226-7230, 1988.
232. A.K. Fahy and S.M. Waldow, "Evaluation of changes in oxygen tension as indicators of RIF-1 tumor response to Nd:YAG laser heating," Lasers Surg. Med. **13**: 312-320, 1993.
233. T. Nakajima, J.G. Rhee, C.W. Song and Y. Onoyama, "Effects of a second heating on rat liver blood flow," Int. J. Hyperthermia **8**: 679-687, 1992.
234. H. Peterson, "Tumor blood flow compared with normal tissue blood flow," in *Tumor blood circulation*, H. Peterson, ed., (Boca Raton, FL: CRC Press, 1979), pp. 103-114.
235. C.W. Song, M.S. Patten, L.M. Chelstrom, J.G. Rhee and S.H. Levitt, "Effect of multiple heatings on the blood flow in RIF-1 tumours, skin and muscle of C3H mice," Int. J. Hyperthermia **3**: 535-545, 1987.
236. A.M. Seifalian, G.P. Stansby and K.E.F. Hobbs, "Measurement of liver blood flow: a review," HPB Surgery 4: 171-186, 1991.
237. H.F. Bowman, "Estimation of tissue blood flow," in *Heat transfer in medicine and biology*, vol. 1, A. Shitzer and R.C. Eberhart, eds., (New York: Plenum Press, 1985), pp. 193-230.
238. A.M. Seifalian, G. Stansby, A. Jackson, K. Howell and G. Hamilton, "Comparison of laser Doppler perfusion imaging, laser Doppler flowmetry, and thermographic imaging for assessment of blood flow in human skin," Eur. J. Vasc. Surg. **8**: 65-69, 1994.
239. D.K. Harrison, N.C. Abbot, J. Swanson Beck and P.T. McCollum, "A preliminary assessment of laser Doppler perfusion imaging in human skin using the tuberculin reaction as a model," Physiol. Meas. **14**: 241-254, 1993.
240. M. Knudsen, "Estimation of tissue blood flow from hyperthermia treatment data," Int. J. Hyperthermia **5**: 653-661, 1989.
241. F.M. Waterman, L. Tupchong, R.E. Nerlinger and J. Matthews, "Blood flow in human tumors during local hyperthermia," Int. J. Radiat. Oncol. Biol. Phys. **20**: 1255-1262, 1991.
242. G. Delhomme, W.H. Newman, B. Roussel M. Jouvet, F. Bowman and A. Dittmar, "Thermal diffusion probe and instrument system for tissue blood flow measurements: validation in phantoms and in vivo organs," IEEE Trans. Biomed. Eng. **41**: 657-661, 1994.
243. W.H. Newman, P.P. Lele and H.F. Bowman, "Limitations and significance of thermal washout data obtained during microwave and ultrasound hyperthermia," Int. J. Hyperthermia **6**: 771-784, 1990.

244. T.S. Sandhu, "Measurement of blood flow using temperature decay: effect of thermal conduction," Int. J. Radiat. Oncol. Biol. Phys. **12**: 373-378, 1986.
245. C. Sturesson, S. Andersson-Engels and S. Svanberg, "A numerical model for the temperature increase in surface-applied laser-induced thermo therapy with applications to tumour blood flow estimations," in *Laser-induced interstitial thermotherapy*, G. Müller and A. Roggan, eds., (Bellingham, WA: SPIE Opt. Eng. Press, 1995), pp. 157-173.
246. P.Å. Öberg, Laser-Doppler flowmetry," Crit. Rev. Biomed. Eng. **18**:125-163, 1990.
247. A.M. Troilius B. Ljunggren, "Evaluation of port wine stains by laser Doppler perfusion imaging and reflectance photometry before and after pulsed dye laser treatment," Acta Derm.Venereol. **76**:291-294, 1996
248. C.W. Song, J.G. Rhee and D.J. Haumschild, "Continuous and non-invasive quantification of heat-induced changes in blood flow in the skin and RIF-1 tumour of mice by laser Doppler flowmetry," Int. J. Hyperthermia **3**: 71-77, 1987.
249. J.G. Rhee, H.A. Eddy, J.J. Hong, M. Sunthralingam and P.W. Vaupel, "Divergent changes of flow through individual blood vessels upon localized heating," Int. J. Hyperthermia **12**: 757-769, 1996.
250. E.G. Salerud and P.Å. Öberg, "Single-fibre laser Doppler flowmetry. A method for deep tissue perfusion measurements," Med. Biol. Eng. Comput. **25**: 329-334, 1987.
251. R. Bonner and R. Nossal, "Model for laser Doppler measurements of blood flow in tissues," Appl. Opt. **20**: 2097-2107, 1981.
252. G.E. Nilsson, T. Tenland and P.Å. Öberg, "Evaluation of a laser Doppler flowmeter for measurement of tissue perfusion," IEEE Trans. Biomed. Eng. **27**: 597-604, 1980.
253. A. Blouin, R.P. Bolender and E.W. Weibel, "Distribution of organelles and membranes between hepatocytes and non-hepatocytes in the rat liver parenchyma. A stereological study," J. Cell Biol. **72**: 441-455, 1977.
254. M.V. St.-Pierre, A.J. Schwab, C.A. Goresky, W. Lee and K.S. Pang, "The multiple-indicator dilution technique for characterization of normal and retrograde flow in once-through rat liver perfusion," Hepatology **9**: 285-296, 1989.
255. G.E. Nilsson, "Signal processor for laser Doppler flowmeters," Med. Biol. Eng. Comput. **22**: 343-348, 1984.
256. C.W. Song, L.M. Chelstrom and D.J. Haumschild, "Changes in human skin blood flow by hyperthermia," Int. J. Radiat. Oncol. Biol. Phys. **18**: 903-907, 1990.
257. A.P. Shepard, G.L. Riedel, J.W. Kiel, D.J. Haumschild and L.C. Maxwell, "Evaluation of an infrared laser-Doppler blood flowmeter," Am. J. Physiol. **252**: G832-839, 1987
258. G.J. Smits, R.J. Roman and J.H. Lombard, "Evaluation of laser-Doppler flowmetry as a measure of tissue blood flow," J. Appl. Physiol. **61**: 666-672, 1986.
259. A. Jakobsson and G.E. Nilsson, "Prediction of sampling depth and photon pathlength in laser Doppler flowmetry," Med. Biol. Eng. Comput. **31**: 301-307, 1993.
260. T. Tenland, E.G. Salerud, G.E. Nilsson and P.Å. Öberg, "Spatial and temporal variations in human skin blood flow," Int. J. Microcirc. Clin. Exp. **2**: 81-90, 1983.
261. Y.I. Kim, T. Ishii, M. Aramaki, T. Yoshida and M. Kobayashi, "The Pringle maneuver induces only partial ischemia of the liver," Hepato-Gastroenterol. **42**: 169-171, 1995.
262. D.K. Kelleher, T. Engel and P.W. Vaupel, "Changes in microregional perfusion, oxygenation, ATP and lactate distribution in subcutaneous rat tumours upon water-filtered IR-A hyperthermia," Int. J. Hyperthermia **11**: 241-255, 1995.
263. T. Menovsky, J.F. Beek, F.X. Roux and S.G. Bown, "Interstitial laser thermotherapy: developments in the treatment of small deep-seated brain tumors," Surg. Neurol. **46**: 568-571, 1996.
264. T.J. Vogl, M.G. Mack, P. Müller, C. Philipp, H. Böttcher, A. Roggan, M. Deimling, D. Knöbber and R. Felix, "MR-guided laser induced thermotherapy of head and neck tumors," in *Laser-induced interstitial thermotherapy*, G. Müller and A. Roggan, eds., (Bellingham, WA: SPIE Opt. Eng. Press, 1995), pp. 493-504.
265. A.C. Steger, "Interstitial laser hyperthermia for the treatment of hepatic and pancreatic tumours," Photochem. Photobiol. **53**: 837-844, 1991.
266. H. Mumtaz, M.A. Hall-Craggs, A. Wotherspoon, M. Paley, G. Buonaccorsi, Z. Amin, I. Wilkinson, M.W. Kissin, T.I. Davidson, I. Taylor and S.G. Bown, "Laser therapy for breast cancer: MR imaging and histopathologic correlation," Radiology **200**: 651-658, 1996.
267. Z.Amin, W.R. Lees and S.G. Bown, "Technical note: interstitial laser photocoagulation for the treatment of prostatic cancer," Br. J. Radiol. **66**: 1044-1047, 1993.
268. R. Muschter and A. Hofstetter, "Technique and results of interstitial laser coagulation," World J. Urol. **13**: 109-114, 1995.
269. C.T. Germer, D. Albrecht, A. Roggan, C. Isbert and H.J. Buhr, "Experimental study of laparoscopic laser-induced thermotherapy for liver tumours," Br. J. Surg. **84**: 317-320, 1997.
270. J. Heisterkamp, R. van Hillegersberg, P.G.H. Mulder, E.L. Sinofsky and J.N.M. Ijzermans, "Importance of eliminating portal flow to produce large intrahepatic lesions with interstitial laser coagulation," Br. J. Surg. 84: 1245-1248, 1997.

271. G.H. Li, S.L. Zhu, J.Q. Li and Y.Q. Zhan, "Evaluation of partial hepatectomy for primary liver cancer," J. Surg. Oncol. **41**: 5-8, 1989.
272. J.C. O'Grady, R.J. Polson, K. Rolles, R.Y. Calne and R. Williams, "Liver transplantation for malignant disease," Ann. Surg. **207**: 373-379, 1988.
273. J.A. Ridge and J.M. Daley, "Treatment of colorectal hepatic metastases," Surg. Gynecol. Obstet. **161**: 597-607, 1985.
274. T.S. Ravikumar, G. Steele, R. Kane and V. King, "Experimental and clinical observations on hepatic cryosurgery for colorectal meatstases," Cancer Res. **51**: 6323-6327, 1991.
275. D. Donath, D. Nori, A. Turnbull, N. Kaufman and J.G. Fortner, "Brachytherapy in the treatment of solitary colorectal metastases to the liver," J. Surg. Oncol. **44**: 55-61, 1990.
276. T. Livraghi, C. Vettori and S. Lazzaroni, "Liver metastases: results of percutaneous ethanol injection in 14 patients," Radiology **179**: 709-712, 1991.
277. D. Hashimoto, M. Takami and M. Idezuki, "In depth radiation therapy by Nd:YAG laser for malignant tumours of the liver under ultrasonic guidance [abstract]," Gastroenterology **88**:A1663, 1985.
278. J. Hahl, R. Haapainen, J. Ovaska, P. Puolakkainen and T. Schröder, "Laser-induced hyperthermia in the treatment of liver tumours," Laser Surg. Med. **10**: 319-321, 1990.
279. C.P. Nolsøe, S. Torp-Pedersen, F. Burcharth, T. Horn, S. Pedersen, N.-E.H. Christensen, E.S. Olldag, P. Haubro Andersen, S. Karstrup, T. Lorenzen and H.H. Holm, "Interstitial hyperthermia of colorectal liver metastases with a US-guided Nd-YAG laser with a diffuser tip: a pilot clinical study," Radiology **187**: 333-337, 1993.
280. C.-T. Germer, D. Albrecht, J. Boese-Landgraf, A. Roggan and C. Isbert, "Laser-induced thermotherapy (LITT) in the treatment of colorectal liver metastases - a clinical pilot study," in *Laser-induced interstitial thermotherapy*, G. Müller and A. Roggan, eds., (Bellingham, WA: SPIE Opt. Eng. Press, 1995), pp. 393-402.
281. T.J. Vogl, M.G. Mack, R. Straub, A. Roggan and R. Felix, "Percutaneous MRI-guided laser-induced thermotherapy for hepatic metastases for colorectal cancer," Lancet **350**: 29, 1997.
282. S.J. Berry S J, D.S. Coffey, P.C. Walsh and L.L. Ewing, "The development of human benign prostatic hyperplasia with age," J. Urol. **132**: 474-479, 1984.
283. R.E. Deering, S.A. Bigler, J. King, M. Choongkittaworn, E. Aramburu and M.K. Brawer, "Morphometric quatitation of stroma in human benign prostatic hyperplasia," Urology **44**: 64-70, 1994.
284. Workshop.Treatment of benign prostatic hyperplasia **3**:1997. Läkemedelsverket.
285. J.P. Blandy *Transurethral resection* 2nd edn. (London: Pitman Medical Publishing Co, 1978), pp. 85-112.
286. Z. Petrovich, F. Ameye, L. Baert, K.H. Bichler, S.D. Boyd, L.W. Brady, R.C. Bruskewich, C. Dixon, P. Perrin and G.M. Watson, "New trends in the treatment of benign prostate hyperplasia and carcinoma of the prostate," Am. J. Clin. Oncol. **16**: 187-200, 1993.
287. W.K. Mebust, H.L. Holtgrewe, A.T.K. Cockett and P.C. Peters, "Transurethral prostatectomy: immediate and postoperative complications. A cooperative study of 13 participating institutions evaluating 3,885 patients," J. Urol. **141**: 243-247, 1989.
288. H.A. Doll, N.A. Black, K. McPherson, A.B. Flood, G.B. Williams and J.C. Smith, "Mortality, morbidity and complications following transurethral resection of the prostate for benign prostatic hyperplasia," J. Urol. **147**: 1566-1573, 1992.
289. N.F. Wasserman, P.K. Reddy, G. Zhang and P.A. Berg, "Experimental treatment of benign prostatic hyperplasia with transurethral balloon dilatation of the prostate: preliminary study in 73 humans," Radiology **177**: 485-494, 1990.
290. K.K. Nielsen, P. Klarskov, J. Nordling, J.T. Andersen and H.H. Holm, "The intraprostatic spiral. New treatment for urinary retention," Br. J. Urol. **65**: 500-503, 1990.
291. G. Rigondet and J.M. Salé, "Place actuelle de la cryochirurgie en urologie," Ann. Urol. **19**: 153-157, 1985.
292. W.L. Strohmaier, K.H. Bichler, S.H. Fluchter and D.M. Wilbert, "Local microwave hyperthermia of benign prostatic hyperplasia," J. Urol. **144**: 913-917, 1990.
293. Y. Homma and Y. Aso, "Transurethral microwave thermotherapy for benign prostatic hyperplasia: a 2-year follow-up study," J. Endourol. **7**: 261-265, 1993.
294. S. Madersbacher, C. Kratzik, M. Susani and M. Marberger, "Tissue ablation in benign prostatic hyperplasia with high intensity focused ultrasound," J. Urol. **152**: 1956-1961, 1994.
295. R.S. Foster, R. Bihrle, N. Sanghvi, F. Fry, K. Kopecky, J. Regan, J. Eble, C. Hennige, L.V. Hennige and J.P. Donohue, "Production of prostatic lesions in canines using transrectally administered high-intensity focused ultrasound," Eur. Urol. **23**: 330-336, 1993.
296. C.C. Schulman, A.R. Zlotta, J.S. Rasor, L. Hourriez, J.C. Noel and S.D. Edwards, "Transurethral needle ablation (TUNA): safety, feasibility, and tolerance of a new office procedure for treatment of benign prostatic hyperplasia," Eur. Urol. **24**: 415-423, 1993.
297. M.J.A.M. De Wildt, A. Tubaro, K. Höfner, S.St.C. Carter, J.J.M.C.H. De La Rosette and M. Devonec, "Responders and nonresponders to transurethral microwave thermotherapy: A multicenter retrospective analysis," J. Urol. **154**: 1775-1778, 1995.

298. A.J. Costello, W.G. Bowsher, D.M. Bolton, K.G. Braslis and J. Burt, “Laser ablation of the prostate with benign prostatic hypertrophy,” Br. J. Urol. **69**: 603-608, 1992.
299. J.N. Kabalin and E.D. Butler, "Costs of minimally invasive laser surgery compared with transurethral electrocautery resection of the prostate," West. J. Med. **162**: 426-429, 1995.
300. A.J. Costello, B.S. Shaffer, H.R. Crowe, “Second generation delivery systems for laser prostatic ablation,” Urology **43**: 262-266, 1994.
301. J.P. Norris, D.M. Norris, R.D. Lee and M.A. Rubenstein, “Visual laser ablation of the prostate: clinical experience in 108 patients,” J. Urol. **150**: 1612-1614, 1993.
302. R.S. Cowles, J.N. Kabalin, S. Childs, H. Lepor, C. Dixon, B. Stein and A. Zabbo, “A prospective randomized comparison of transurethral resection to visual laser ablation of the prostate for the treatment of benign prostatic hyperplasia,” Urology **46**: 155-160, 1995.
303. T. Uchida, S. Egawa, M. Iwamura, M. Ohori, E. Yokoyama, T. Endo and K. Koshiba, “A non-randomized comparative study of visual laser ablation and transurethral resection of the prostate in benign prostatic hyperplasia,” Int J Urol, **3**:108-112, 1996.
304. K. Anson, J. Nawrocki, J. Buckley, C. Fowler, R. Kirby, W. Lawrence, P. Paterson and G.A. Watson, “A multicenter, randomized, prospective study of endoscopic laser ablation versus transurethral resection of the prostate,” Urology, **46**:305-310, 1995.
305. R. Muschter, A. Hofstetter, S. Hessel, E. Keiditsch and P. Schneede, “Interstitial laser prostatectomy: experimental and first clinical results (abstract),” J. Urol. **149**: 346A, 1993.
306. R. Muschter and A. Hofstetter, “Interstitial laser therapy outcomes in benign prostatic hyperplasia,” J. Endourol. **9**: 129-135, 1995.
307. D.M. Cromeens, R.E. Price and D.E. Johnson, “Pathologic changes following transurethral canine prostatectomy with a cylindrically diffusing fiber,” Lasers Surg. Med. **14**: 306-313, 1994.
308. T. Suzuki, K. Kurokawa, K. Suzuki, H. Nakazato, K. Imai and H. Yamanaka, “In vivo effects of transurethral balloon laser prostatectomy on the canine prostate,” J. Urol. **151**: 1092-1095, 1994.
309. T. Suzuki, K. Kurokawa, H. Yamanaka, M.L. Liong and N. Daikuzono, “Prostatectomy by transurethral balloon laserthermiaTM (ProstalaseTM) in the canine,” Lasers Surg. Med. **14**: 71-82, 1994.
310. S. Furuya, T. Tsukamoto, Y. Kumamoto, N. Daikuzono, and M.L. Liong, "Transurethral balloon laser thermotherapy for symptomatic benign prostatic hyperplasia: Preliminary clinical results," J. Endourol. **9**: 145-149, 1995.
311. M. Devonec, N. Berger and P. Perrin, “Transurethral microwave heating of the prostate - or from hyperthermia to thermotherapy,” J. Endourol. **5**: 129-135, 1991.
312. V. Eppert, S. Trembly and H.J. Richter, “Air cooling for an interstitial microwave hyperthermia antenna: Theory and experiment,” IEEE Trans. Biomed. Eng. **38**: 450-460, 1991.
313. M.M. Yeh, S. Trembly, E.B. Douple, T.P. Ryan, P.J. Hoopes, E. Jonsson and J.A. Heaney, ”Theoretical and experimental analysis of air cooling for intracavitary microwave hyperthermia applicators,” IEEE Trans. Biomed. Eng. **41**: 874-881, 1994.
314. F.C. D'Ancona, E.A. Francisca, W.P. Witjes, L. Welling, F.M. Debruyne and J.J. De-La-Rosette, “Transurethral resection of the prostate vs high-energy thermotherapy of the prostate in patients with benign prostatic hyperplasia: long-term results,” Br. J. Urol. **81**: 259-264, 1998.
315. M.J.A.M. de Wildt, F.M.J. Debruyne and J.J.M.C.H de la Rosette, “High-energy transurethral microwave thermotherapy. A thermoablative treatment for benign prostatic hyperplasia,” Urology **48**: 416-423, 1996.
316. J.J.M.C.H. de la Rosette, F.C.H. D’Ancona and F.M.J.DeBruyne, “Current status of thermotherapy of the prostate,” J. Urol. 157: 430-438, 1997.
317. S.S.C. Carter and C.W. Ogden, “Intraprostatic temperature versus clinical outcome in TUMT. Is the response heat-dose dependent (abstract 416A),” J.Urol. **151**: 756, 1994.
318. T. Inaba, "Quantitative measurements of prostatic blood flow and blood volume by positron emission tomography," J. Urol. **148**: 1457-1460, 1992.
319. L.S. Marks, B. Treiger, F.J. Dorey, Y.S. Fu and J.B. DeKernion, “Morphometry of the prostate: I. Distribution of tissue components in hyperplastic glands,” Urology **44**: 486-492, 1994.